NASA TECHNICAL MEMORANDUM

NASA TM X-71961

COPY NO.

NASA TM X-

RECOMMENDED RADIATIVE PROPERTY DATA FOR VENUSIAN ENTRY CALCULATIONS

By

J. J. Jones, R. E. Boughner, K. V. Haggard,
J. E. Nealy, D. R. Schryer and E. V. Zoby

This informal documentation medium is used to provide accelerated or special release of technical information to selected users. The contents may not meet NASA formal editing and publication standards, may be revised, or may be incorporated in another publication.

NATIONAL AERONAUTICS AND SPACE ADMINISTRATION
LANGLEY RESEARCH CENTER, HAMPTON, VIRGINIA 23665

1. Report No.	2. Government Accession No.	3. Recipient's Catalog No.
TM X-71961		

4. Title and Subtitle	5. Report Date
Recommended Radiative Property Date for Venusian Entry Calculations	May 1974
	6. Performing Organization Code

7. Author(s)	8. Performing Organization Report No.
J. J. Jones, R. E. Boughner, K. V. Haggard, J. E. Nealy, D. R. Schwaner and E. V. Zoby	
	10. Work Unit No.

9. Performing Organization Name and Address	11. Contract or Grant No.
Advanced Entry Analysis Branch/SSD NASA-Langley Research Center Hampton, VA 23665	
	13. Type of Report and Period Covered
12. Sponsoring Agency Name and Address	Technical Memorandum
NASA-Langley Research Center Hampton, VA 23665	14. Sponsoring Agency Code

15. Supplementary Notes

In preparation as a NASA SP

16. Abstract

A compilation of experimental and calculated data on the radiative properties species important in Venusian entry is presented. Molecular band systems, atomic lines, free-bound, and free-free continua are considered for the principal radiating species of shock heated carbon dioxide. A limited amount of data pertinent to the species in the ablation layer is also included. The assumption is made that the Venus atmosphere so closely approximates pure CO_2 that the invidcid layer radiation is due almost entirely to thermally excited CO_2. The only exception is the inclusion of data on the Violet band system of CN. For the principal contributors, recommendations are made as to best property values for radiative heating calculations. A review of the basic equations and the relationships of the various emission-absorption gas properties is also included.

17. Key Words (Suggested by Author(s)) (STAR category underlined)	18. Distribution Statement
Carbon Dioxide, Oscillator Strength, Molecular radiation, Atomic radiation Venus Entry, Opacity	No restriction

19. Security Classif. (of this report)	20. Security Classif. (of this page)	21. No. of Pages	22. Price*
Unclassified	Unclassified	129	$4.75

*Available from { The National Technical Information Service, Springfield, Virginia 22151
STIF/NASA Scientific and Technical Information Facility, P.O. Box 33, College Park, MD 20740

ABSTRACT

A compilation of experimental and calculated data on the radiative properties of species important in Venusian entry is presented. Molecular band systems, atomic lines, free-bound, and free-free continua are considered for the principal radiating species of shock heated carbon dioxide. A limited amount of data pertinent to the species in the ablation layer is also included. The assumption is made that the Venus atmosphere so closely approximates pure CO_2 that the inviscid layer radiation is due almost entirely to thermally excited CO_2. The only exception is the inclusion of data on the Violet band system of CN. For the principal contributors, recommendations are made as to best property values for radiative heating calculations. A review of the basic equations and the relationships of the various emission-absorption gas properties is also included.

SUMMARY

A compilation of experimental and calculated data on the radiative properties of species important in Venusian entry is presented. Molecular band systems, atomic lines, free-bound, and free-free continua are considered for the principal radiating species of shock heated carbon dioxide. A limited amount of data pertinent to the species in the ablation layer is also included. The assumption is made that the Venus atmosphere so closely approximates pure CO_2 that the inviscid layer radiation is due almost entirely to thermally excited CO_2. The only exception is the inclusion of data on the Violet band system of CN. For the principal contributors, recommendations are made as to best property values for radiative heating calculations. A review of the basic equations and the relationships of the various emission-absorption gas properties is also included.

INTRODUCTION

Calculations of radiative heat transfer to an entry vehicle require a determination of the concentration of gas species in the shock layer and the radiative contribution of all major species. Such calculations are therefore dependent on inputs of the radiative properties of each species to be considered. These radiative properties, variously presented as cross section, oscillator strength (f-number), transition moment, transition probability, radiative lifetime, absorption coefficient, etc. are based on fundamental atomic structure and, ideally, could be calculated. For some cases calculations are in fact available, which are sufficiently accurate for radiative heating calculations. For most cases, however, no satisfactory calculations have as yet been undertaken, and resort must be made to experimental determinations. A large number of such experimental measurements have been made and reported in the literature in the past decade for many gas species with emphasis on the gas species which are present in shock heated air; but the gases prevalent in the atmospheres of the other planets have also been treated to a lesser degree.

In the present paper, entry into the atmosphere of the planet Venus is considered. For direct entry, radiative heating is approximately equivalent to convective heating. Thus, heating calculations must consider the radiative contribution in some detail, and such calculations require inputs of the radiative properties not only

of the inviscid layer species, but also the major species of the ablation layer.

The lower atmosphere of Venus is presently believed to consist almost entirely of carbon dioxide. Reference 1, for instance, concludes that carbon dioxide comprises about 97 percent or more by volume of the lower atmosphere, with nitrogen as the next most abundant gas. The radiation spectrum from the shock layer of a Venus probe would therefore be expected to be dominated by species resulting from shocked CO_2, with contributions from CN, NO, or nitrogen playing a lesser role.

For most of the gas species expected to be present in the shock layer, experimental determinations of the radiative properties are reported in the literature, and for some of these species, the number of experiments reported is rather large. The disagreement of the various reported values is also frequently large and is an indication of the difficulty of such experiments and the differing assumptions which were made in order to reduce the data. Thus, different calculations of shock layer radiation may vary considerably as a result of using the various reported values for the radiative properties available in the literature.

The present work compiles and compares the radiative property data that are available in the open literature for Venus entry shock layer radiation. Recommendations are then made as to best

values to use in radiative heating calculations, based on what are believed to be the most accurate data. To some degree the species of the ablation layer have also been considered, but comparatively little data are available. For example, data for several species thought to be emitted from phenolic carbon heat shields could not be found.

No clear cut criteria were apparent to determine what radiating species ought to be included. Species included herein are normally considered in various radiative computational programs. But other species might well be included if data were available. The primary list of radiators considered is:

Molecular Band Systems

C_2 Swan

CO Fourth Positive

CO^+ Comet Tail

CN Violet

CH A-X, B-X, C-X

CF

C_3

Atomic Lines

C

O

Free-Bound Continua

C

O

C+

C-

O-

Free-Free Continua

Electron-ion

Electron neutral

The band systems of CH, CF, and C_3 are included because, for certain ablator materials, these will play important roles in the ablation layer. C_2 Swan band system may also be expected to be more important in the ablation layer than in the shock layer. Summaries of the literature found for other band systems, which have been considered of secondary importance, are contained in the appendix. However, there is no conclusive basis to identify each radiation species as being of primary or secondary importance.

SYMBOLS

A	a neutral atom
A^+	a singly ionized atom
A_{UL}	Einstein coefficient for spontaneous emission
$A_{v'v''}$	Einstein emission coefficient for a vibrational band
$A_{v'}$	summation of $A_{v'v''}$ over all lower vibrational states, $= \sum_{v''} A_{v'v''} = \frac{1}{\tau}$
c	velocity of light
D_o	molecular dissociation energy
d	total degeneracy
E	energy of atomic state
e	electronic charge
e^-	electron
f_{el}	absorption electronic oscillator strength
$f_{v'v''}$	absorption band oscillator strength
$f_{J'J''}$	absorption rotational line oscillator strength
G	Gaunt factor
g	statistical weight
h	Planck constant
I	energy radiated per unit solid angle per second in a transition
I_o	ionization energy

$I_{v'v''}$	energy radiated per unit volume per unit solid angle per second in a vibrational band transition
J	total angular momentum quantum number
j	volume emission coefficient
k	Boltzmann constant
k_ν	spectral absorption coefficient
M	magnetic quantum number
M_e	electric dipole moment of a molecule
m_e	electron rest mass
N	number of particles per unit volume
n	principal quantum number in an atom
p	parity substates due to Λ - doubling
Q	internal partition function
$q_{v'v''}$	Franck-Condon factor
R_{rad}	portion of total dipole moment which includes vibration and electronic motion
$R_e(r)$	electronic transition moment of a band system
R_Y	Rydberg constant
r	internuclear separation distance
$\bar{r}$	r-centroid
r_μ	position vector of particle from center of mass
S	electron spin quantum number
$S_{J'J''}$	Hönl London factor
s	parameter in equation 42

T	temperature
$\bar{V}$	vector velocity of particle relative to center of mass
X	matrix element of electric dipole moment
Z	nuclear charge
Z_{eff}	effective nuclear charge in electron-neutral interaction
α	parameter in equation 41
$\delta_{0,\Lambda}$	Kronecker symbol. $\delta_{0,\Lambda} = 0$ if $\Lambda \neq 0$, $\delta_{0,\Lambda} = 1$ if $\Lambda = 0$
ε_0	permittivity of free space
Λ	quantum number of the angular momentum of the electrons about the internuclear axis
λ	wavelength, nanometers
λ_{th}	threshold wavelength for photoionization
μ	number of particles in an interacting system
ν	frequency
Σ	quantum number of electron spin component in the direction of the internuclear axis
σ	cross section
$\sigma_{n,f}$	free-bound cross-section from quantum number n level
σ_n	free-bound cross-section for hydrogenic model
σ_{th}	threshold photoionization cross section
τ	radiative lifetime
τ_e	element of configuration space
ψ	wave function

Subscripts

Following standard notation, prime denotes upper state, double prime denotes lower state of a molecular transition

A	refers to atom
e^-	refers to electron
f	free (unbound electron) state
J	rotational quantum number
n	bound state principal quantum number
U, L	generalized notation for upper and lower states respectively of a transition
v	vibrational quantum number
μ	refers to each fundamental particle in an interacting system.

The International System of Units (SI) is used for all physical quantities in the present study except where specifically noted. Conversion of the equations to cgs units may be accomplished by removing the term $4\pi\varepsilon_0$, which as been left intact in the equations.

BASIC RELATIONSHIPS

Once the thermodynamic properties (temperature, density, species concentration) are known at each point in the shock layer, the radiative heating can be calculated from the equation of transfer. The solution of this equation requires, in addition, knowledge of the total absorption by the shock-layer gas at each point. This latter quantity in turn is obtained by summing over each radiative absorption process of each species which contributes at the frequency of interest. In other words, the volumetric or linear absorption coefficient, k_ν, of the shock layer gas is given by

$$k_\nu = \sum_i \sum_p \nu i,p$$

where the subscript i denotes a particular species and p signifies a radiative absorption process. It is often easier and more convenient to work with the absorption cross-section σ_ν rather than k_ν since much of the dependence upon temperature is eliminated. These two quantities are related through the expression

$$k_{\nu,i,p} = N_{i,L}\sigma_{\nu,i,p}$$

where N_L represents the total number of absorbing particles of species i per unit volume. Those radiative processes making a contribution to the absorption in a high temperature shock layer include discrete transitions in atoms, ions, and molecules (including

individual rotational lines, collections of lines comprising a band, and groups of bands forming a band system), photoionization (atomic and molecular), which is also commonly referred to as a bound-free transition, and free-free transitions or bremsstrahlung. For each radiative process, there are a great many species that could be considered. However, in this report, attention has been restricted to those species and radiative processes which are important in the inviscid and ablation layers for Venusian entry. In addition, the radiative processes that contribute between the frequencies of about 2 to 12ev (wavelength range 100-600 nm) are emphasized. These limits, although somewhat arbitrary, were selected because for temperatures typical of Venusian entry trajectories most of the energy is contained within this spectral interval.

The spectral absorption coefficient k_ν or the more fundamental quantity, the absorption cross-section, σ_ν, can be obtained experimentally or be calculated by recourse to the theory of quantum mechanics. Both procedures are extensively employed, and in many instances, they are used together, with experiment providing values for those parameters that are not possible or practical to calculate with present technology. In the following paragraphs, a brief outline is given of the quantum theory for calculating absorption coefficients, and how these theoretical relations are employed to interpret the experimental measurements.

Line Radiation

The radiation emitted when electronically excited atoms undergo transitions to lower levels gives rise to line radiation of frequency ν_{UL} in which the photon energy of such a transition is

$$h\nu_{UL} = E_U - E_L \tag{1}$$

The intensity of the line is given by

$$I_{UL} = \frac{1}{4\pi} N_U A_{UL} h\nu_{UL} \tag{2}$$

Since

$$\frac{N_U}{N_L} = \frac{g_U}{g_L} \exp\left(\frac{-h\nu_{UL}}{kT}\right) \tag{3}$$

equation (2) becomes

$$I_{UL} = \frac{N_L}{4\pi} \frac{g_U}{g_L} A_{UL} h\nu_{UL} e^{-\left(\frac{h\nu_{UL}}{kT}\right)} \tag{4}$$

The relationship between the spontaneous transition probability and the absorption oscillator strength, or f-number is (ref. 2)

$$A_{UL} = \frac{g_L}{g_U} \frac{8\pi^2 e^2 \nu_{UL}^2}{4\pi\varepsilon_o m_e c^3} f_{LU} \tag{5}$$

Also, since

$$N_L = \frac{N}{Q} g_L e^{-E_L/kT}$$

the integrated absorption coefficient for an individual atomic line may be written as

$$\int k_\nu d\nu = \frac{N}{Q} e^{-E_L/kT} \frac{g_L f_{LU}}{4\pi\varepsilon_o} \frac{\pi e^2}{mc \nu_{UL}^3} \left(1 - e^{-\left(\frac{h\nu_{UL}}{kT}\right)}\right) \qquad (6)$$

where equations 4 and 5 have been combined and used in Kirchoff's law:

$$I_{UL} = \int k_\nu B_\nu d\nu = B\nu_{LV} \int k_\nu d\nu$$

Equation 6 gives no information about the spectral profile of the line.

Spectral line profiles are dependent on the state of the gas in which the line is emitted (pressure, temperature, electron density, etc.). The inclusion of the important line broadening mechanisms into a prediction of half-widths for polyelectronic atoms is very complicated, and usually has a significant degree of uncertainty. However, in high temperature plasmas, the energy contained in the wings of the lines is of importance and broadening must be accounted for. Due to the wide ranges of the various parameters that affect line shapes, and the complexity of the pertinent theories, no description of this aspect of line radiation will be included here. State-of-the-art discussions of this problem may be found, for

example, in the texts by Penner, Griem, and Armstrong and Nicholls (ref. 2-4).

Diatomic Molecular Systems

The absorption strength of a diatomic molecular band system is generally stated in terms of an overall electronic absorption oscillator strength f_{el} which is frequently treated as a constant fo the band system. This concept for molecular systems derives dire by analogy to its use in the integrated absorption intensity of a single line transition. This extension has been criticized by several investigators (Schadee, ref. 5, Wentink, ref. 6 and 7, and Tatum, ref. 8) since it introduces ambiguities. These investigators also indicate that use of a single f_{el} value for an entire band system has little real meaning. To appreciate these comments fully, it is first necessary to understand how the band system oscillator strength is obtained. This derivation is briefly outlined below, employing the notation adopted by Schadee.

To define an electronic oscillator strength for a band system we begin with the oscillator strength for an individual rotational line and then sum this expression over all rotational lines in a given band and over all bands comprising a band system. The f-number for absorption from lower rotational state J" to upper state J' is given by (e.g. ref. 5 and 9)

$$f_{J'J''} = 4\pi\varepsilon_o \frac{me\ c\ \lambda^2_{J'J''}}{8\pi^2\ e^2} \frac{d_{J'}}{d_{J''}} A_{J'J''} \qquad (7)$$

where $\lambda_{J'J''}$ is the wavelength of the transition, $d_{J'}$ and $d_{J''}$ the upper and lower state degeneracies, respectively, and $A_{J'J''}$ is Einstein's coefficient for spontaneous emission. According to quantum theory and the Born-Oppenheimer approximation (ref. 9), the Einstein spontaneous emission coefficient for a diatomic molecule is written as

$$A_{J'J''} \frac{64\pi^4}{4\pi\varepsilon_c 3h \lambda^3_{J'J''}} \frac{R_{rad} S_{J'J''}}{d_{J'}} \tag{8}$$

where $S_{J'J''}$ is the Hönl-London (HL) factor (ie., rotational line intensity factor) and R_{rad} is the portion of the dipole moment that involves the vibrational and electronic motions. In more explicit terms, this quantity becomes

$$R_{rad} = \sum \left| \int \psi_{v'} R_e(r) \psi_{v''} dr \right|^2 \tag{9}$$

with

$$R_e(r) = \int \psi_{v'} M_e \psi_{v''} d\tau_e \tag{10}$$

and the summation being over all degenerate levels of the upper and lower states of the transition. $R_e(r)$ is commonly referred to as the electronic transition moment, and as implied by the functional notation, generally varies with internuclear separation distance, r. M_e is the dipole moment.

Several types of degeneracy occur in a diatomic molecule. The first is the rotational degeneracy associated with the magnetic quantum number M (M = -J, -J + 1, ... , J). In the absence of a magnetic field, these 2J + 1 levels coincide. A second degeneracy is the Λ doubling of each rotational line in molecules whose electronic angular momentum $\Lambda \neq 0$. This splitting is due to a finer interaction between the rotational and electronic motions. The two Λ components are rarely resolved and thus lead to a degeneracy of $2 - \delta_{0,\Lambda}$. The (2S + 1) electronic-spin multiplicity of an electronic state is usually treated as a (2S + 1)- fold degeneracy since the energy differences of the resulting substates is small in most cases. Schadee (ref. 5) uses the symbolism M, p, and Σ to distinguish these three degeneracies and the same notation is employed here.

The Hönl-London factors obey a sum rule, but because different normalizations have been employed, many tabulations of HL-factors differ to within a constant factor. (See ref. 5, 8, and 9). Each normalization implies a slightly different treatment of rotational statistical weights. The normalization used in this report is (ref. 5)

$$\sum_{\Sigma'\Sigma''} \sum_{J''} S_{J'J''} = (2S + 1)(2J' + 1) \qquad (11)$$

or in other words, the sum of the HL-factors for all transitions from the levels with equal J' is equal to the number of initial sublevels. The factor $(2 - \delta_o)$ does not appear in equation (11) because $S_{J'J''}$ as defined in equation (8) represents the average angular

factor for the two Λ components.* It is important to emphasize that with this normalization, the HL-factors, transition probabilities, and oscillator strengths, of the two Λ components are always equal. Intensities, and such phenomena as intensity alterations in homonuclear molecules, are governed by the populations of the component levels. Tatum, (ref. 8), provides an excellent discussion, with several examples, of how to incorporate properly the electronic and rotational degeneracies when calculating level populations.

When equations (8), (9), and (10) are combined with equation (7), the result becomes

$$f_{J'J''} = \frac{8\pi^2 m_e c}{3he^2 \lambda_{J'J''}} \frac{\sum_{p'p''} \sum_{\Sigma'\Sigma''} | R_{ev'v''} |^2}{(2 - \delta_{o,\Lambda''})(2S'' + 1)} \frac{S_{J'J''}}{(2J'' + 1)} \qquad (12)$$

The quantity $\sum | R_{ev'v''} |^2$ is another way of representing equation (9). If the interaction between the rotation and electronic-vibrational motions is negligible, and in most cases this interaction can be safely neglected, $\sum | R_{ev'v''} |^2$ is the same for each rotational line of the band (v',v''). Equation (12) may then be summed over all rotational transitions and averaged over the substates to yield a band oscillator strength as follows:

---

*Schadee (ref. 5) gives a bibliography of HL-factors for various molecular transitions.

$$f_{v'v''} = \frac{8\pi^2 m_e c}{3he^2 \lambda_{v'v''}} \frac{\sum |R_{ev'v''}|^2}{(2 - \delta_{o\Delta''})(2S'' + 1)} = \frac{m_e c \lambda_{v'v''}^2}{8\pi^2 e^2} \tag{13}$$

$$\frac{(2 - \delta_{o,\Lambda'})(2S' + 1)}{(2 - \delta_{o,\Lambda''})(2S'' + 1)} A_{v'v''}$$

In performing this summation, the ratio $\frac{\lambda_{v'v''}}{\lambda_{J'J''}}$ was taken as unity. This ratio deviates from unity only slightly in nearly all cases, and thus introduces little error.

Equation (13) cannot, in general, be simplified further. However, if the electronic and vibrational motions are strictly independent, which is equivalent to stating that R_e is not a function of r, the electronic transition moment can be removed from the integral in equation (9), substitution of this approximation into equation (13) gives

$$f_{v'v''} = \frac{8\pi^2 m_e c}{3he^2 \lambda_{v'v''}} \frac{q_{v'v''} \sum R_e^2}{(2 - \delta_{o\Lambda''})(2S'' + 1)} \tag{14}$$

where $q_{v'v''}$ is the square of the vibrational overlap integral or, as it is more commonly referred to, the Franck-Condon factor. This parameter specifies the vibrational contribution to the total transition probability. To obtain an oscillator strength characteristic of a band system, equation (14) is summed over all vibrational bands. In performing this manipulation, the $\lambda_{v'v''}$ are replaced by a

reference wavelength, (usually that of the 0-0 transition λ_{0-0}) and factored from the summation. When the sum rule

$$\sum_{v'} q_{v'v''} = \sum_{v''} q_{v'v''} = 1$$

is applied, there results

$$f_{el} = \frac{8\pi^2 m_e c}{3he^2 \lambda_{00}} \frac{\sum R_e^2}{(2 - \delta_{o\Lambda''})(2S'' + 1)} \qquad (15)$$

and upon combining with equation (14)

$$f_{el} = f_{v'v''} \frac{\lambda_{v'v''}}{\lambda_{00} q_{v'v''}} \qquad (16)$$

a form that is frequently seen in the literature.

There are two obvious shortcomings associated with equation (16). In band systems which encompass a wide frequency interval, replacement of $\lambda_{v'v''}$ by the reference wavelength λ_{00} can lead to errors. A second error arises from use of a constant R_e^2 value for the entire band system. It has now been established for many band systems that the interaction between the vibrations and electronic motions is appreciable, thus making the electronic transition moment dependent on the vibrational transition. This variation, as well as that of the wavelength, makes it difficult to define a meaningful overall electronic oscillator strength. Despite these limitations, equation (16) continues to be employed since it provides a convenient and simple means for estimating the absorption strength of band systems.

When the electronic-vibrational interaction is non-negligible, the factorization shown in equation (14) can still be achieved by means of the r-centroid approximation, a concept based on the Franck-Condon principle and first introduced by Jarmain and Fraser (ref. 10). In this approximation, the electronic transition moment is evaluated at the r-centroid, $\bar{r}_{v'v''}$, defined as the internuclear separation of atomic nuclei at which the electronic-vibrational transition occurs. This quantity, along with $q_{v'v''}$, may be calculated from the vibrational wavefunctions, but it is not yet feasible for many-electron molecules to establish theoretically the relationship between $\sum R_e^2$ and $\bar{r}_{v'v''}$. For several transitions, this relation has been determined experimentally from measured vibrational band intensities (see, for example, the survey by Schadee). When this dependence is known and is employed in conjunction with equation (14), it is preferable to use of equation (16).

Nicholls (ref. 11) has shown on the basis of a Morse approximation to the potential function that $\bar{r}_{v'v''}$ is a unique and monotonic function of $\lambda_{v'v''}$. As a consequence, one may also expect $\sum R_e^2$ to be a unique function of $\lambda_{v'v''}$. The computations made by Schadee (ref. 5) tend to confirm this expectation. Because of this relationship between $\sum R_e^2$ and $\lambda_{v'v''}$, Schadee concludes that it is meaningful to define

$$f_{el}(\lambda) \equiv \frac{8\pi^2 m_e c}{3he^2 \lambda} \frac{\sum R_e^2(r)}{(2 - \delta_{o\Lambda''})(2S'' + 1)} \qquad (17)$$

as a wavelength dependent electronic f-number, rather than try to establish a constant overall oscillator strength. With better potential approximations, such as RKR, the $f_{el}(\lambda)$ values may deviate slightly from the mean value defined by equation (17). However, for transitions where calculations based on both the Morse and RKR potentials are available, the difference between $f_{el}(\lambda)$ results is generally less than 10 percent. Such a discrepancy falls within the limits of observational accuracy, and equation (17) is still a meaningful definition. In this report, we present electronic oscillator strengths according to equation (17) since this form directly accounts for the explicit wavelength variation of f_{el} as well as the wavelength dependence implicit in $\sum(R_e)^2$. Whenever sufficient experimental data were available, we have also constructed empirical formulas which express f_{el} as a function of wavelength. This form should be particularly useful in radiative transport calculations, or other applications, since knowledge of the r-centroids is not required.

A comparison of equation (17) with equation (14) shows that the electronic oscillator strength f_{el} can be obtained from measured vibrational band oscillator strengths $f_{v'v''}$ by division by the appropriate Franck-Condon factor; that is

$$f_{el}(\lambda) = \frac{f_{v'v''}}{q_{v'v''}} \qquad (18)$$

For bands where $f_{v'v''}$ is unavailable, the known variation of the electronic transition moment with $\bar{r}_{v'v''}$ can be used directly in equation (14) to calculate f_{el}. As pointed out previously, a priori calculations of $\sum R_e^2$ have not yet proven feasible in a multi-electron molecule. Consequently, $\sum R_e^2$ must be determined through suitable experimentation. The techniques frequently employed involve measurements of radiative lifetimes τ of excited vibrational levels, measurements of the total power emitted per unit volume $I_{v'v''}$ by a vibrational band, and the integrated absorption $\int k_\nu d\nu$ of selected rotational lines within a vibrational band. These quantities are related to the electronic transition moment through Einstein's coefficient for spontaneous emission, $A_{v'v''}$ as follows:

$$I_{v'v''} = \frac{1}{4\pi} N_{v'} A_{v'v''} h\nu_{v'v''} \tag{19}$$

$$\frac{1}{\tau} = \sum_{v''} A_{v'v''} \equiv A_{v'} \tag{20}$$

$$\int k_\nu d\nu = \frac{\pi e^2}{4\pi\varepsilon_o m_e c} N_{J''} f_{J'J''} \left(1 - e^{-\frac{h\nu_{J'J''}}{kT}}\right) \tag{21}$$

where the induced emission term has been incorporated.

Although the above equations are written in terms of frequency, hereafter, following common practice, wavelength is used. Thus, the relations for $A_{v'v''}$ and $f_{J'J''}$ are

$$A_{v'v''} = \frac{64\pi^4}{4\pi\varepsilon_o 3h} \frac{1}{\lambda^3_{v'v''}} \frac{q_{v'v''} \sum R_e^2(r)}{(2 - \delta_{0\Lambda'})(2S' + 1)} \qquad (22)$$

and

$$f_{J'J''} = f_{el}(\lambda_{v'v''})\, q_{v'v''} \frac{\lambda_{v'v''}}{\lambda_{J'J''}} \frac{S_{J'J''}}{(2J'' + 1)} \qquad (23)$$

which follows from equations (12), (13), (17), and (18).

Although the above parameters are directly related to $\sum R_e^2$ (or equivalently $f_{el}(\lambda)$), its determination is not without difficulty. Approximations needed to obtain $\sum R_e^2$ can strongly influence the accuracy of the final result. In emission and absorption measurements, perhaps the biggest difficulty is accurate specification of the number of absorbing or emitting particles per unit volume (ie., $N_{v'}$ or $N_{J''}$). This requires determination of state properties and the assumption that local thermodynamic equilibrium conditions prevail so that the fraction of molecules in a given energy may be calculated according to the Boltzman distribution. Furthermore, the total number of molecules of a particular type must also be known. This quantity can be obtained from energy conservation principles, provided the molecule's dissociation energy is known. Uncertainties in this latter parameter can strongly influence the value deduced for the electronic transition moment.

The value of $\sum R_e^2$ inferred from radiative lifetime measurements is independent of the dissociation energy because in this method, one only monitors the relative change, with time, of the

excited state population. The time constant for this decay is the inverse of the radiative lifetime which is connected to $\sum R_e^2$ through equations (20) and (22). Equation (20) demonstrates that the measured decay time involves the total spontaneous transition from the excited state v' to all lower states v''. To obtain $A_{v'v''}$ for a particular vibrational transition, information about vibrational branching ratios (ie., how $A_{v'}$ is partitioned among the $A_{v'v''}$) is needed. But this requires, at least, knowledge of the relative variation of $\sum R_e^2$ between vibrational bands, which is not known a priori. To circumvent this difficulty approximate vibrational branching ratios, expressed in terms of the Franck-Condon factors which are more readily calculated, are often employed. These quantities are obtained by substituting equation (22) into equation (20) yielding

$$A_{v'} = \sum_{v''} A_{v'v''} = 4\pi\varepsilon_o \frac{64\pi^4}{3h} \frac{1}{(2 - \delta_{o\Lambda'})(2s' + 1)} \sum_{v''} \lambda_{v'v''}^{-3}. \qquad (24)$$

$$q_{v'v''} \sum R_e^2(\bar{r}_{v'v''})$$

If $\sum R_e^2(\bar{r}_{v'v''})$ is assumed to be constant, it can be factored from the summation to give

$$A_{v'} = 4\pi\varepsilon_o \frac{64\pi^4}{3h} \frac{\langle \sum R_e^2 \rangle}{(2 - \delta_{o\Lambda'})(2s' + 1)} \sum_{v''} \lambda_{v'v''}^{-3} q_{v'v''} \qquad (25)$$

where $\langle \sum R_e^2 \rangle$ represents the average value of $\sum R_e^2$. The combination of equations (25) and (22) with the same assumption, then results in

$$\frac{A_{v'v''}}{A_{v'}} = \frac{\lambda_{v'v''} \, q_{v'v''}}{\sum_{v''} \lambda_{v'v''}^{-3} \, q_{v'v''}} \tag{26}$$

or in terms of the measured lifetime

$$A_{v'v''} = \frac{1}{\tau} \frac{\lambda_{v'v''}^{-3} \, q_{v'v''}}{\sum_{v''} \lambda_{v'v''}^{-3} \, q_{v'v''}} \tag{27}$$

The band absorption oscillator strength follows immediately from equation (13)

$$f_{v'v''} = 4\pi\varepsilon_o \frac{m_e c}{8\pi^2 e^2} \frac{1}{\lambda_{v'v''}} \frac{(2 - \delta_{o\Lambda'})(2s' + 1)}{(2 - \delta_{o\Lambda''})(2s'' + 1)} \frac{1}{\tau} \frac{q_{v'v''}}{\sum_{v''} \lambda_{v'v''}^{-3} \, q_{v'v''}} \tag{28}$$

and the corresponding electronic oscillator strength is

$$f_{el}(\lambda) = \frac{f_{v'v''}}{q_{v'v''}} = 4\pi\varepsilon_o \frac{m_e c}{8\pi^2 e^2} \frac{1}{\lambda_{v'v''}} \frac{(2 - \delta_{o\Lambda'})(2s' + 1)}{(2 - \delta_{o\Lambda''})(2s'' + 1)} \tag{29}$$

$$\frac{1}{\tau} \frac{1}{\sum_{v''} \lambda_{v'v''}^{-3} \, q_{v'v''}}$$

It should be noted that equation (29) is essentially equivalent to equation (16) since a constant value for $\sum R_e^2$ has been assumed. Although this equation is frequently used in the literature for

converting radiative decay times to electronic oscillator strengths, it should, of course, be applied only to those transitions for which the conditions of its validity are reasonably met.

Equation (29) can be simplified further for electronic band systems where the wavelength variation along a v'' progression is small or the vibrational bands in the progression decrease rapidly in intensity (ie., a nearly vertical transition in which $v' = v''$).* For these cases, the factor $\lambda_{v'v''}^{-3}$ can be replaced by an average value and removed from the summation. Application of the vibrational sum rule, $\sum_{v''} q_{v'v''} = 1$, then gives

$$f_{el} \simeq 4\pi\varepsilon_o \frac{m_e c}{8\pi^2 e^2} \lambda_{ave}^2 \frac{(2 - \delta_{\quad})(2s' + 1)}{(2 - \quad_{v''})(2s'' + 1)} \frac{1}{\tau} \qquad (30)$$

The CH molecule is an example where this equation can be used with some degree of confidence. Equation (30) is frequently employed to define an effective f_{el} for electronic transitions where it does not strictly apply.

The lifetime technique can also supply information about the transition moment variation by measuring τ for several excited states. This is generally accomplished by replacing $\sum R_e^2(\bar{r}_{v'v''})$ in equation (24) with a truncated Taylor series expansion, and

---

*For these transitions, only the diagonal elements of the Franck-Condon factor array have appreciable values whereas the off-diagonal elements are zero or nearly equal to zero.

using the experimental values of τ in conjunction with calculated Franck-Condon factors to solve for the unknown coefficients.

Free-Bound Radiation

As its name implies, free-bound radiation occurs when a free electron combines with an ion and excess energy is emitted as a photon:

$$A^+ + e^- \rightarrow A + h\nu$$

Such processes are also referred to in the literature as recombination radiation and the inverse process as photoionization.

For a hydrogen-like atom the absorption cross-section (for the inverse process above) may be expressed by a relatively simple equation (see, for example, ref. 2):

$$\sigma_n = \frac{64\pi^4}{3\sqrt{3}} \frac{e^{10} m_e Z^4 \lambda^3 G}{(4\pi\varepsilon_o)^5 h^6 c^4 n^5}, \qquad \lambda \leq \lambda_{th} \qquad (31)$$

when λ is in nm. Here σ_n is the cross-section for photoionization from the nth quantum level, and exists only for wavelengths less than the threshold wavelength, λ_{th}.

In order to extend the above to nonhydrogenic species, several factors should be taken into consideration. For the absorption process, only allowed transitions between the parent atom and its ion should be included. In addition, the hydrogenic formula (eq. 31) is inaccurate for transitions involving the ground state and lower-lying levels of the parent atom. It becomes increasingly more applicable for higher levels, or increasing values of n.

As in done in reference 12 an effective Z^2 is defined by

$$Z^2_{eff} = n^2(E_u - E_\ell)/R_Y \qquad (32)$$

The cross-section then becomes

$$\sigma_n = \frac{16}{3\sqrt{3}} \frac{Ge^2}{4\pi\varepsilon_o c^2 m_e} \frac{\lambda^3 (E_U - E_L)^2}{n} \qquad (33)$$

where the value of the Rydberg constant $\left[R_Y = 2\pi^2 m_e \frac{e^4}{h^3 c\ (4\pi\varepsilon_o)^2}\right]$ has been used. For the hydrogen-like particle of ionization energy I_o,

$$\sigma_n = \frac{16}{3\sqrt{3}} \frac{Ge^2}{4\pi\varepsilon_o c^2 m_e} \frac{\lambda^3 I_o^2}{n^5} \qquad (34)$$

The absorption coefficient is found by summing the product of σ_n and the particle number density of level n:

$$k_\nu = \sum_n N_n \sigma_n = \frac{N}{Q} \frac{32}{3\sqrt{3}} \frac{Ge^2 I_o^2}{4\pi\varepsilon_o c^2 m_e} e^{-I_o/kT} \sum_n \frac{1}{n^3} e^{-I_o/n^2 kT} \qquad (35)$$

where the approximate hydrogenic upper level degeneracy, $g_n = 2n^2$, has been used.

For purposes of shock layer transfer calculations, the above formulation is considered adequate for C and O atoms for $n \geq 3$. This applies to the wavelength range from the near UV into the IR. In this range other processes are generally more important (lines, bands, and ionic free-free). Comparison of the hydrogenic cross-sections

with more exact computations for C-atoms are given in reference 13, where equation (35) gives absorption coefficients that deviate from the detailed calculations by no more than 45 percent between 300 and 600 nm.

As with the other radiative processes, detailed quantum theory calculations are difficult, and when extensive transfer calculations are to be made, a measure of empiricism is desirable. This is particularly important for the lower-lying levels--the deviation from hydrogenic cross-sections is most severe, and for high temperatures these levels are among the most important contributors. Recourse to quantum theory for individual cross-sections with subsequent development of empirical formulas appears to be the most expedient way of handling the problem.

For a photoionization process, quantum theory gives the following formula for the cross-section (ref. 14):

$$\sigma_{nf} = \frac{8\pi^3}{3\lambda} \frac{1}{g_n} \sum_n \sum_f \left| \int \psi_f^* \sum_\mu \left(e_u \, r_\mu \right) \psi_n \, d\tau' \right|_e \qquad (36)$$

where ψ_n is the wave function for the initial state of statistical weight g_n. ψ_f is the wave function for the final state of the original particles in which one of the electrons is free. The charge of the μth particle of the system is e_μ and r_μ is the position vector of the particle with respect to the system center of mass.

The major part of the problem is embodied in the evaluation of the dipole matrix elements

$$X_{nf} = \int \psi_n^* \sum_\mu \left(e_\mu r_\mu \right) \psi_f \, d\tau' \qquad (37)$$

The above formulation is referred to as the dipole length. An equivalent expression

$$X_{nf} = \frac{h^2}{4\pi^2 m_e E_{nf}} \int \psi_f^* \sum_\mu (e_\mu \bar{V}_\mu) \psi_n \, d\tau' \qquad (38)$$

is called the dipole velocity formulation.

The various detailed calculations of specific cross-sections involve a number of assumptions about the wave functions and the potential function which appears in the Schrödinger equation. It is not reasonable here to go into detail on these aspects, but rather to present results of a number of the calculations for comparison among themselves and with experiment.

Free-Free Radiation

Free-free radiation arises as a result of the process

$$A + e^- \rightarrow A + e^- + h\nu$$

$$A^+ + e^- \rightarrow A^+ + e^- + h\nu$$

in which a free electron, e^-, interacts with the coulomb field of another particle, A. The consequent change in energy of the electron results in an emitted photon. The cross-section for the process is normally evalueated in units of cm^5, which when multiplied by the

number density product $N_A N_e$- yields the linear absorption coefficient in reciprocal centimeters. Detailed quantum-mechanical calculations of these cross-sections are complex. An excellent procedural outline on such calculations is given in the text by Armstrong & Nicholls, reference 4.

The classical expression for the emission cross-section of a free electron accelerated in the field of a particle of charge Z was developed by Kramers (see, for instance, ref. 2) and may be written:

$$\sigma_{ff} = 4\pi\varepsilon_o \frac{16\pi^2}{3\sqrt{3}} \frac{e^6}{hc^4 (2\pi m_e)^{3/2}} \frac{\lambda^3 Z^2}{(kT)^2} \qquad (39)$$

For λ in nm and T in degrees of K,

$$\sigma_{ff} = 1.35(10)^{-43} \frac{\lambda^3 Z^2}{T^{\frac{1}{2}}} \text{ cm}^5 \qquad (40)$$

The corresponding emission coefficient is

$$j_{ff} = 1.63\text{x}10^{-34} \frac{N_e N_A Z^2}{\lambda^2 T^{\frac{1}{2}}} \exp\left(\frac{-14388000}{\lambda T}\right) \qquad (41)$$

for λ in nm. For electrons interacting with ions, this expression appears to give reasonable results, (ref. 14a) and is considered to be sufficiently accurate for shock layer transfer calculations.

For electrons interacting with neutral particles, it is tempting to measure or deduce an effective Z^2 for the particle in question, and apply the Kramers equation, 40. This may be done to give rough

order-of-magnitude cross-sections for a limited temperature and frequency range. This has been done in reference 15 over an extensive λ, T range, but might be justified by the fact that free-free radiation from neutrals is not a significant process in the high-temperature radiance of equilibrium gas mixtures.

DISCUSSION AND RECOMMENDATIONS

Molecular Band Systems

C_2 Swan Band System $d^3\Pi_g \leftrightarrow a^3\Pi_u$

Both experiment and calculation have been used to obtain oscillator strengths for this well-known band system of diatomic carbon. Table I summarizes the experimental measurements, (ref. 16-25), and the calculated values are presented in Table II, (ref. 26-31).

The experimental techniques which have been employed to measure the f-number include furnaces (emission and absorption), shock tubes (incident shock and reflected shock, emission and absorption), and lifetime measurements (phase-shift and laser excitation). All the available data, experimental and calculated, are presented in figure 1. The experimental values of f_{el} extend from 0.006 to 0.043 while the calculations span a range from 0.024 to 0.24.

Note that most of the experimental data were evaluated at the 0-0 bandhead at 516 nm (all the calculated values in Table II used approximately this wavelength). There is relatively little information regarding the variation with wavelength. Five of the most recent and most through sources (ref. 7, 19, 21-23) report values of the f-number between 0.025 and 0.035 at the 0-0 bandhead. The correct value surely lies within this range. We have elected to select the mean of this range and recommend $f_{el}(0,0) = 0.030$.

As noted previously, only very limited data are available to indicate the variation of f-number with wavelength. Mentall and Nicholls, reference 32, and Jeunehomme and Schwenker, reference 16, have each developed empirical expressions for the variation of the transition moment with internuclear separation. These two relations differ slightly but are in essential agreement. The Mentall and Nicholls relation was used with the r-centroid values of reference 33 to determine the wavelength variation of oscillator strength, and this in turn was normalized to $f_{el}(0,0) = 0.30$. The result is shown in figure 1. As Arnold, reference 19, points out, this method gives good relative agreement with his measurements at the $\Delta v = 0$ and $\Delta v = 1$ sequences. A simple expression that adequately defines this wavelength variation,

$$f_{el}(\lambda) = 0.030(516.5/\lambda)^{2.8}$$

(wavelength in nanometers)

is shown on figure 1 and is our recommendation.

CO Fourth Positive Band System $A\,^2\Pi - X\,^1\Sigma^+$ This extensive system in the vacuum ultraviolet is the most important molecular radiator in shock heated carbon dioxide. A number of investigators have reported its radiative properties using a variety of techniques; yet considerable uncertainty remains as to its oscillator strength. The fact that the wavelength region is in the vacuum ultraviolet (110 to 280 nm) adds to the experimental difficulties. When observed in emission, the bands are mostly overlapped. Since the system's lower state is the ground state, it can be observed in absorption, and this technique has been used to advantage. An excellent summary of all carbon monoxide bands is given in reference 34.

Figure 2 summarizes the f-number data available. Hexter (ref. 35) used the crystal field splitting of solid state CO to determine a value of $f_{el} = 0.148$ at the 2,0 band, which is the most intense. In a similar manner Brith and Schnepp (ref. 36) obtained a value of about 0.16. Lassettre and Silverman (ref. 37) used an electron impact technique to obtain $f_{el} = 0.24$. However, this experiment was performed again at higher resolution and a revised value of $f_{v'v''}(2,0) = 0.0429$ obtained. Using their relative intensity measurements, and the fact that $f_{el} = \sum_{v'} f_{v',o}$ they obtained $f_{el} = 0.195$. The prior value of $f_{el} = 0.24$ is not shown on figure 2, but the values for $v' = 0$ to 10 are shown from reference 38. Meyer and Lassettre (ref. 39) altered the experiment of reference 38 to permit measuring the electron impact spectra at zero scattering angle and obtained good agreement with the former result.

Vargin, Pasynkova, and Trekhov (ref. 40) measured the emission from the Fourth Positive band system in an arc discharge in the wavelength region 221 to 230 nm, and determined $f_{el} = 0.079$. Using a phase shift technique, Hesser and Dressler (ref. 41) determined a lifetime of 10 ± 0.5 nanoseconds for the $v' = 2$ transition. In reference 42, they report a revised value of 10.5 ± 1 nanoseconds. In reference 43, Hesser interprets this measurement with the aid of relative emission data to derive $f_{v'v''}$ for $v' = 0$ to 5, $v'' = 0$ to 12. For this data, figure 2 shows $f_{el} = \frac{f_{v'v''}}{q_{v'v''}}$ using the Franck-Condon factors of reference 44.

[illegible]ich, reference 45, used a shock tube to heat CO to about 5000 K, and measured absorption for a number of bands. His reported values of $f_{v'v''}$ have been converted to f_{el} and are shown on figure 2. Jeunehomme (ref. 46) measured a radiative lifetime of 10 ± 2 nsec, in good [illegible]t with other investigators. However, he also performed ex[illegible]ve absorption and relative intensity measurements, shown on [illegible]gure 2, which are higher than other measurements and for which he [illegible] equivalent radiative lifetime of 2.5 ± .2 nsec. This dis[illegible]cy is [illegible]ined, but his absorption measurements were run [illegible]o [illegible]ensity, and wall absorption may have been a problem. Penner, [illegible] [illegible]noir's out that wall absorption of CO can cause large [illegible]s in concentration, even for pressures 100 times greater than [illegible] reference 46.

Radiative lifetime was also measured by Wells and Isler (ref. 47) using a level-crossing technique and they obtained $\tau = 9 \pm 1$ nsec for the $v' = 2$ state. No conversion to f-number was made in reference 47. Chervenak and Anderson (ref. 48) measured lifetimes for the first six vibrational levels ($v' = 0$ to 5) which ranged from 14.3 to 16.6 nsec. They report $f_{v'v''}(0,0) = 0.0097$ which would yield $f_{el} = 0.086$. Their longer lifetimes as compared to references 41, 42, 46 and 47 is unexplained.

The curve-of-growth method was employed by Pilling, Bass, and and Braun (ref. 49), who determined f_{el} for $v' = 3$ to 8 ranging from 0.128 to 0.175. Mumma, Stone, and Zipf, reference 50, using electron collision spectra, determined relative transition probabilities which they converted to an absolute scale by normalizing to other published values. On this basis, they quote $f_{el} = 0.15$. Their transition probabilities have been converted to oscillator strengths and included on figure 2.

Several experimentors have obtained oscillator strengths for this system near $f_{el} = 0.15$. In most of these cases the data were based on measurements on the 2,0 band ($\lambda = 147.7$ nanometers). The variation with wavelength has been studied by several of the investigators, and their findings are in essential agreement. In reference 50, the variation of transition moment with r-centroid was found to be $R_e = R_{e,o}(1 - 0.6\bar{r})$. Jeunehomme's power series in frequency closely

approximated the same result. The recommended curve on figure 2,

$$f_{el} = 0.15 \left(\frac{68}{\lambda - 80} \right)^2$$

(with λ in nanometers) has been selected to go through $f = 0.15$ at 148 nanometers and is in good agreement with the curve fits of references 50 and 46. It is also in general accord with other studies that covered a significant wavelength range. The evidence suggests the correct value of f_{el} lies within $\pm$ 30 percent of the recommended curve.

CO^+ Comet-Tail Band System $A^2\Pi_i - X^2\Sigma^+$ This band system received its name from the fact that it is the most prominent band system observed in the tails of comets. It is also observed in fluorescent spectra from the atmosphere of Venus. The first investigator to present values of the band oscillator strength, $f_{v'v''}$, for a large number of bands was Nicholls, reference 51. He combined radiative lifetime data of Bennett and Dalby, reference 52, with the data of Robinson and Nicholls, reference 53, to obtain absolute values of $f_{v'v''}$. However, the lifetime values of Bennett and Dalby have been challenged by Anderson, Sutherland, and Frey, (ref. 54), whose more recent and presumably better values are significantly larger.

Whereas Nicholls used Franck-Condon factors based on Morse potentials, Jain and Sahni, reference 55, analyzed the data of Robinson and Nicholls using Franck-Condon factors and r-centroids based on RKR potential functions. They then used Nicholls' technique and Bennett and Dalby's radiative lifetime data to calculate absolute values of $f_{v'v''}$.

Spindler and Wentink, reference 56, obtained values of $f_{v'v''}$ from Bennett and Dalby's lifetime measurements by a much more direct technique than that used by Nicholls and Jain and Sahni. Despite the fact that Spindler and Wentink's Franck-Condon factors and r-centroids were calculated using Morse potentials, their work probably constitutes the best reduction of the data of reference 52. The values of $f_{v'v''}$ reported in reference 56 are, in most cases, about double those of Nicholls and Jain and Sahni.

Anderson, Sutherland, and Frey, (ref. 54), calculated $f_{v'v''}$ values from lifetime measurements using a technique described by Anderson, (ref. 57), which is similar to that used by Spindler and Wentink. They used their own lifetime measurements together with unpublished Franck-Condon factors and r-centroids calculated by Albritton* using RKR potentials. Their values generally lie between those of Spindler and Wentink and those of Nicholls and Jain and Sahni, and are believed to be the best currently available. The values $f_{v'v''}$ from reference 54 have been converted to $f_{el}(\lambda) = \frac{f_{v'v''}}{q_{v'v''}}$ using the Franck-Condon factors due to Albritton.

The equation

$$f_{el} = 7.24 \times 10^{-3} \exp[-(7.73 \times 10^{9} + 8.9 \times 10^{-4}\lambda^{5})/\lambda^{4}]$$

has been found to fit the results quite well. This function is shown in figure 3.

It should be noted that although the r-centroid approximation has been questioned by some investigators, its validity for the Comet-Tail System is demonstrated by the results of Krupenie and Benesch, reference 58.

---

*D. L. Albritton; Environmental Research Laboratory, National Oceanic and Atmospheria Administration, Boulder, Colo.

CN Violet Band System $B^2\Sigma^+ \leftrightarrow X^2\Sigma^+$ The violet system of the CN radical has been extensively studied in the past. Recently, Arnold and Nicholls (ref. 59) reviewed the work performed within the past decade, along with making their own measurement of the electronic transition moment. Their results and survey are recapitulated in Table III where, for convenience, the same format employed by them in their Table IV is used. In addition, earlier sources not considered by them have been included. In order to facilitate comparisons between experimenters, the transition data have been converted to a wavelength-dependent electronic oscillator strength.

The results given by Dunham (ref. 60), White (ref. 61 and 62), and Tsang, et al (ref. 63) are probably not too reliable. Dunham stated that his f-value was only tentative since his computed CN concentration was sensitive to the dissociation potential and vapor pressure assumed for carbon, Kudryartsev, (ref. 64), reviewed White's work, (ref. 61), and expressed doubt as to whether the CN concentration was predicted correctly. In a subsequent paper, White, (ref. 62), considered this question, and indicated that his previous estimate for the CN concentration may have been too high by a factor of 3-4 since he failed to account for secondary dissociation of CN by electrical dischange through C_2N_2. He, therefore, revised his earlier f-value upward. In regard to the result deduced by Tsang, et al (ref. 63), the authors claimed only an order of magnitude agreement with the true value.

Oscillator strengths deduced [illegible] ballistic range measurements are strongly dependent [illegible]ation energy assumed for CN. This sensitivity is demonst[illegible]rn's results, (ref. 65), and as Table III shows, a wide [illegible]ssociation energies have been used. Consequently, the seeming [illegible]agreement among the $f_{el}(\lambda)$ values obtained from recent [illegible] and ballistic range studies is somewhat deceptive. When corrected to a common dissociation energy, large disparities can occur.

Arnold and Nicholls, (ref. 59), simultaneously determined the dissociation energy and the electronic transition moment by making measurements at widely separated temperatures. Their observations yielded an $f_{el}(\lambda)$ at 386nm of 0.033 and a $D_{o,CN} = 7.89eV$. Since they exercised considerable care in their measurements, this result has been used herein as a standard against which the other shock tube results have been compared. Correction to $D_{o,CN} = 7.89eV$ can be accomplished by noting that (ref. 59)

$$f_{el}(\lambda) \propto \exp\left(-\frac{D_{o,CN}}{kT}\right)$$

where T is to be considered a constant (equal to the temperature actually observed during the absorption or emission measurement). Arnold and Nicholls have performed such a comparison and found that the f-values obtained by Menard, et al (ref. 66, 67), Kudryavtsev, (ref. 64), and Ambartsuumyan, et al (ref. 68), are lower than their result by about a factor of 2. Similarly, Harrington's unpublished

value reported by Wentink, et al. (ref. 7, is higher by approximately 40 percent. Reis' (ref. 69), and McKenzie and Arnold's, (ref. 70), earlier measurements were found to agree well with the results of reference 59 when corrected to $D_{o,CN} = 7.89eV$. Levitt and Parson's, (ref. 71), value is low, but it should be noted that they assumed $f_{el} = 0.027$ was correct and employed measured CN emissions to deduce a dissociation energy which agrees well with the Arnold and Nicholls value.

Oscillator strengths found by the radiative lifetime technique are independent of dissociation energy uncertainties, and as Table III shows, bracket the result found by Arnold and Nicholls. The electronic f-number given for Liszt and Hesser, (ref. 72), is an average of their (0,0), (1,1), and (2,2) band f-values converted to $f_{el}(\lambda)$ values, which were nearly constant. Liszt and Hesser tried to compare their phase shift results as closely as possible with those of Moore and Robinson in reference 73 (who were in good agreement with the earlier work of Bennett & Dalby in reference 74), but were unable to reveal any reason for the disparity between the two measurements. After a review of all the results reported in Table III, the present authors must agree with Arnold and Nicholls that the true electronic f-number lies in the range bounded by the lifetime results. Until additional measurements are made to narrow this range, it is recommended that Arnold and Nicholls' result be adopted as the mean value for the $\Delta v = 0$ sequence electronic f-number at 386nm, with the

radiative decay measurements providing the lower and upper limits of uncertainty.

The variability of the electronic transition moment with internuclear separation was studied in references 75 to 78 and in a recent review by Klemsdel, (ref. 79). Nicholls, (ref. 75), claimed an appreciable variation of R_e, but his result disagrees substantially with all the other investigations which show little or no variation. Parthasarathi, et al. (ref. 76), found R_e was practically constant even for high vibrational levels. Reis, (ref. 69), indicated that the ratio of R_e for the $\Delta v = +1$ to $\Delta v = -1$ band sequence was 0.90, a value which compares well with Arnold and Nicholls' recent measurements $[R_e(\Delta v = +1)/R_e(\Delta v = -1) = 0.904]$. The phase shift measurements of Moore and Robinson, (ref. 73), also showed a slow variation of R_e, $[R_e(\Delta v = +1)/R_e(\Delta v = -1) \simeq 0.94]$. Thus, based on a summary of prior work, the conclusion is that R_e is practically constant. Although the precise variation is yet to be determined, this assumption should be adequate for most radiative calculations. A constant transition moment, as discussed previously, implies $f_{e1}(\lambda) \simeq \lambda^{-1}$ so the present recommendation for the Violet system is

$$f_{e1}(\lambda) = 0.035 \left(\frac{388}{\lambda}\right)$$

CH Molecule

Data pertaining to the electronic oscillator strengths of the $A^2\Delta - X^2\Pi$, $B^2\Sigma^- - X^2\Pi$, and $C^2\Sigma^+ - X^2\Pi$ band systems of the CH radical are summarized in Tables IV and V. These tables are felt to be reasonably complete, although the possibility of omissions cannot be excluded. To facilitate comparisons between theory and experiment, the data are grouped into experimental measurements and analytical calculations. Pertinent features of each experiment or calculation are included under the Remarks column. The wavelength to which the oscillator strength corresponds is also listed.

Except for Dunham's, (ref. 60), and Linevsky's, (ref. 81), absorption measurements, the experimental results were radiative decay measurements which have been converted to an equivalent electronic oscillator strength by means of the expression:

$$f_{e\ell}(\lambda) = \frac{4\pi\varepsilon_o m_e c\lambda^2}{8\pi^2 e^2} \frac{d'}{d''} \frac{1}{\tau}$$

where τ is the lifetime, and λ the (weighted) wavelength at which the measurement was made. In most cases, the values for λ and $f_{e\ell}$ listed in Table IV are taken directly from the original sources. As pointed out in an earlier section, the above relationship must generally be used with caution, but for the CH bands, it should provide an excellent approximation to the electronic oscillator strengths since the assumptions involved in its derivation are fairly well met.

Dunham measured the absorption by the $R_2(1)$ line of the (0,0) band of CH in a graphite tube maintained at 3130 K, and derived a tentative f-number based upon a calculated CH concentration, which he stated was sensitive to the values adopted for the dissociation potential and vapor pressure of carbon. As can be seen, his result is about an order of magnitude larger than the more recent decay measurements, and since it is approximate, should not be given much weight.

Of the four lifetime measurements made on the $A^2\Delta - X^2\Pi$ system, only Jeunehomme and Duncan's, (ref. 82), results are in disagreement. They did not provide any explanation for the discrepancy. Hesser and Lutz, (ref. 83), have noted in a footnote to their paper that two lifetimes reported by Jeunehomme and Duncan in Reference 82 were revised, and have interpretated this as an indication that some problem was apparently encountered in the measurement of the A-State lifetime, which should therefore, be disregarded. Without additional information on which to make a judgement, the present authors concur in this assessment.

The value $f_{e\ell} = 0.0012$ given by Bennett and Dalby, (ref. 84), for the B-X band system was based on a preliminary measurement of the $B^2\Sigma^-$ lifetime. This value is low by a factor of 2.5 in comparison to that for the other two decay measurements and to Linevsky's relative absorption measurement, and probably should not be given much weight. Since Bennett and Dalby used a 10nm band pass centered

at 390nm, their observed B-state lifetime may have been influenced by emission from the atomic hydrogen line at 397nm. Both Fink and Welge, (ref. 24), and Hesser and Lutz employed a narrower band pass (2nm and .5nm) and thus were able to exclude this foreign emission.

Linevsky's relative absorption measurement appears to be the only experimental data available on the $C^2\Sigma^+ - X^2\Pi$ band system. Hesser and Lutz, (ref. 83), did measure the C-state lifetime, but found that the data could not be represented by a single exponential decay. The possibility of radiative cascading from higher lying excited states was excluded because such states have not been observed in emission. Their observations were adequately described in terms of overlapping emissions from states with two distinct lifetimes, both of which were considerably smaller than the radiative decay time expected on the basis of Linevsky's f-number. This was interpretated as evidence for predissociation of the C-state.

Comparison between the theoretical predictions of $f_{e\ell}$, (ref. 85-87), and the corresponding experimental quantities show only an order of magnitude agreement. Nicholls, (ref. 85), states that this is about the limit of accuracy achievable with a modern single configuration formulation. She also computed transition probabilities using the length and velocity forms of the transition operator in an attempt to determine which form was preferable to use with approximate wavefunctions. Since both forms gave results with comparable accuracy, no conclusion could be drawn.

None of the experimental studies listed in Table IV specifically examined the variability of the electronic dipole-transition moment with internuclear separation. Huo, (ref. 85), however, theoretically investigated the effect of electronic-vibrational interactions on the A-X transition and found the influence, for all practical purposes, to be negligible. Clearly, further studies are needed to define the variation of $R_e(r)$ for each band system.

Recommended values for the electronic oscillator strengths of the A-X, B-X, and C-X band systems of CH, based upon a review of the results contained in Tables IV and V are given below. The values for the A-X and B-X systems can be considered as being reasonably well established and, therefore, not subject to further large changes. However, the $f_{e\ell}$ for the C-X transition may have to be revised as more data becomes available.

RECOMMENDED ELECTRONIC f-NUMBERS FOR BAND SYSTEMS OF CH

System	$f_{e\ell}$	λ (nm)
$A^2\Delta - X^2\Pi$	0.0053	431.4
$B^2\Sigma^- - X^2\Pi$	0.003	387.1
$C^2\Sigma^+ - X^2\Pi$	0.0063	314.3

CF Molecule

Electronic transition moment data for band systems of the CF radical are scarce. The only sources uncovered are the shock tube studies made by Harrington and his colleagues, (ref. 22 and 88), pertaining to the $A^2\Sigma^+ - X^2\Pi$ transition and the radiative decay measurements of Hesser, (ref. 42, 43), for the $A^2\Sigma^+ - X^2\Pi$ and $B^2\Sigma - X^2\Pi$ systems. Due to a computational error, the f-values originally given by Harrington, et al. (ref. 22), for CF were too low by a factor of 10; revised f-numbers were reported in reference 88. The reader should be warned that the numbers actually quoted are emission oscillator strengths rather than absorption f-values which are employed in this report. The relationship between the two is:

$$f_{ems} = \frac{d_L}{d_U} f_{abs}$$

Wentink and Isaacson, (ref. 89), calculated equivalent electronic oscillator strengths using Hesser's earlier lifetime measurements, (ref. 42), and compared them to the corrected shock tube results of Harrington, et al. (ref. 88). The calculations were made assuming R_e = constant. Reference 89 also tabulates Franck-Condon factors based on a Morse potential for the A-X and B-X band systems. In a later paper, Hesser, (ref. 43), remeasured several of the excited state lifetimes reported in his previous paper, (ref. 42), employing an improved experimental technique. The new lifetime results for the A and B states of CF were essentially identical to his old values. Hesser used these lifetimes in conjunction with the Franck-

Condon factors of reference 89 to compute $f_{v'v''}$ arrays under the assumption that R_e is a constant. In addition, he assumed that 95 percent of the observed B-state lifetime was due to transitions into the ground state while the remainder was due to the spectroscopically unobserved B-A transition. A comparison of the various measured and calculated oscillator strengths is presented in Table VI. We have converted Hesser's band f-numbers to $f_{e\ell}(\lambda)$ values by dividing by the appropriate Franck-Condon factor taken from reference 89. Only $f_{e\ell}$ corresponding to the 0-0 transition wavelength is listed for Hesser because, since he took R_e = constant, the $f_{e\ell}$ at another wavelength can be obtained from the expression:

$$f_{e\ell}(\lambda) = \frac{\lambda_{o,o}\, f_{e\ell}\,(\lambda_{o,o})}{\lambda}$$

As the table shows for the A-X transition, there is reasonably good agreement between the f-numbers derived from Hesser's lifetime measurement and Harrington, et al,'s emission data on the basis of shock tube determined CF_2 and CF heats of formation. It should be pointed out, however, that Harrington, et al. also analysed their data using JANAF heats of formation and obtained f-numbers that were a factor of 10 higher. Wentink and Isaacson, (ref. 89), have argued that these latter values are unrealistically high. Moreover, oscillator strengths derived from lifetime data are independent of the thermochemical properties, and in this case, tend to favor the lower value. Until more measurements are made and more data becomes available, we recommend the following tentative values:

$A^2\Sigma^+ - X^2\Pi$	$f_{e\ell}(\lambda) = 0.026$	at	λ = 233 nm
$B^2\Sigma^+ - X^2\Pi$	$f_{e\ell}(\lambda) = 0.016$	at	λ = 202,5 nm

heats of formation

CF_2	-39.7 kcal/mole
CF	49.2 kcal/mole

The variation of electronic transition moment with internuclear separation is not known for these two band systems of CF. Harrington, et al. computed $f_{e\ell}$ values from their measured emission data for the (0,0), (0,1), and (0,3) band sequences at 232.9, 237,7 and 254.7nm of the A-X transition. An examination of the equation they used to theoretically predict the emitted intensity reveals that they essentially assumed R_e was constant. However, their reported f-values display a much greater variation than expected on the basis of an inverse wavelength dependence (ie., R_e = constant). This is perhaps an indication that R_e is variable, but further work is needed to clarify this point.

Since the Morse-potential Franck-Condon factors given in reference 89 are apparently the only ones published, we recommend that they be used until more accurate arrays based on realistic potential functions become available. This is an area requiring further study because there is experimental evidence (ref. 90) that vibrational levels of the A-State with $v' > 2$ are predissociated.

Triatomic Carbon, C_3

Data on the absorption spectrum of gaseous C_3 are extremely scarce. The few sources that have been uncovered in the literature range between the extremes of absorption measurements made at cryogenic temperatures (20 and 4 K), (refs. 91 to 95), and absorption measurements made in a graphite furnace characterized by temperatures in excess of 3000 K, (ref. 96). The spectra obtained for these two situations differ significantly from one another. At extremely low temperatures, only transitions from the lowest vibrational level of the ground electronic state are observed and display a discrete line structure; at the temperatures found in a graphite furnace the absorption spectrum shows a complex structure characterized by discrete transitions in the neighborhood of the well-known Swing bands at 405 nm superimposed upon an underlying continuum. Brewer and Engelke, (ref. 96), have demonstrated that the underlying continuous absorption is not a true continuum but involves transitions between the same two electronic levels that are responsible for the Swing bands. In fact, they were able to qualitatively explain their observed spectra in terms of a blending of many weak, closely spaced rotational lines into a pseudocontinuum, upon which a few rotational lines of particularly strong bands stood out. The subsequent rotational-vibrational analysis of gaseous C_3 by Gausset, et al. (ref. 97), has clarified the reason for the appearance of numerous rotational lines and hence C_3's spectral complexity. In

both electronic states, C_3 is linear with a bending frequency in the ground level of approximately 70 cm^{-1}. The bending mode of the excited electronic state, on the other hand, was found to have a large Renner effect (ie., interaction between the vibrational and electronic motions) which removes the degeneracy associated with this mode. The particular significance of these findings is that the absorption spectrum of C_3 should be strongly dependent on temperature. Consequently, extrapolation of results obtained from absorption measurements made at cryogenic temperatures to ablation layer conditions will be difficult, if not impossible, without explicit knowledge of its temperature variation.

Interpretation of cryogenic measurements is also made difficult by so-called "matrix" or solid state effects (refs. 91, 92, 94). In this phenomenon carbon vapor is trapped in an inert solid matrix, such as Argon or Neon, formed at extremely low temperatures, typically 20 K or lower. Although only the lowest vibrational level of the ground electronic state is populated at these low temperatures, thereby simplifying the spectral analysis, the solid matrix perturbs the trapped C_3 molecule, and such perturbations are easily detectable. For example, the observed absorption spectra are found to be shifted relative to the gaseous spectra by differing amounts depending on the matrix employed. Weltner, Walsh, and Angell, (ref. 91), noted subbands appearing in addition to the principal bands which they attributed to the existence of multiple matrix sites offering different invironments.

The f-number of the 405 nm line group was reported in references 92 and 94 but these values disagree by approximately two orders of magnitude. This variance among f-numbers is probably indicative of their reliability. It is obvious that many more measurements, encompassing a wide range of temperatures, is needed to better define the absorption spectrum of C_3. In the interim, use of Brewer and Engelke's data, (ref. 96), is recommended, since their measurements were made at a temperature typical of that expected in the ablation layer.

Figure 4 gives a plot of absorption cross section versus frequency, while Table VII provides numerical values. These results were obtained by digitizing Brewer and Engelke's absorption curve and dividing by the value they gave for the C_3 concentration appropriate to their experimental conditions ($N = 3.268 \times 10^{16}$ cc^{-1}). The uncertainty in cross section is about a factor of two since this is the accuracy quoted by Brewer and Engelke for their estimate of the C_3 number density. This is exclusive of measurement and digitizing errors.

The reader should also note that the results presented in Figure 4 and Table VII pertain to a temperature of 3200 K and in accord with our previous comments will vary with temperature.

Franck-Condon Factors

Franck-Condon factors based on Morse potentials are available for all of the band systems of interest here; for many of them improved potential models such as the Rydberg-Klein-Rees and Klein-Dunham potentials have been employed. Table VIII indicates sources of tabulated Franck-Condon factors for the various band systems. Also, Tables IX to XV reproduce limited arrays from certain of these references. The references selected based their calculations on either RKR or KD potential model.

Cross Sections for Free-Bound Continua

The available pertinent literature sources have been examined which deal with free-bound processes from neutrals as well as for positive and negative ions. Most important are those dealing with carbon and oxygen neutrals, since Venus entry shock layer conditions are such that significant radiative transfer results from the emission due to electron capture. Of lesser importance, but worthy of inclusion in radiative transfer calculations, are the free-bound processes for the species C^+, C^-, and O^-.

Because of the large amounts of energy involved and the relatively high concentrations of C and O in the shock layer, transitions of the type:

$$A + h\nu \rightarrow A^+ + e^-$$

from the lower-lying levels of the parent atoms require special attention. These transitions occur for photon energies in the vacuum-ultraviolet region of the spectrum.

Oxygen atom cross sections have been extensively studied for earth entry applications as well as for upper atmospheric photochemical processes. For oxygen the pertinent transitions and their corresponding photoionization edges are:

OI		OII	λ edge, nm
^3P	→	$^4S^o$	91.1
^3P	→	$^2D^o$	73.2
^3P	→	$^2\,o$	66.6

^1D	→	$2p^o$	82.8
^1D	→	$2_p{}^o$	74.4
^1S	→	2_p	85.8

The transitions resulting from a single energy level in the parent atom result in cross-sections which are atomic constants. For OI there are three such temperature-invariant cross-sections of importance, all in the far ultraviolet (λ < 100 nm). Theoretical calculations of cross sections reported in the literature exhibit a variety of spectral dependence, primarily due to the different approximations and assumptions made in performing the computations. Use of more accurate wave functions should provide more reliable information.

Experimental data for the VUV cross sections of oxygen are relatively scarce and generally of insufficient accuracy to indicate clearly the spectral variation. Plots of these cross sections for O are given in Figures 5a, 5b, 5c, showing the results of several authors, (refs. 12, 113-117). These plots exhibit the disparity of the various computations and how the experimentally obtained values compare with the various theories. In general, experimental values are somewhat higher than the computed cross-sections. Reference 118 gives empirical curve fits to the data of reference 117.

References dealing with carbon atom photoionization are fewer in number than for the corresponding oxygen processes and are generally of more recent vintage. The relevant processes appear to be:

CI		CII	λ edge, nm
^3P	→	$^2P^o$	110
^3P	→	^4P	74.7
^1D	→	$^2P^o$	123.9
^1D	→	$^2P^o$	144.4
^5S	→	^4P	99.8

The transitions ^3P-^4P, ^5S-^4P have not been discussed in the literature, probably because of their relative unimportance in comparison with the others. A summary of the available sources is presented in Figures 6a, b, c, showing results of references 113, 114, 119, and 120.

The cross section for the process:

$$C^+ + h\nu \rightarrow C^{++} + e^-$$
$$(^2P) \qquad (^1S) \qquad \lambda \text{ edge} = 50.86 \text{ nm}$$

is of lesser importance due to the short wavelength threshold. Results of Henry, (ref. 113), are presented in Figure 7 along with a Kramer's calculation. Cross section for the O^+ processes have even shorter wavelength thresholds, and are not considered to be of sufficient importance to include in radiative transfer calculations.

For all of the carbon and oxygen free-bound vacuum ultraviolet cross-sections, the work of Hentry, (ref. 113), appears to offer most consistency in that the cross-section formulas give a good compromise to the various theoretical calculations. These formulas compare with the existing measurements better than most of the theories, and are

presented in reference 113 in a convenient formulation for inclusion in radiative transfer computations. Furthermore, there is a scarcity of recent vacuum UV measurements using latest techniques, and it is felt that at the present time, detailed calculations of individual free-bound cross-sections have a better reliability than do most of the measurements. For these reasons, the recommendation is that these cross-section formulas be used for the transitions involved.

Some representative calculations have been made for the C and O VUV free-bound transitions. The general formula of reference 113:

$$\sigma(\lambda) = \sigma_{edge} \left\{\alpha[\lambda/\lambda_o]^S + (1 - \alpha)[\lambda/\lambda_o]^{S+1}\right\} \qquad (42)$$

has been used to generate absorption coefficients for the combined pertinent transitions and the corresponding spectral radiance. The values of the empirical constants as given in reference 113 and used in the calculations are:

	S	α	$\sigma_{edge} \times 10^{-18}$ cm^2
$C(^3P) - C^+(^2P)$	2.0	3.317	12.19
$C(^1D) - C^+(^2P)$	1.5	2.789	10.30
$C(^1S) - C^+(^2P)$	1.5	3.501	9.59
$C^+(^2P) - C^{++}(^1S)$	3.0	1.950	4.60
$O(^3P) - O^+(^4S)$	1.0	2.661	2.94
$O(^3P) - O^+(^2D)$	1.5	4.378	3.85
$O(^3P) - O^+(^2P)$	1.5	4.311	2.26
$O(^1D) - O^+(^2D)$	1.5	6.829	4.64
$O(^1D) - O^+(^2P)$	1.5	4.800	1.95
$O(^1S) - O^+(^2P)$	1.5	5.124	7.65

Figures 8 and 9 show the absorption coefficient per particle, or total cross-section, for O and C at temperatures of 8000 and 12,000 K. It is evident that this spectral quantity is notably insensitive to temperatures in this range.

Figure 10 (a, b, c) show some representative radiance calculations for the C and O transitions in the vacuum UV at temperatures of 8000, 10,000, and 12,000 K. The number densities of C and O used are those corresponding to equilibrium conditions in thermally excited CO_2 at a pressure of $1.013(10)^5$ N/m^2 (1 atm.) The outstanding feature of the radiance calculations is the dominance of the carbon transitions. This is due to the influence of the Planck function as used in Kirchhoff's Law. Since these temperatures are representative of Venus entry shock layer conditions, more importance must be given the carbon transitions for shock-heated CO_2.

Even though negative ion concentrations are small, bound-free photodetachment processes warrant some attention since the cross sections are relatively large over considerable portions of the spectrum. The relevant processes are:

$$\begin{cases} C^- \\ \\ O^- \end{cases} + h\nu \rightarrow \begin{cases} C + e^- & \lambda_{edge} = 990 \text{ nm} \\ \\ O + e^- & \lambda_{edge} = 855 \text{ nm} \end{cases}$$

Fortunately, experiment and theory appear to agree quite well for both ions, as can be seen on Figures 11 and 12. Figure 11 shows the O^- cross section as computed from references 121, 122 and the

measurements of reference 123. The C^- data of reference 124 shows some differences at long wavelengths between measurement and theory, but the discrepancy should not seriously affect overall radiative transfer. The dipole velocity calculations of references 125 and 126 are in good agreement. Henry, (ref. 125), illustrates the difference in the dipole-length and dipole-velocity formulations and the data at the shorter wavelengths suggests that the latter formulation is preferable. The present recommendation is to use the calculation of Cooper and Martin, reference 122, for both C^- and O^- photodetachment.

Atomic Lines

Transition probabilities for carbon and oxygen lines can be obtained from Wiese, Smith, and Glennon, reference 127, who have carefully surveyed sources in the literature and compiled recommended f-numbers. Data may be found for many more lines than are important in radiative heating calculations. Wilson and Nicolet, reference 128, have applied specified criteria to screen those transitions which ought to be included, and have supplemented the NBS tables of reference 127 with calculated f-numbers for additional lines. Reference 128, therefore, presents a good compilation for use in radiation calculations, but the values from reference 127 which are based on experimental measurement are to be preferred. Also, references 129 to 131 present additional experimental transition probabilities for carbon lines. The recommended transition values, Tables XVI to XIX were thus obtained by combining the above sources. It should be noted that reference 127 is indicated in the tables even though this is not the prime source for certain experimentally determined transitions. The sources of these experiments may be obtained by referral to reference 127.

For cases where absorption becomes important, a knowledge of the line width and absorption shape is required. Tables of line half width and line shift data are included in reference 128, based on the theory of electron impact broadening as set forth by Griem, reference 3. This broadening mechanism leads to a Lorentz, or dispersion profile,

and for lines which are optically very thick indicates that for practical problems a substantial amount of energy is contained in the line wings. In situations where moderate-to-high ionization occurs and line radiation contributes less than about 15-20 percent of the total radiant transfer, electron impact broadening theory should yield acceptable results. In other situations, a more detailed analysis is required--other broadening mechanisms become important and lead to different line widths and profiles. For example, in gases composed primarily of neutral atoms and relatively few electrons, Doppler and resonance effects are the dominant broadening mechanisms. A good description of these effects is found in reference 132, where a detailed analysis for NI atomic line radiation is presented. In this paper it is also shown that for line series associated with high quantum numbers, mathematical simplifications may be made which treat these line series as a continuum. (See also ref. 133).

Cross Sections for Free-Free Continua

An excellent survey of theoretical methods for computing the radiation from free-free transitions is given by Johnson in reference 134. Several theoretical studies are available in the open literature, for example references 135-140.

Experiments show that ion-electron interactions (Kramer's radiation) are adequately described by applying a correction for quantum effects (Gaunt factor) to the semiclassical Kramer's cross section, see references 141-143. We have found no evidence that significant improvement in the cross section for Kramer's radiation can be made by departing from this relatively simple calculation. Thus it is recommended that cross sections be obtained by using Kramer's cross sections and appropriate Gaunt factors, reference 139.

The scattering of electrons by neutrals (neutral Bremsstrahlung) is more complicated, since the effective scattering force is produced by polarization of the atom by the incident electron. References 135, 137, 140, and 144 show that for oxygen and nitrogen, theory and experiment are in poor agreement for this process. Experimental results are usually formulated as effective values of Z^2 for use in Kramer's formula, but Kramer's formula does not correctly describe the wavelength or temperature dependence. For oxygen, the experimental cross sections (ref. 144 and 145) are about 2 percent as large for the neutral as for the ion. No experimental data has been found for carbon. For many cases it may be appropriate to neglect the neutral Bremsstrahlung.

When it is deemed necessary to include, experimental data close to the desired thermodynamic state will be required for reasonably accurate cross sections.

SUMMARY OF RECOMMENDATIONS

As a result of the survey of published measurements and calculations, the following values are recommended for use in radiative heating calculations for Venus entry:

Molecular Band Systems

C_2 Swan	$f_{el} = 0.03(516.5/\lambda)^{2.8}$
CO Fourth Positive	$f_{el} = 0.15\left(\frac{68}{\lambda-80}\right)^2$
CO^+ Comet-Tail	$f_{el} = 7.24\times10^{-3} \exp\left[\frac{-(7.73\times10^{9} + 8.91\times10^{-4}\lambda^5}{\lambda^4}\right]$
CN Violet	$f_{el} = 0.035(388/\lambda)$
CH A-X	$f_{el} = 0.0053$
CH B-X	$f_{el} = 0.003$
CH C-X	$f_{el} = 0.0063$
CF A-X	$f_{el} = 0.026$
CF B-X	$f_{el} = 0.016$

(The above relations use λ in nanometers)

Free-Bound Continua

For both carbon and oxygen photoionization use the cross section formula of Hentry, reference 113; for photodetachment of C^- and O^-, use the calculations of Cooper and Martin, reference 122.

Atomic Lines

Use f-numbers as compiled in Tables VIII to XI.

Free-Free Continua

Ion-electron interactions are adequately described by Kramer's formulation with Gaunt factors from Karzas and Latter, reference 139. Neutral-electron interactions may usually be neglected, but if included, they must be based on experimental data close to the desired thermodynamic state.

APPENDIX
OTHER BAND SYSTEMS

Some data have been collected concerning other band systems of C_2, CN, CO, and CO^+. These other band systems have, in general, been studied less extensively than those discussed in the main body of this report, and in most radiative heating calculations they have been neglected. (The Red system of CN is usually considered for earth entry, but for Venus atmospheric models with little nitrogen, it is frequently neglected.) The possible importance of these "minor" band systems has not been investigated, so the extent of the errors incurred by neglecting them are not known. The brief, not necessarily inclusive, summary of absolute intensity studies which follows represents the extent of the work which has been uncovered for these band systems. No recommendations as to best values are made.

C_2 Phillips System $A'\Pi - X\ '\Sigma^+$. A value of $f_{el} = 0.0165$ at the 0,0 bandhead (λ = 1210 nm) is given by Wentink, et al. reference 7. Clementi, reference 28, calculated a value of $f_{el} = 0.0027$ with hybridization considered. Hicks, reference 25, reported a ratio

$$\frac{f(2,0)\text{Phillips}}{f(1,0)\text{Swan}} = 0.468 \pm 0.028$$

which was based on experimental measurements. Using the present recommendation for the Swan system, Hicks' result would yield $f_{el} = .025$ for the Phillips system.

C_2 Deslandres d'A zumbuja System - $C'\Pi_g$ - $A'\Pi_u$. A value of f_{el} = 0.0061 at the 0-0 bandhead was reported by Wentink et al. (ref. 7) based on radiative lifetimes measured in laser blow-off experiments. Shull, reference 29, and Clementi, reference 28, calculated f-numbers considering hybridization and reported values of 0.17 and 0.065 respectively. In reference 26, Stephenson did not consider hybridization and computed a value of 0.039.

C_2 Freymark System $E\ ^1\Sigma_g^+$ - $A\ ^1\Pi_u$. Wentink et al., reference 7, estimated from calculations a radiative lifetime of 33 nanoseconds from which they compute f_{el} at 0-0 = 0.011.

C_2 Fox Herzberg System $e\ ^3\Pi_g$ - $a\ ^3\Pi_u$. Sviridov et al., reference 21, estimated an upper limit for $f_{el} < 0.011$. Wentink et al., reference 7, give a calculated value = 0.00312. Clementi, reference 28, calculated f_{el} = 0.8184.

C_2 Mulliken System $D\ ^1\Sigma_u^+$ - $X\ ^1\Sigma_g^+$. Wentink et al., reference 7, give a probable lower bound as f_{el} = 0.0203. Clementi, reference 28, calculated f_{el} = 0.1025 using a value of 8.5 percent of hybridization. Smith, reference 25, obtained f_{el} = .055 in a lifetime measurement.

C_2 Ballik - Ramsay System $b\ ^3\Sigma_g^-$ -- $a\ ^3\Pi_u$. Clementi, (ref. 28), reports a calculated f_{el} = .0066.

CN Red System $A\ ^2\Pi_i$ - $X\ ^2\Sigma^+$. The variation of the transition moment was determined from relative intensity measurements by Dixon and Nicholls, reference 146. Wentink, Isaacson, and Morreal, reference

147, measured a lifetime of 3.5 microseconds from which they quoted a corresponding a band oscillator strength $f_{v'v''}(0,0) = 0.0037$. Jeunehomme, (ref. 148), measured lifetimes of 6.4 to 7.4 microseconds and calculates $f_{v'v''}(0,0) = 0.0034$. The inconsistency of these two sets of data is attributed by Jeunehomme to neglect of a degeneracy term in the former result, and he states the Wentink, Isaacson, and Morreal result should be interpreted as $f_{v'v''}(0,0) = 0.0074$. Schadee, (ref. 5), used the Dixon and Nicholls measurements, normalized to Jeunehomme's result at the 0-0 bandhead and obtained a wavelength variation of $f_{el}(\lambda)$. His result can be closely approximated by $f_{el} = \frac{7}{\lambda}$ (λ in nanometers).

CO Cameron Band System $a\,^3\Pi_r - X\,^1\Sigma^+$. The $a\,^3\Pi$ state of CO is metastable, and transition to the singlet ground state is forbidden because of spin change. The transition is observed, however, because of spin-orbit mixing with the $A\,^1\Pi$ state. A wide range of lifetimes and f-numbers are quoted in the literature, (ref. 149 to 160), as shown in Table A1. A best value of f_{el} appears to be about 6×10^{-7} at the 0-0 band. This value was obtained by Hasson and Nicholls, (ref. 155), and is in good agreement with the value obtained by Fairbairn, (ref. 153, 154), and the calculation by James, (ref. 160). Very little trend in f_{el} with wavelength was observed by Lawrence and Seitel, (ref. 157), for $v' = 0$ to 5, $v'' = 0$, so a constant oscillator strength appears justified.

CO Hopfield - Birge System B $^1\Sigma^+$ - X $^1\Sigma^+$. Lassettre and Silverman, (ref. 37), quoted an integrated oscillator strength f_{el} = 0.03 based on electron scattering. Later work, reference 38, suggested this should be reduced by the factor 0.727. Meyer et al., (ref. 161), measured electron impact spectra and obtained f_{el} = 0.0224. Hesser, reference 43, measured a radiative lifetime of 25 nanoseconds. They system is narrow in wavelength, as are several other ultraviolet systems of CO, so a wavelength-dependence of the oscillator strength is not required.

CO Hopfield - Birge System C $^1\Sigma^+$ - X$^1\Sigma^+$. Lassettre and Silverman's, (ref. 37), electron scattering measurements led to an estimated f_{el} = 0.28, but they state this value may not be too reliable. By the same reasoning as was applied to the B-X transition, Lassettre and Skerbele, reference 38, conclude the earlier value should be reduced by the factor 0.727. Meyer, Skerbele, and Lassettre, reference 161, reported a value f_{el} = 0.33. Hesser, in reference 43, reported an experimental radiative lifetime τ = 1.4 nanoseconds.

CO Third Positive Band System b $^3\Sigma^+$ - a $^3\Pi_r$. Barrow et al., reference 162, measured the relative intensity of the vibrational bands in this system but made no absolute measurements. Robinson and Nicholls, (ref. 163), measured relative intensities and fit the relation

$$R_e \simeq (-1 + 0.943\bar{r})$$

to their data through the use of calculated r-centroid values. Tawde and Patil, in reference 164, performed a similar analysis using the data of reference 162 and obtained

$$R_e \alpha (1 - 0.6433\bar{r})$$

Schwenker, (ref. 165), measured a radiative lifetime of 86 nanoseconds from which he quotes $f_{el} = 8.9 \times 10^{-3}$. Fowler and Holzberlein, (ref. 166), measured $\tau = 40$ nanoseconds while Moore and Robinson, (ref. 73), measured 97 nanoseconds.

CO Angstrom Band System $B\ ^1\Sigma^+ - A\ ^1\Pi$. Robinson and Nicholls, (ref. 163), measured relative intensities for the $v' = 0$ progression. Fowler and Holzberlein, (ref. 166), obtained $\tau = 75$ nanoseconds, while Moore and Robinson, (ref. 73), quoted a transition probability for the $v' = 0$ progression:

$$A_{B-A} = 1.11 \times 10^7 \text{ sec}^{-1}$$

which would correspond to a radiative lifetime of 90 nanoseconds. Using this latter value and the Franck-Condon factors given in reference 73, equation 29 yields:

$$f_{el} = 0.03$$

CO Asundi Band System $a'\ ^3\Sigma^+ - a\ ^3\Pi_r$. The Asundi Bands extend through most of the visible, [illegible]re not very intense. Wentink et al., (ref. 7), performed extensive lifetime measurements and concluded a best fit was obtained for a constant transition moment, which corresponds to $f_{el}(0,0) = 1.56 \times 10^{-3}$.

CO^+ First Negative Band System $B^2\Sigma^+ - X^2\Sigma^+$. Experimentally determined values of the radiative lifetime for various levels of the B-X transition have been reported in references 42, 43, 165, and 169-172.

All of the sources with the exception of references 165 and 169, obtained lifetimes in the range 44 to 60 nanoseconds. The variation of the transition moment with r-centroid has been studied in references 167, 168, 173 and 174 without a conclusive determination, but the variation of R_e would appear to be small. By using the lifetime measurements of Hesser, (ref. 43), Isaacson et al., (ref. 167), calculated $f_{el} = 0.0144$, assuming a constant transition moment. They obtained $f_{el} = 0.0192$ for a varying transition moment. However, in view of the apparent small variation of the transition moment, the former value ($f_{el} = 0.0144$ at the 0,0 bandhead) seems preferable.

TABLE A1

CO Cameron Band System $a\ ^3\Pi - X\ ^1\Sigma$

Source	Ref.	Radiative Lifetime	f_{el}	Comment
Hansche	149	∿ 10 microsec.		rough estimate
Meyer, Smith, & Spitzer	150	100 microsec. to 3 millisec.		matrix
Donovan & Husain	151	12 millisec.		prediction
Borst & Zipf	152	1 millisec.		electron beam
Fairbairn	153 154		5.5×10^{-7}	absorption
Hasson & Nicholls	155		$f_{oo} = 1.62 \times 10^{-7}$	absorption
Lawrence	156	7.5 millisec.	$(f_{el} = 5.53 \times 10^{-7})^*$	
Lawrence & Seitel	157		$f_{el} \sim 6 \times 10^{-7}$	relative to ref. 155 data
Johnson & Van Dyck	158	10 - 10 millisec.		time of flight
Slanger & Black	159	4.4 msec.		photon absorption
James	160		$f_{oo} = 1.63 \times 10^{-7}$ $(f_{el} = 5.56 \times 10^{-7})^*$	calculated

*Calculated using the Franck-Condon factor of reference 107.

Reference List

1. Noll, R. B.; and McElroy, M.V.: Engineering Models of the Venus Atmosphere. Presented at 11th Aerospace Sci Meeting Washington D.C.; AIAA 73-130, Jan. 1973.

2. Penner, S.S.: Quantitative Molecular Spectroscopy and Gas Emissivities. Addison-Wesley Publ. Co., London, Eng., 1959.

3. Griem, H.R.: "Plasma Spectroscopy". McGraw-Hill Publ. Co., 1964.

4. Armstrong, B.H.; and Nicholls, R.W.: Emission, Absorption and Transfer of Radiation in Heated Atmospheres. Pergamon Pres. New York, 1972.

5. Schadee, A.: The Relation Between the Electronic Oscillator Strength and the Wavelength for Diatomic Molecules . J. Quant. Spectrose. Radiat. Transfer., Vol. 7, pp. 169-183, 1967.

6. Wentink, T.; Davis, J.; Isaacson, L.; and Spindler, R.: Electronic Oscillator Strengths of Diatomic Molecules. AVCO/RAD TM 64-33, July 1964.

7. Wentink, T.; Marram, E.P.; Isaacson, L.; and Spindler, R.J.: Ablative Material Spectroscopy. Vol. I, Experimental Determination of Molecular Oscillator Strengths, Air Force Weapons Lab. TR 67-30, (1967).

8. Tatum, J.B.: The Interpretation of Intensities in Diatomic Molecular Spectra. Astrophysical Journal, Supplement Series, Supp. No. 124, Vol. 14, pp. 21-56, (1967).

9. Herzberg, G.: Molecular Spectra and Molecular Structure, I. Spectra of Diatomic Molecules. D. Van Nostrand Co., Princeton, N.J., (1950).

10. Jarmain, W.R.; and Fraser, P.A.: Vibrational Transition Probabilities of Diatomic Molecules II. Proc. Phys. Soc. A, Vol. 66, pp. 1153-1157, (1953).

11. Nicholls, R.W.: On the Relationship Between r-centroid and Band Frequency. Proc. Phys. Soc., Vol. 85, pp. 159-162, (1965).

12. Hahne, G.E.: The Vacuum Ultraviolet Radiation From N^+ and O^+ Electron Recombination in High Temperature Air. NASA-TN D-2794, June 1965.

13. Praderie, F.: Calcul Quelques Sections de Photoionisation du Carbone Neutre. Annales D'Astrophysique, No. 3, pp. 129-140, (1964).

14. Atomic and Molecular Processes. Edited by D.R. Bates, Academic Press N.Y., (1962).

14a. DeVore, R.V.: Absorption and Bremsstrahlung Cross Sections of Nitrogen for Slow Electrons. Phys. Rev., Vol. 136, No. 3A, pp. A666-A668, (1964).

15. Allen, R.A.: Air Radiation Graphs: Sectrally Integrated Fluxes Including Line Contributions and Self Absorption. Avco Everett Res. Lab. Research Report: 230, (1965).

16. Jeunehomme, M.; and Schwenker, R.P.: Focused Laser-Beam Experiment and the Oscillator Strength of the Swan System. J. Chem. Phys., Vol. 42, No. 7, pp. 2406-2408, (1965).

17. Arnold, J.O.: A Shock Tube Determination of the Electronic Transition Moment of the C_2 (Swan), Bands. Journ. Quant. Spect. and Rad. Trans., Vol. 8, No. 11, pp. 1781-1794, November 1968.

18. Hagan, L.G.: The Absolute Intensity of C_2 Swan Bands. Ph. D. Thesis, Univ. of California, Berkeley, California, (1963).

19. Fairbairn, A.R.: A Shock-Tube Study of the Oscillator Strength of the C_2 Swan Bands. Journ. Quant. Spect. and Rad. Trans., Vol. 6, pp. 325-336, (1966).

20. Sviridov, A.G.; Sobolev, N.N.; and Sutovskii, V.M.: Determination of the Matrix Element of the Dipole Moment of an Electronic Transition of the Swan-Band System of C_2 Molecules. Journ. Quant. Spect. and Rad. Trans., Vol. 5, pp. 525-543, (1965).

21. Sviridov, A.G.; Sobolev, N.N.; and Novgorodov, M.Z.: Determination of the Matrix Element of the Dipole Moment of an Electron Transit in the Swan Band System of Carbon Molecules. II. Absorption Method. Journ. Quant. Spect. and Rad. Trans., Vol. 6, pp. 337-349, (1966).

22. Harrington, J.A.; Modica, A.P.; and Libby, D.R.: Shock-Tube Determination of the C_2 ($A^3\Pi \rightarrow X^3\Sigma$) and CF ($A^2\Sigma^+ \rightarrow X^2\Pi$) Band System Oscillator Strengths. J. Chem. Phys., Vol. 44, pp. 3380-3387, (1966).

23. Hicks, W.T.: Spectroscopy of High Temperature Systems. Rad. Lab. Report OCRL 3696, University of California, Berkley, (1957).

24. Fink, E.H.; and Welge, K.H.: Lifetime Measurements on $CH(A^2\Delta)$ $CH(B^2\Sigma^-)$ and $C_2(A^3\Pi_a)$ by the Phase Shift Method. Journ. Chem. Phys., Vol. 46, No. 11, pp. 4315-4318, (1967).

25. Smith, W.H.: Transition Probabilities for the Swan and Mulliken C_2 Bands. Astrophy. Journ., Vol. 156, pp. 791-794, (1969).

26. Stephenson, G.: Calculation of the Oscillator Strengths for Certain Band-Systems of N_2 and C_2. Proc. Phys. Soc., Vol. A64, pp. 99-100, (1951).

27. Lyddane, R.H.; and Rogers, F.T.: The Abundances of Molecules in the Solar Reversing Layer. Phys. Rev., Vol. 60, pp. 281-282, July-December, (1941).

28. Clementi, E.: Transition Probabilities for Low-Lying Electronic States in C_2. Astrophysical Journ., Vol. 132, pp. 898-904, (1960).

29. Shull, H.: Transition Probabilities for C_2 and N_2^+. Astrophy. Journ., Vol. 114, No. 2, p. 546, (1951).

30. Spindler, R.J.: Franck-Condon Factors Based on RKR Potentials With Applications to Radiative Absorption Coefficients. Journ. Quant. Spect. and Rad. Trans., Vol. 5, pp. 165-204, (1965).

31. Coulson, C.A.; and Lester, G.R.: Some Consequences of Orthonalization in Molecular-Orbital Theory. Faraday Society Trans., Vol. 15, Pt. 12, pp. 1605-1611, (1965).

32. Mentall, J.E.; and Nicholls, R.W.: Absolute Band Strengths for the C_2 Swan System. Proc. Phys. Soc., Vol. 86, pp. 873-876, (1965).

33. Jain, D.C.: Transition Probability Parameters of the Swan and the Fox-Herzberg Band Systems of the C_2 Molecule. Journ. Quant. Spect. and Rad. Trans., Vol. 4, pp. 427-440, (1964).

34. **Krupenie, P.H.:** The Band Spectrum of Carbon Monoxide. **National Bureau of Stds., NSRDS-NBS-5, July 1966.**

35. **Hexter, R.M.:** Evaluation of Lattice Sums in the Calculation of Crystal Spectra. Journ. Chem. Phys., Vol. 37, pp. 1347-1356, (1962).

36. **Brith, M.; and Schnepp, O.:** The Absorption Spectra of Solid CO and N_2. Mol. Phys., Vol. 9, pp. 473-488, (1965).

37. **Lassettre, E.N.; and Silverman, S.M.:** Inelastic Collision Cross Sections of Carbon Monoxide. Journ. Chem. Phys., Vol. 40, No. 5, pp. 1256-1261, (1964).

38. **Lassettre, E.N.; and Skerbele, A.:** Absolute Generalized Oscillator Strength for Four Electronic Transitions in Carbon Monoxide. Journ. Chem. Phys., Vol. 54, No. 4, pp. 1597-1607, February 1971.

39. **Meyer, V.D.; and Lassettre, E.N.:** Experimental Determination of Oscillator Strengths for the CO $A\,^1\Pi \leftarrow X\,^1\Sigma$ Bands. Journ. Chem. Phys., Vol. 54, No. 4, pp. 1608-1610, February 1971.

40. **Vargin, A.N.; Pasynkova, L.M.; and Trekhov, E.S.:** Experimental Determination of the Absolute Value of $|R_e|^2$ for the 4^+ System of the CO Molecule. Zh. Prik. Spek., Vol. 13, pp. 662-666, October 1970.

41. **Hesser, J.E.; and Dressler, K.:** Absolute Transition Probabilities in the Ultraviolet Spectrum of CO. Astrophy. Journ. Letters, Vol. 142, pp. 389-390, April 1965.

42. **Hesser, J.E.; and Dressler, K.:** Radiative Lifetimes of Ultraviolet Molecular Transitions. Journ. Chem. Phys., Vol. 45, pp. 3149-3150, (1966).

43. **Hesser, J.E.:** Absolute Transition Probabilities in Ultraviolet Molecular Spectra. Journ. Chem. Phys., Vol. 48, No. 6, pp. 2518-2535, (1968).

44. **Nicholls, R.W.:** Laboratory Astrophysics. Journ. Quant. Spect. and Rad. Trans., Vol. 2, pp. 443-449, (1962).

45. **Rich, J.C.:** f Values of Bands of the Carbon Monoxide Fourth Positive System. Astrophy. Journ., Vol. 153, No. 1, pp. 327-329, (1968).

46. **Jeunehomme, M.:** Transition Probability Parameters for the Fourth-Positive Band System of Carbon Monoxide. NASA CR-73462, (1970).

47. **Wells, W.C.; and Isler, R.C.:** Measurement of the Lifetime of the $A^1\Pi$ State of CO by Level-Crossing Spectroscopy. Phys. Rev. Letters, Vol. 24, No. 13, pp. 705-708, March 1970.

48. **Cheryenak, J.G.; and Anderson, R.A.:** Radiative Lifetime of the $A^1\Pi$ State of CO. Journ. Optical Society of America, Vol. 61, No. 7, pp. 952-954, (1971).

49. **Pilling, M.J.; Bass, A.M.; and Braun, W.:** A Curve of Growth Determination of the f-Values for the Fourth Positive System of CO and the Lyman-Birge-Hopfield System of N_2. Journ. Quant. Spect. and Rad. Trans., Vol. 11, pp. 1593-1604, (1971).

50. **Mumma, M.J.; Stone, E.J.; and Zipf, E.C.:** Excitation of the CO Fourth Positive Band System by Electron Impact on Carbon Monoxide and Carbon Dioxide. Journ. Chem. Phys., Vol. 54, No. 6, pp. 2627-2634, (1971).

51. **Nicholls, R.W.:** Franck-Condon Factors and r-centroids to High Vibrational Quantum Numbers for Three Band Systems of CO^+ and Absolute Band Strengths for the Comet-Tail System. Canadian Journal of Physics, Vol. 40, pp. 1772-1783, (1962).

52. **Bennett, R.G.; and Dalby, E.W.:** Experimental Oscillator Strength of the Comet-Tail System of CO^+. Journ. Chem. Phys., Vol. 32, No. 4, pp. 1111-1113, (1960).

53. **Robinson, D.; and Nicholls, R.W.:** Intensity Measurements on the CO^+ Comet Tail, and the BO^α and β Molecular Band Systems. Proc. Phys. Soc., Vol. 75, No. 6, pp. 817-825, (1960).

54. **Anderson, R.; Sutherland, R.; and Frey, N.:** Radiative Lifetimes of the $A^2\Pi$ State of CO^+. Journ. Optical Society of America, Vol. 62, No. 10, p. 1127, 1130, October 1972.

55. **Jain, D.C.; and Sahni, R.C.:** Transition Probability Parameters of the Band Systems of CO^+. Journ. Quant. Spect. and Rad. Trans., Vol. 6, pp. 705-715, (1966).

56. **Spindler, R.J.; and Wentink, T.Jr.:** Franck-Condon Factors and Electronic Transition Moment of CO^+ Comet Tail System. Avco Corp. Tech. Mem., RAD-TM-63-55, (1963).

57. Anderson, R.: A Compilation of Measured Lifetimes of Gaseous Diatomic Molecules. Atomic Data, Vol. 3, pp. 227-240, (1971).

58. Krupenie, P.H.; and Benesch, W.: Electronic Transition Moment Integrals for First Ionization of CO and the A-X Transition in CO^+. Some Limitation on the Use of the r-Centroid Approximation. J. Res. N. B. S. - A Physics and Chemistry Vol. 72A, No. 5, pp. 495-503, (1968).

59. Arnold, J.O.; and Nicholls, R.W.: A Shock Tube Determination of the CN Ground State Dissociation Energy and the CN Violet Electronic Transition Moment. Journ. Quant. Spect. and Rad. Trans., Vol. 13, pp. 115-133, (1973).

60. Dunham, T.Jr.: The Concentration of Interstellar Molecules. Proc. of Amer. Astron. Soc., Vol. 10, pp. 123, 124, (1941).

61. White, J.U.: Spectroscopic Measurements of Gaseous CN I. Dissociation in the Electric Discharge. Journ. Chem. Phys., Vol. 8, pp. 79-90, (1940).

62. White, J.U.: Spectroscopic Measurements of Gaseous CN. II. Thermal Dissociation of Cyanogen. J. Chem. Phys., Vol. 8, pp. 459-465, (1940).

63. Tsang, W.; Bauer, S.H.; and Cowperthwaite, M.: Dissociation Energy and Rate of Decomposition of C_2N_2. Journ. Chem. Phys., Vol. 36, No. 7, pp. 1768-1775, (1962).

64. Kudryavtsev, E.M.: Experimental Determination of the Matrix Element of the Dipole Moment of Electronic Transition of the Violet System of Cyanogen Bands. Proc. P. N. Lebedev, Phys. Inst., Vol. 35, pp. 69-143, (1966).

65. Fairbairn, A.R.: Spectrum of Shock Heated Gases Simulating the Venus Atmosphere. AIAA Journal, Vol. 2, pp. 1004-1007, June 1964.

66. Thomas, G.M.; and Menard, W.A.: Experimental Measurements of Nonequilibrium and Equilibrium Radiation From Planetary Atmospheres. AIAA Journal, Vol. 4, No. 2, pp. 227-237, Feb. 1966.

67. Menard, W.A.; Thomas, G.M.; and Helliwell, T.M.: Experimental and Theoretical Study of Molecular, Continuum, and Line Radiation From Planetary Atmospheres. AIAA Paper No: 67-323, (1967).

68. Ambartsumyan, Ye.A.; Ionor, P.V.; and Kon'kov, A.A.: An Experimental Determination of the Oscillator Strength of the Violet System of the CN Radical. NASA TTF 505 pp. 76-85, (1968).

69. Reis, V.H.: Oscillator Strength of the CN Violet System. Journ. Quant. Spect. and Rad. Trans., Vol. 5, pp. 585-594, (1965).

70. McKenzie, R.L.; and Arnold, J.O.: Experimental and Theoretical Investigations of the Chemical Kinetics and Nonequilibrium CN Radiation Behind Shock Waves in CO_2-N_2 Mixtures. AIAA Thermophysics Specialist Conf. New Orleans, AIAA 67-322, (1967).

71. Levitt, B.P.; and Parsons, A.B.: Emissivity and Heat of Dissociation of CN. Trans. Faraday Soc., Vol. 65, p. 1199, 1207, (1969).

72. Liszt, H.S.; and Hesser, J.E.: Transition Probabilities for the Cyanogen B-X Transition. Astrophy. Journ., Vol. 159, p. 1101, 1105, (1970).

73. Moore, J.H.; and Robinson, D.W.: Study of Some Electronic Transition Probabilities in CO and CN. Journ. Chem. Phys., Vol. 48, No. 11, pp. 4870-4874, (1968).

74. Bennett, R.G.; and Dalby, F.W.: Experimental Oscillator Strength of the Violet System of CN. Journ. Chem. Phys., Vol. 36, pp. 399-400, (1962).

75. Nicholls, R.W.: The Interpretation of Intensity Distributions in the CN Violet, C_2 Swan, OH Violet, And O_2 Schumann-Runge Band Systems by Use of Their r-Centroids and Franck-Condon Factors. Proc. Phys. Soc., Vol. 69, pp. 741-753. (1956).

76. Parthasarathi S.; Sastri, V.D.P.; and Joshi, K.C.: Electronic Transition Moment Variation of the CN Violet System. Journ. Quant. Spect. and Rad. Trans., Vol. 6, pp. 903-908, (1966).

77. Prasad, K.; and Prasad, S.S.: Electronic Transition Moment Variation in CN Violet Band System. Journ. Phys. (B) Atomic Mol. Ph., Vol. 2, Ser. 2, pp. 725,726, (1969).

78. Prasad, S.S.: On The Variation of Electronic Transition Moment R_e in CN Violet Band Systems. Indian J. Phys., Vol. 34, pp. 584, 585, (1960).

79. Klemsdal, H.: The Variation of the Electronic Transition Moment R_e in the Intensity Theory of Diatomic Molecules. Journ. Quant. Spect. and Rad. Trans., Vol. 13, pp. 517-541, (1973).

80. Dickerman, P.J.: Radiative Energy Transfer on Entry into Mars and Venus. IIT Res. Inst. Report, p. 6048, (1969).

81. Linevsky, M.J.: Relative Oscillator Strengths of CH. The Heat of Dissociation of CH. Journ. Chem. Physics, Vol. 47, No. 9, pp. 3485-3490, (1967).

82. Jeunehomme, M.; and Duncan, A.B.F.: Absolute Measurements of Some Excited States of Nitrogen, Nitric Oxide, and Formaldehyde. Journ. Chem. Phys., Vol. 41, No. 6, pp. 1692-1699, (1964).

83. Hesser, J.E.; and Lutz, B.L.: Probabilities for Radiation and Predissociation II. The Excited States of CH, CD, and CH^+, and Some Astrophysical Implications. Astrophysical Journ., Vol. 159, pp. 703-718, (1970).

84. Bennett, R.G.; and Dalby, F.W.: Experimental Oscillator Strengths of CH and NH. Journ. Chem. Phys., Vol. 32, pp. 1716-1719, (1960).

85. Huo, W.M.: Valence Excited States of NH and CH and Theoretical Transition Probabilities. Journ. Chem. Physics, Vol. 49, No. 4, pp. 1482-1492, (1968).

86. Stephenson, G.: Calculation of the Oscillator Strength for the $^2\Pi$ - $^2\Delta$ Transition in the CH Molecule. Proc. Phys. Soc., Vol. A64, pp. 666-667, (1951).

87. Hurley, A.C.: The Electronic Structure of the First Row Hydrides BH, CH, NH, OH II. Excited States. Proc. Phys. Soc., Vol. 249A, pp. 402-413, (1959).

88. Harrington, J.A.; Modica, A.P.; and Libby, D.R.: Erattum: Shock Tube Determination of the $C_2(A^3\Pi - X^3\Pi$ and $CF(A^2\Sigma^+ - X^2\Pi)$ Band System Oscillator Strengths. Journ. Chem. Phys., Vol 45, p. 2720, (1966).

89. Wentink, T.Jr.; and Isaacson, L.: Oscillator Strengths of CF and Comments on Heats of Formation of CF and CF_2. Journ. Chem. Phys., Vol. 46, pp. 603-605, (1967).

90. Wentink, T.Jr.; Isaacson, L.; Economou, G.J.; and Flinn, D.: Ultraviolet Emission from CF Bands and Continua. Avco Report RAD-TM-63-53, July 1963.

91. Weltner, W.Jr.; Walsh, P.N.; and Angell, C.L.: Spectroscopy of Carbon Vapor Condensed in Rare Gas Matrices at 4° and 20°K I. Journ. Chem. Phys., Vol. 40, No. 5, pp. 1299-1305, (1964).

92. Weltner, W.Jr.; and McLeod, D.Jr.: Spectroscopy of Carbon Vapor Condensed in Rare-Gas Matric at 4° and 20°K II. Journ. Chem. Phys., Vol. 40, No. 5, pp. 1305-1316, (1964).

93. Weltner, W.Jr.; and McLeod, D.Jr.: Spectroscopy of Carbon Vapor Condensed in Rare Gas Matrices at 4° and 20°K III. Journ. Chem. Phys., Vol. 45, No. 8, pp. 3096-3105, (1966).

94. Barger, R.L.; and Broida, H.P.: Spectra of C_3 in Solidified Gases at 4° and 20°K. Journ. Chem. Phys., Vol. 43, No. 7, pp. 2364-2370, (1965).

95. Barger, R.L.; and Broida, H.P.: Absorption Spectrum of Carbon Vapor in Solid Argon at 4° on 20°K. Journ. Chem. Phys., Vol. 37, pp. 1152-1153, (1962).

96. Brewer, L.; and Engelke, J.L.: Spectrum of C_3. Journ. Chem. Phys., Vol. 36, pp. 992-998, (1962).

97. Gausset, L.; Herzberg, G.; Lagerquist, A.; and Rosen, B.: Analysis of the 4050Å Group of the C_3 Molecule. Astrophy. Journ., Vol. 142, pp. 45-76, (1965).

98. Nicholls, R.W.; Fraser, P.A.; Jarmain, W.R.: Transition Probability Parameters of Molecular Spectra Arising from Combustion Processes. Comb. and Flames, Vol. 3, pp. 13-38, (1959).

99. Ortenberg, F.S.: Calculation of Franck-Condon Factors for the NO, C_2, and CO Band Systems. Optika i Spektroskopiya, Vol. 6, pp. 398-400, (1964).

100. Nicholls, R.W.: Franck-Condon Factors to High Quantum Numbers. VI. C_2 Band Systems. Journ. Res. NBS, Vol. 69A, No. 5, pp. 397-400, (1965).

101. Halman, M.; and Laulicht, I1: Isotope Effects on Transition Probabilities. IV. Electronic Transitions of Isotopic C_2, CO, CN, H_2, and CH Molecules. Suppl. Journ. Astrophysics, Vol. 12, pp. 307-321, (1966).

102. Fraser, P.A.; Jarmain, W.R.; and Nicholls, R.W.: Vibrational Transition Probabilities of Diatomic Molecules: Collected Results. II. N_2^+, CN, C_2, O_2, TiO. Astrophys. Journ., Vol. 119, pp. 286-290, (1954).

103. Liszt, H.S.; and Smith, W.H.: RKR Franck-Condon Factors for Blue and Ultraviolet Transitions for Some Molecules of Astrophysical Interest and Some Comments on the Interstellar Abundance of CH, CH^+, and SiH^+. Journ. Quant. Spect. and Rad. Trans., Vol. 12, No. 5, pp. 947-959, (1972).

104. Childs, D.R.: Vibrational Wave Functions and Franck-Condon Factors of Various Band Systems. Journ. Quant. Spect. and Rad. Trans., Vol. 4, pp. 283-290, (1964).

105. Nicholls, R.W.: Franck-Condon Factors to High Vibrational Quantum Numbers. III: CN. Journ. Res. Nat. Bur. Std., A. Phys. and Chem., Vol. 68A, No. 1, pp. 75-78, Jan./Feb. 1964.

106. Fraser, P.A.: Vibrational Transition Probabilities of Diatomic Molecules. III. Proc. Phys. Soc. Lond., Vol. 67, pp. 939-941, (1954).

107. McCallum, J.C.; Jarmain, W.R.; and Nicholls, R.W.: Franck-Condon Factors and Related Quantities for Diatomic Molecular Band System. 1970 Spectroscopic Report, No. 5, York Univ., C.R.E.S.S., March 1970.

108. Popova, T.N.; and Saschenko, N.M.: Franck-Condon Factors for Some Vibrational Transitions in the Fourth Positive System of CO. Opt. Spect., Vol. 12, pp. 447-448, (1962).

109. Jarmain, W.R.; Ebisuzaki, R.; and Nicholls, R.W.: Franck-Condon Factors and r-Centroids for Some Bands of the CO Fourth Positive ($A\Pi - X\Sigma$) Band System. Can. Journ. Phys., Vol. 38, pp. 510-512, (1960).

110. Singh, N.L.; and Jain, D.C.: Franck-Condon Factors and r-Centroids for the Triplet Band System of CO Molecule. Proc. Phys. Soc. Vol. 78, pp. 399-403, (1961).

111. Nicholls, R.W.; Fraser, P.A.; Jarmain, W.R.; and McEachran, R.P.: Vibrational Transition Probabilities of Diatomic Molecules: Collected Results. IV. BeO, BO, CH^+, CO, NO, SH, O_2, O_2^+. Astrophy. Journ., Vol. 131, No. 2, pp. 399-406, March 1960.

112. Jarmain, W.R.; Fraser, P.A.; and Nicholls, R.W.: Vibrational Transition Probabilities of Diatomic Molecules; Collected Results. III. N_2, NO, O_2, O_2^+, OH, CO, CO^+. Astrophy. Journ., Vol. 122, pp. 55-61, (1955).

113. Henry, R.J.W.: Photoionization Cross Sections for Atom and Ions of Carbon, Nitrogen, Oxygen, and Neon. Astrophy. Journ., Vol. 161, pp. 1153-1155, Sept. (1970).

114. Thomas, G.M.; and Helliwell, T.M.: Photoionization Cross Sections of Nitrogen, Oxygen, Carbon, and Argon for the Slates-Klein-Brueckner Potential. Journ. Quant. Spect. and Rad. Trans., Vol. 10, pp. 423-448, (1970).

115. Sherman, M.P.; and Kulander, J.L.: Free-Bound Radiation from Nitrogen Oxygen and Air. Gen. Elect. R65 SD 15, May 1965.

116. Dalgarno, A.: Planetary Atmosphere Studies VII: Photoionization of Atomic Oxygen and Nitrogen. Geophysics Corp. of Amer. GCA TR 60-5-N N-62-16005, (Dec. 1960).

117. Cairns, R.B.; and Samson, J.A.R.: Total Absorption Cross-Section of Atomic Oxygen Below 910Å. Phys. Rev., Vol. 139, No. 5A, pp. A1403-A1407, August 1965.

118. Stolarski, R.S.; and Johnson, N.P.: Photoionization and Photo-absorption Cross Sections for Ionospheric Calculations. Journ. of Atmospheric and Terrestrial Phys., Vol. 34, pp. 1691-1701, (1972).

119. Hofmann, W.; and Weissler, G.L.: Measurement of the Photoionization Cross Section in the Resonance Continuum of CI Using a Wall-Stabilized Arc. J. Opt. Soc. Am., Vol. 61, No. 2, Feb. 1971, pp. 228-230.

120. Norman, G.E.: Photoionization Cross-Sections of the Lower Excited States and Oscillator Strengths of Certain Lines of Carbon and Nitrogen Atoms. Opt. Spect., Vol. 14, No. 5, pp. 315-317, (1963).

121. Garrett, W.R.; and Jackson, H.T., Jr.: Electron Photodetachment from O^- and Elastic Scattering from Atomic Oxygen. Phys. Rev., Vol. 153, No. 1, pp. 28-35, January 1967.

122. Cooper, J.W.; and Martin, J.B.: Electronic Photodetachment from Ions and Elastic Collision Cross Sections for O, C, Cℓ, and F. Phys. Rev., Vol. 129, pp. 1482-1486, May 1962.

123. Branscomb, L.M.; Burgh, S.S.; Smith, S.J.; and Geltman, S.: Photodetachment Cross Section and Electron Affinity of Atomic Oxygen. Phys. Rev., Vol. 111, pp. 504-513, (1958).

124. Seman, M.L.; and Branscomb, L.M.: Structure and Photodetachment Spectrum of the Atomic Carbon Negative Ion. Phys. Rev., Vol. 125, No. 5, pp. 1602-1607, (1962).

125. Henry, R.J.W.: Photcionization Cross Sections for C^-, N, and O^+. Journ. of Chem. Phys., Vol. 44, pp. 4357-4359, June 1966.

126. Myerscough, V.P.; and McDowell, M.R.C.: Continuous Absorption By the Carbon Negative Ion II. Free-Free Absorption. Mon. Nat. R. Astr. Soc., Vol. 132, pp. 457-461, (1966).

127. Wiese, W.L.; Smith, M.W.; and Glennon, B.M.: Atomic Transition Probabilities, Hydrogen through Neon. Vol. 1, NBS, NSRDS, NBS 4, May 1966.

128. Wilson, K.H.; and Nicolet, W.E.: Spectral Absorption Coefficients of Carbon, Nitrogen, and Oxygen Atoms. Journ. Quant. Spect. and Rad. Trans., Vol. 7, No. 6, pp. 891-941, Nov./Dec. 1967.

129. Miller, M.H.: Thermally Insensitive Determinations of Transition Probabilities for CI, OI, NeI, AℓII, SiI, SiII, PI, PII, SI, SII, and CℓI. Univ. of Md. Tech. Note BN-550, May 1968.

130. Bengtson, R.D.: The Measurement of Transition Probabilities and Stark Widths for CI, FI, CℓI, CℓII, BrI, and BrII. U. Maryland, TN BN-559, July 1968.

131. Roberts, J.R.; and Eckerle, K.L.: Measurements of Relative Oscillator Strengths of Some CII Multiplets. Phys. Rev., Vol. 153, No. 1, pp. 87-90, (1967).

132. Hunt, B.L.; and Sibulkin, M.: Radiative Transfer in a Gas of Uniform Properties in Local Thermodynamic Equilibrium. Office of Naval Research, Rep't No.'s. Nonr - 562 (35)/16 to 562(35)/ 18, December 1966.

133. Hunt, B.L.; and Sibulkin, M.: A Simple Method for Calculating the Frequency-Integrated Radiation Due to Weak, Closely Spaced Lines in a Uniform Gas. Journ. Quant. Spectros. and Rad. Trans., Vol. 7, pp. 951-964, 1967.

134. Johnson, R.R.: Free-Free Radiation Transitions, A Survey of Theoretical Results. Journ. Quant. Spect. and Rad. Trans., Vol. 7, pp. 815-835, (1967).

135. Kivel, B.: Neutral Atom Bremsstrahlung. Avco RR 247, June 1966.

136. Kivel, B.: Bremsstrahlung in Air. Avco RR 249, June 1966.

137. Biberman, L.M.; and Norman, G.E.: Emission of Recombination Radiation and Bremsstrahlung of a Plasma. Journ. Quant. Spect. and Rad. Trans., Vol. 3, pp. 221-245, (1963).

138. Biberman, L.M.; and Norman, G.E.: Continuous Spectra of Atomic Gases and Plasma. Soviet Phys. Uspekhi, Vol. 10, No. 1, July/August 1967.

139. Karzas, W.J.; and Latter, R.: Electron Radiative Transitions in a Coubomb Field. Astrophy. Journ. Suppl., No. 6, p. 167, (1961).

140. Geltman, S.: Free-Free Radiation in Electron-Neutral Atom Collisions. Journ. Quant. Spect. and Rad. Trans., Vol. 13, pp. 601-613, (1973).

141. Morris, J.C.; Krey, R.U.; and Bach, G.R.: Bremsstrahlung and Recombination Radiation of Atomic and Ionic Oxygen. Phys. Rev., Vol. 159, No. 1, pp. 113-119, (1967).

142. Morris, J.C.; Krey, R.U.; and Garrison, R.L.: Bremsstrahlung and Recombination Radiation of Neutral and Ionized Nitrogen. Physical Rev., Vol. 180, No. 1, pp. 167-183, April 1968.

143. Allen, R.A.; Textoris, A.; and Wilson, J.: Measurements of the Free-Bound and Free-Free Continua of Nitrogen, Oxygen and Air. AVCO Research Report: 195, (1964). Also Journ. Quant. Spect. and Rad. Trans., Vol. 5, pp. 95-108, (1965).

144. Allen, R.A.; Taylor, R.L.; and Textoris, A.: Kramers' and Line Radiation from Nitrogen and Air Shocks. AVCO Rept. AMP-113, May 1963.

145. Taylor, R.L.; and Caledonia, G.: Experimental Determination of the Cross Section for Neutral Bremsstrahlung II. High Temperature Air Species O, N, N_2^*. AVCO RR 312, (1968).

146. Dixon, R.N.; and Nicholls, R.W.: An Experimental Study of the Band Intensities in the CN Red System. Con. Journ. Phy., Vol. 36, pp. 127-133, (1958).

147. Wentink, T.; Isaacson, L.; and Morreal, J.: Radiative Lifetime of the $^2\Pi$ State of the CN Red System. Journ. Chem. Phys., Vol. 41, No. 1, pp. 278-279, July 1964.

148. Jeunehomme, M.: Oscillator Strength of the CN Red System. Journ. Chem. Phys., Vol. 42, No. 12, pp. 4086-4088, June 1965.

149. Hansche, G.E.: Conditions Influencing the Intensity of the $^3\Pi - {}^1\Sigma$ Cameron Bands of CO. Phys. Rev., Vol. 57, pp. 289-291, (1940).

150. Meyer, B.; Smith, J.J.; and Spitzer, K.: Phosphorescent Decay of Matrix-Isolated GeO, GeS, SnO, and SnS, and the Lifetime of the Cameron Bands of CO-Type Diatomics. Journ. Chem. Phys., Vol. 53, No. 9, pp. 3616-3620, (1970).

151. Donovan, R.J.; and Husain, D.: Vibrational Excitation of Carbon Monoxide Following Quenching of the a $^3\Pi$ State. Trans. Faraday Soc., Vol. 63, pp. 2879-2887, (1967).

152. Borst, W.L.; and Zipf, E.C.: Lifetimes of Metastable CO and N_2 Molecules. Phys. Rev. A, Vol. 3, No. 3, pp. 979-989, (1971).

153. Fairbairn, A.R.: Band Strengths in Forbidden Transitions: The Cameron Bands of CO. Journ. Quant. Spect. and Rad. Trans., Vol. 10, pp. 1321-1328, (1970).

154. Fairbairn, A.R.: Errata - Band Strengths in Forbidden Transitions: The Cameron Bands of CO. Journ. Quant. Spect. and Rad. Trans., Vol. 11, p. 1289, (1971).

155. Hasson, V.; and Nicholls, R.W.: Absolute Absorption Oscillator Strength Measurements on the ($a^3\Pi - X^1\Sigma$) Cameron Band System of CO. Journ. Phys. B, Vol. 4, pp. 681-683, (1971).

156. Lawrence, G.M.: Quenching and Radiation Rates of CO ($a^3\Pi$). Chem. Phys. Lett., Vol. 9, No. 6, pp. 575-577, (1971).

157. Lawrence, G.M.; and Seitel, S.C.: Oscillator Strengths in the Cameron System of Carbon Monoxide. Journ. Quant. Spect. and Rad. Trans., Vol. 13, pp. 713-716, (1973).

158. Johnson, C.E.; and VanDyck, R.S.: Lifetime of the $a^3\Pi$ Metastable State of Carbon Monoxide. Journ. Chem. Phys., Vol. 56, No. 4, pp. 1506-1510, (1972).

159. Slanger, T.G.; and Black, G.: CO($a^3\Pi$), Its Production, Detection, Deactivation, and Radiative Lifetime. Journ. Chem. Phys., Vol. 55, No. 5, pp. 2164-2173, (1971).

160. James, T.C.: The Transition Moments, Franck-Condon Factors, and Lifetimes of Forbidden Transitions. Calculation of the Intensity of the Cameron System of CO. Journ. Chem. Phys., Vol. 55, No. 8, pp. 4118-4124, Oct. 1971.

161. Meyer, V.D.; Skerbele, A.; and Lassettre, E.N.: Intensity Distribution in the Electron Impact Spectrum of Carbon Monoxide at High-Resolution and Small Scattering Angles. Journ. Chem. Phys., Vol. 43, pp. 805-816, (1965).

162. Barrow, R.F.; Gratzer, W.B.; and Malherbe, J.F.: Intensities of Bands in the System $b^3\Sigma^+ - a^3\Pi$ of Carbon Monoxide. Proc. Phys. Soc., Vol. A69, pp. 574, 576, (1956).

163. Robinson, D.; and Nicholls, R.W.: Intensity Measurements on the O_2^+ Second Negative CO Angstrom and Third Positive and NO γ and β Molecular Band Systems. Proc. Phys. Soc., Vol. 71, pp. 957-964, (1958).

164. Tawde, N.R.; and Patil, B.S.: The Evaluation of the Electronic Transition Moment for the $b^3\Sigma^+ - a^3\Pi$ System of CO. Ind. Journ. Phys., Vol. 33, pp. 505-510, (1959).

165. Schwenker, R.P.: Experimental Oscillator Strengths of CO and CO^+. Journ. Chem. Phys., Vol. 42, No. 6, pp. 1895-1897, (1965).

166. Fowler, R.G.; and Holzberlein, T.M.: Transition Probabilities for H_2, D_2, N_2, N_2^+, and CO. Journ. Chem. Phys., Vol. 45, No. 1, pp. 1123-1125, (1966).

167. Isaacson, L.; Marram, E.P.; and Wentink, T.Jr.: Electronic Transition Moment of CO + $B^2\Sigma - X^2\Sigma$. Journ. Quant. Spect. and Rad. Trans., Vol. 7, p. 691, (1967).

168. Joshi, K.C.; Sastri, V.D.P.; and Parthasarathi, S.: Absolute Transition Probabilities, Oscillator Strengths, and Electronic Transition Moments for the First Negative System of CO^+. Journ. Quant. Spect. and Rad. Trans., Vol. 6, p. 215, (1966).

169. Lawrence, G.M.: Lifetimes and Transition Probabilities in CO^+. Journ. Quant. Spect. and Rad. Trans., Vol. 5, pp. 359-367, (1965).

170. Fink, E.H.; and Welge, K.H.: Lebensdauern und Löschquerschnitte elektronisch angeregter Zustände von N_2O^+, CO^+, und CO. Zeit Naturforsch, Vol. 23A, pp. 358-376, (1968).

171. Desesquelles, J.; duFay, M.; and Poulizac, M.C.: Lifetime Measurement of Molecular States with an Accelerated Ion Beam. Physics Letters, Vol. 27A, No. 2, pp. 96-97, (1968).

172. Fowler, R.G.; Skwerski, P.R.; Anderson, R.A., Copeland, G.E.; and Holzberlein, T.M.: Radiative Lifetime of the $B^2\Sigma^+$ State of CO^+. Journ. Chem. Phys., Vol. 50, No. 10, pp. 4133-4135, May 1969.

173. Judge, D.L.; and Lee, L.C.: Electronic Transition Moments for the A→X, B→X, and B→A Transitions in CO^+ and the A←X and B←X Moments for the CO→CO^+ Systems; Absolute Cross Sections for the Absorption Processes. Journ. Chem. Phys., Vol. 57, No 1, pp. 455-462, (1972).

174. Aarts, J.F.M.; and DeHeer, F.J.: Emission Cross Sections of the $A^2\Pi$ and $B^2\Sigma^+$ States of CO^+. Physica, Vol. 49, pp. 425-440, (1970).

TABLE I - MEASURED ELECTRONIC f-NUMBERS FOR C_2 SWAN SYSTEM

Source Date	Ref.	Wavelength of Measurement, Nanometers	f_{el}	Method
Arnold 1968	17	516.5 471	0.035 ± .005 0.043 ± .006	Shock Tube emission
Fairbairn 1966	19	509-529	0.033 ± .012	Shock Tube emission
Fink & Welge 1967	24		0.022	Phase Shift
Hagan 1963	18	516	0.007 ± .004	Furnace, emission, and absorption
Harrington, Modica, and Libby 1966	22	516	.028 ± .009	Shock Tube emission
Hicks 1957	23	516	0.026 (a)	Furnace
Jeunehomme, Schwenker 1965	16		0.006	Laser excitation
Smith 1969	25	471	0.025 ± .003	Phase Shift
Sviridov, et. al. 1965	20		0.022 ± .008	Shock Tube, emission

TABLE I - (Continued)

Sviridov et. al. 1966	21		0.028 ± .009	Shock Tube
Wentink et. al. 1967	7		0.0133	Laser excitation

(a) original value of 0.034 adjusted by Fairbairn

TABLE II CALCULATED f-NUMBERS FOR C_2 SWAN SYSTEM

Source Date	Ref.	f_{el}	Remarks
Clementi 1960	28	0.048	Considers hybridization
Coulson & Lester 1955	31	0.24	A general estimate based on hybridization and orthogonalization
Lyddane, Rogers 1941	27	0.024	
Shull 1950	29	0.13	Considers hybridization
Stephenson 1950	26	0.029	
Spindler 1965	30	0.0357	Based on Jeunehomme's lifetime measurement (ref. 16)

TABLE III MEASURED ELECTRONIC f-NUMBER FOR CN VIOLET

Source Date	Ref.	Experimental Method	Assumed D_o, eV	Wavelength Region of Measurement (nm)	Bandpass Nanometers	$f_{el}(\lambda)$
Arnold & Nicholls (1973)	59	Shock Tube (incident shock) emission	7.89	358.0 386.0 417.0 421.5	4.7 4.7 4.7 2.35	0.031 ± 0.005 0.035 ± 0.005 0.033 ± 0.005 0.034 ± 0.005
Dickerman (1969)	80	Shock Tube (incident shock) emission	8.1	388.0	1.5	0.033 ± 0.003
Levitt & Parsons (1968)	71	Shock Tube (incident shock) emission	7.8 ± 0.2	421.5	7.5	0.027
Kudryavtsev, et. al. (1968)	64	Shock Tube (reflected shock) absorption	7.54	388.0 & 421.5	Rot. Line Anal.	0.030 ±0.004
Ambartsyumyan, Ionov & Kon'kov (1968)	68	Shock Tube (reflected shock) absorption	7.5	388.0	~1.5	0.027 ± 0.006
Menard, et. al. (1966-67)	66 67	Shock Tube (incident shock) emission	7.7	421.6 - 358.0	3.2	0.027
McKenzie & Arnold (1967)	70	Shock Tube (incident shock) emission	8.2	421.6	2.9	0.023 ± 0.003
Harrington (1967)	7	Shock Tube (emission)	7.5 - 7.6	?	?	0.026 ± 0.0066

TABLE III - Concluded MEASURED ELECTRONIC f-NUMBER FOR CN VIOLET

Source Date	Ref.	Experimental Method	Assumed D_o, eV	Wavelength Region of Measurement (nm)	Bandpass Nanometers	$f_{el}(\lambda)$
Reis (1965)	69	Ballistic Range (emission)	8.2	358.0 417.0	~10 ~10	0.019 ± 0.004 0.020 ± 0.004
Fairbairn (1964)	65	Shock Tube (reflected shock) emission	8.35 7.6	~420.0	-- --	0.016 ± 0.008 0.031 ± 0.015
Tsang, Bauer, & Cowperthwaite (1962)	63	Shock Tube (incident shock) absorption	7.95	388.3 421.6	0.75	0.013 0.008
White (1940)	61	Absorption measurements at room temp. CN formed by electric discharge through C_2N_2.	--	388.3	Rot. Line Anal.	0.026 ± 0.006
White (1940)	62	Reanalysis of data in earlier paper	--	388.3	Rot. Line Anal.	0.1 ± 0.05
Dunham (1941)	60	Absorption measurement in a high temp. graphite furnace (2300 K)	--	387.4	Rot. Line Anal.	0.07
Liszt & Hesser (1970)	72	Lifetime	--	388.0	0.6	0.039 ± 0.004
Moore & Robinson (1968)	73	Lifetime	--	388.0	0.5	0.028 ± 0.003
Bennett & Dalby (1962)	74	Lifetime	--	390.0	10	0.027 ± 0.003

TABLE IV MEASURED ELECTRONIC f-NUMBERS FOR CH BAND SYSTEMS

Source	Ref.	$A^2\Delta - X^2\Pi$		$B^2\Sigma^- - X^2\Pi$		$C^2\Sigma^+ - X^2\Pi$		Remarks
		f_{el}	λ(nm)	f_{el}	λ(nm)	f_{el}	λ(nm)	
Bennett & Dalby	84	0.0049 ± 0.0005	427	0.0012 ± 0.0004	400[a]	--	--	Interrupted electron beam radiative lifetime meas. spec. resol. ≃ 10nm
Fink & Welge	24	0.0052 ± 0.0004	430	0.0028 ± 0.0005	388.8	--	--	Radiative lifetime measurement using phase shift technique spec. resol. = 2nm
Jeunehomme & Duncan	82	0.0093	~431.4	--	--	--	--	Interrupted electron beam radiative lifetime meas. spec. resol. ≃ 5 - 10nm
Hesser & Lutz	83	0.0059	431.2	0.0033	387.1	--	--	Radiative lifetime meas. using phase shift technique spec. resol. ~.5 - .8nm
Dunham	60	0.06	430	--	--	--	--	Absorption measurement on $R_2(1)$ line made in a high temp. (~2800 C) graphite furnace
Linevsky	81	--	--	0.003	~385.0	0.0063	~314.3	Absorption measurements made on selected rotational lines in a graphite furnace (T~3000°K). Measured f(B-X)/f(A-X) = 0.62 and f(C-X)/f(A-X) = 1.26 ratios put on absolute basis using f(A-X) = 0.005.

[a]Wavelength calculated from equation 30 using quoted f-value and measured lifetime.

TABLE V CALCULATED ELECTRONIC f-NUMBERS FOR CH

Source Date	Ref.	$A^2\Delta - X^2\Pi$		$B^2\Sigma^- - X^2\Pi$		$C^2\Sigma^+ - X^2\Pi$		Remarks
		f_{el}	λ(nm)	f_{el}	λ(nm)	f_{el}	λ(nm)	
Stephenson 1951	86	0.008	432.0	--	--	--	--	One-electron approximation with dipole length form at transition moment
Hurley 1959	87	0.014	--	0.012	--	0.0092	--	Intra atomic correlation correction using dipole length form
Huo 1968	85	0.0036 0.0046	~431.5	0.0027 0.001	~385	0.0048 0.0032	~341.3	Active electron approx. using a) dipole length b) dipole velocity

TABLE VI MEASURED ELECTRONIC f-NUMBERS FOR CF BAND SYSTEMS[a]

Source Date	Ref.	Method	Transition	Wavelength region of measurement (nm)	Bandpass Nanometers	$f_{el}(\lambda)$
Harrington, et. al. (1965)	88	Shock Tube	$A^2\Sigma^+ - X^2\Pi$	232.9	~5.6	0.026 ± 0.0075[b]
	22	(reflected shock)		237.7		0.018 ± 0.0065
		emission		254.7		0.0195 ± 0.0055
Hesser & Dressler (1966)	42	Lifetime	$A^2\Sigma^+ - X^2\Pi$	233.0	0.8	0.0271[c]
		(phase-shift)	$B^2\Sigma^+ - X^2\Pi$	202.5	0.8	0.0167[d]
Hesser (1968)	43	Lifetime	$A^2\Sigma^+ - X^2\Pi$	233.0	0.8	0.0244[e]
		(phase-shift)	$B^2\Sigma^+ - X^2\Pi$	202.5	0.8	0.0161[f]

[a]The state and wavelength assignments are those used in Refs. 43 and 89. Assignment of the B state as a $^2\Sigma^+$ state is uncertain, and therefore the statistical-weight factor entering the lifetime-to oscillator strength conversion is uncertain. Oscillator strengths given for the B-X transition assume the upper state is $^2\Sigma^+$.

[b]Emission oscillator strengths quoted in Ref. 88 converted to absorption f-values using $f_{abs} = \frac{2}{4} f_{emis}$.

[c]Electronic f-number calculated in Ref. 89 assuming τ for $v' = 0$ same as for $v' = 1$ ($\tau = 19$ nsec), which was measured, and using $q_{o,o} = 0.1064$.

[d]Electronic f-number calculated in Ref. 89 using measured $\tau(\tau = 19$ nsec) and $q_{o,o} = 0.6765$.

[e]Calculated using $f_{el} = \frac{f_{v'v''}}{q_{v'v''}}$ where $f_{o,o} = 2.6\times10^{-3}$ and $q_{o,o} = 0.1064$.

[f]Calculated using $f_{el} = \frac{f_{v'v''}}{q_{v'v''}}$ where $f_{o,o} = 1.09\times10^{-2}$ and $q_{o,o} = 0.6765$.

TABLE VII C_3 ABSORPTION CROSS SECTION

T = 3200 K
N = 3.268 E + 16 cc^{-3}

λ, nm	σ, cm^2	λ, nm	σ, cm^2
497.51	3.508E-18	415.80	1.590E-17
492.13	3.745E-18	413.05	1.722E-17
486.38	3.988E-18	410.68	1.893E-17
480.31	4.240E-18	409.16	2.064E-17
474.61	4.626E-18	407.50	2.248E-17
467.73	5.317E-18	405.68	2.419E-17
461.25	5.864E-18	403.39	2.591E-17
455.58	5.979E-18	401.61	2.693E-17
453.31	6.444E-18	399.36	2.755E-17
450.25	7.066E-18	397.46	2.787E-17
448.43	7.658E-18	395.57	2.806E-17
447.03	8.378E-18	393.86	2.797E-17
445.63	8.689E-18	393.08	2.744E-17
443.07	8.885E-18	391.85	2.665E-17
440.72	9.073E-18	390.32	2.641E-17
438.98	9.946E-18	388.80	2.576E-17
437.25	1.067E-17	385.36	2.476E-17
434.22	1.157E-17	382.26	2.416E-17
431.41	1.237E-17	379.22	2.370E-17
427.72	1.325E-17	375.37	2.299E-17
423.37	1.460E-17	372.72	2.238E-17
420.87	1.480E-17	369.96	2.191E-17
418.41	1.514E-17		

TABLE VIII SUMMARY OF FRANCK-CONDON FACTOR SOURCES

BAND SYSTEM	REFERENCE NUMBERS	
	Rydberg-Klein-Rees or Klein-Dunham potential	Morse Potential
C_2 Swan	33, 30	98, 99, 100, 101, 102
C_2 Deslandres d'Azambuja	7	98
C_2 Mulliken		98, 100, 101
C_2 Phillips	30	98, 99, 100, 101
C_2 Fox Herzberg B-X	7, 33	98, 100, 101
C_2 Balik-Ramsey A'-X		100, 101
CF		89
CH A-X	103	101, 104
CH B-X	103	101, 104
CH C-X	103	7, 101
CN Violet	30	10, 98, 101, 102, 104, 105, 106
CN Red	30	102, 105
CO Fourth Positive	7, 107	39, 99, 101, 108, 109
CO Triplet	107	110
CO Third Positive		99, 111
CO Angstrom		99, 111
CO Cameron	107	44, 101, 112
CO Asundi	107	101, 112
CO^+ Comet-Tail	55, 107	51, 101, 112, 56
CO^+ First Negative	55, 107	44, 51, 101

TABLE VII C_3 ABSORPTION CROSS SECTION

T = 3200 K
N = 3.268 E + 16 cc^{-3}

λ, nm	σ, cm^2	λ, nm	σ, cm^2
497.51	3.508E-18	415.80	1.590E-17
492.13	3.745E-18	413.05	1.722E-17
486.38	3.988E-18	410.68	1.893E-17
480.31	4.240E-18	409.16	2.064E-17
474.61	4.626E-18	407.50	2.248E-17
467.73	5.317E-18	405.68	2.419E-17
461.25	5.864E-18	403.39	2.591E-17
455.58	5.979E-18	401.61	2.693E-17
453.31	6.444E-18	399.36	2.755E-17
450.25	7.066E-18	397.46	2.787E-17
448.43	7.658E-18	395.57	2.806E-17
447.03	8.378E-18	393.86	2.797E-17
445.63	8.689E-18	393.08	2.744E-17
443.07	8.885E-18	391.85	2.665E-17
440.72	9.073E-18	390.32	2.641E-17
438.98	9.946E-18	388.80	2.576E-17
437.25	1.067E-17	385.36	2.476E-17
434.22	1.157E-17	382.26	2.416E-17
431.41	1.237E-17	379.22	2.370E-17
427.72	1.325E-17	375.37	2.299E-17
423.37	1.460E-17	372.72	2.238E-17
420.87	1.480E-17	369.96	2.191E-17
418.41	1.514E-17		

TABLE VIII SUMMARY OF FRANCK-CONDON FACTOR SOURCES

BAND SYSTEM	REFERENCE NUMBERS	
	Rydberg-Klein-Rees or Klein-Dunham potential	Morse Potential
C_2 Swan	33, 30	98, 99, 100, 101, 102
C_2 Deslandres d'Azambuja	7	98
C_2 Mulliken		98, 100, 101
C_2 Phillips	30	98, 99, 100, 101
C_2 Fox Herzberg B-X	7, 33	98, 100, 101
C_2 Balik-Ramsey A'-X		100, 101
CF		89
CH A-X	103	101, 104
CH B-X	103	101, 104
CH C-X	103	7, 101
CN Violet	30	10, 98, 101, 102, 104, 105, 106
CN Red	30	102, 105
CO Fourth Positive	7, 107	39, 99, 101, 108, 109
CO Triplet	107	110
CO Third Positive		99, 111
CO Angstrom		99, 111
CO Cameron	107	44, 101, 112
CO Asundi	107	101, 112
CO^+ Comet-Tail	55, 107	51, 101, 112, 56
CO^+ First Negative	55, 107	44, 51, 101

TABLE IX

FRANCK-CONDON FACTORS

C_2 SWAN BAND SYSTEM

Reference 30

v'	v''							
	0	1	2	3	4	5	6	7
0	0.7213	0.2206	0.0476	0.0088	0.0015	0.0002	0.0000	0.0000
1	0.2506	0.3371	0.2803	0.0999	0.0254	0.0054	0.0010	0.0002
2	0.0272	0.3742	0.1381	0.2621	0.1377	0.0453	0.0119	0.0027
3	0.0008	0.0659	0.4255	0.0477	0.2112	0.1572	0.0647	0.0202
4	0.0000	0.0022	0.1055	0.4446	0.0143	0.1576	0.1592	0.0782
5		0.0000	0.0028	0.1341	0.4585	0.0046	0.1137	0.1525
6			0.0002	0.0019	0.1492	0.4831	0.0042	0.0804
7			0.0000	0.0008	0.0001	0.1413	0.5192	0.0103

TABLE X - FRANCK-CONDON FACTORS FOR CH A-X

V'	V"0	1	2	3
0	.9930 .9996 .9923	--- .0002 .0071	--- .0000 .0005	--- .0000 ---
1	--- .0002 .0074	.9867 .9986 .9843	--- .0001 ---	--- .0000 ---
2	--- .0000 .0002	--- .0001 ---	.9894 .9947 ---	--- .0028 ---
3	--- .0000 ---	--- .0000 ---	--- .0032 ---	--- .9819 ---

1st ref. 103 RKR
2nd ref. 104 Morse
3rd ref. 101 Morse

TABLE XI- FRANCK-CONDON FACTORS FOR CH B-X

V'	0	1	2	3
0	.8623 .5937 .7042	.1187 .0006 ---	.0179 .1691 .0278	--- .0525 ---
1	.1231 .0013 .1557	.5538 .2176 .1239	.2110 .0167 ---	.0967 .1116 ---
2	--- .1845 .0379	--- .0166 ---	--- .0004 ---	--- .0162 ---
3	--- .0000 .0077	--- .2174 ---	--- .0012 ---	--- .0745 ---

TABLE XII - FRANCK-CONDON FACTORS FOR CH C-X BAND SYSTEM

V' \ V''	0	1	2	3
0	.9995 .9997 .9997	--- 1.57×10^{-5} ---	--- 2.35×10^{-4} ---	--- 6.29×10^{-6} ---
1	--- --- ---	.9979 --- .9963	--- --- ---	--- --- ---
2	--- --- ---	--- --- ---	.9860 --- .9740	--- --- ---
3	--- --- ---	--- --- ---	--- --- ---	.9487 --- .9046

1st value 103 RKR potential
2nd value 101 Morse potential
3rd value 7 Morse potential

TABLE XIII

FRANCK-CONDON FACTORS

CN VIOLET BAND SYSTEM

Reference 30

v'	v''							
	0	1	2	3	4	5	6	7
0	0.9179	0.0760	0.0058	0.0003	0.0000			
1	0.0809	0.7795	0.1240	0.0143	0.0012	0.0001	0.0000	0.0000
2	0.0012	0.1417	0.6754	0.1550	0.0239	0.0026	0.0002	0.0000
3	0.0000	0.0028	0.1905	0.5929	0.1745	0.0342	0.0046	0.0005
4		0.0000	0.0043	0.2318	0.5279	0.1825	0.0452	0.0071
5		0.0000	0.0001	0.0054	0.2668	0.4824	0.1781	0.0554
6			0.0000	0.0002	0.0050	0.2933	0.4583	0.1640
7				0.0000	0.0007	0.0032	0.3095	0.4554

TABLE XIV FRANCK-CONDON FACTORS

CO FOURTH POSITIVE BAND SYSTEM

Reference 107

v'	v''							
	0	1	2	3	4	5	6	7
0	0.1140	0.2640	0.2850	0.1950	0.0947	0.0346	0.0099	0.0023
1	0.2200	0.1540	0.0023	0.0800	0.1950	0.1840	0.1050	0.0424
2	0.2340	0.0104	0.0947	0.1130	0.0035	0.0627	0.1680	0.1640
3	0.1830	0.0246	0.1150	0.0001	0.0943	0.0788	0.0000	0.0754
4	0.1180	0.0954	0.0289	0.0642	0.0606	0.0099	0.1010	0.0443
5	0.0666	0.1290	0.0017	0.0903	0.0004	0.0855	0.0164	0.0396
6	0.0342	0.1170	0.0413	0.0347	0.0509	0.0347	0.0295	0.0682
7	0.0165	0.0858	0.0841	0.0003	0.0741	0.0014	0.0703	0.0005

TABLE XV

FRANCK-CONDON FACTORS

CO^+ COMET-TAIL BAND SYSTEM

Reference 107

v'	v''							
	0	1	2	3	4	5	6	7
0	0.0423	0.1520	0.2500	0.2520	0.1740	0.0864	0.0322	0.0091
1	0.1130	0.1930	0.0812	0.0005	0.0918	0.1910	0.1770	0.1000
2	0.1670	0.0987	0.0028	0.1080	0.0856	0.0004	0.0726	0.1740
3	0.1800	0.0141	0.0726	0.0705	0.0036	0.0969	0.0630	0.0010
4	0.1590	0.0045	0.0961	0.0010	0.0765	0.0371	0.0188	0.0988
5	0.1220	0.0414	0.0498	0.0305	0.0581	0.0079	0.0788	0.0063
6	0.0850	0.0789	0.0067	0.0703	0.0039	0.0620	0.0151	0.0419
7	0.0549	0.0952	0.0034	0.0586	0.0140	0.0485	0.0116	0.0567

TABLE XVI LINES OF NEUTRAL CARBON, CI

Line No.	Wavelength nm	Energy, ev	f-number	Ref.
1	1973.7	0.628	1.06E-01	128
2	1858.3	0.667	9.85E-01	128
3	1788.6	0.693	1.52E-01	128
4	1786.0	0.694	1.03E+00	128
5	1753.2	0.707	1.04E+00	128
6	1688.6	0.734	7.40E-01	127
7	1603.5	0.773	1.14E+00	128
8	1502.5	0.825	1.81E-01	128
9	1461.7	0.848	1.86E-01	128
10	1454.8	0.852	2.75E-01	128
11	1441.2	0.860	7.24E-01	128
12	1270.0	0.976	1.59E-01	128
13	1259.1	0.985	2.49E-01	127
14	1235.8	1.003	1.63E-01	128
15	1220.0	1.016	1.66E-01	128
16	1177.1	1.053	2.31E-01	128
17	1175.5	1.055	7.00E-01	127
18	1166.4	1.063	9.60E-01	127
19	1164.1	1.065	1.32E-01	127
20	1145.8	1.082	1.75E-01	128
21	1133.0	1.094	6.30E-01	127
22	1069.5	1.159	2.54E-01	128
23	1069.5	1.159	5.00E-01	127
24	1041.6	1.190	1.34E-02	128
25	1012.4	1.225	2.62E-01	127
26	960.1	1.291	1.00E-01	127
27	833.5	1.487	3.20E-02	130
28	828.0	1.497	1.90E-02	128
29	750.3	1.652	2.10E-02	128
30	716.9	1.729	2.20E-02	128
31	667.5	1.857	2.40E-02	128
32	660.7	1.876	1.00E-02	128
33	658.8	1.882	8.46E-03	129
34	631.4	1.964	2.50E-02	128
35	579.8	2.138	1.06E-03	129
36	538.0	2.304	7.47E-03	129
37	505.2	2.454	1.11E-02	129
38	504.1	2.459	1.02E-03	130
39	493.2	2.514	4.27E-03	129
40	482.6	2.569	4.40E-04	129
41	481.7	2.574	4.52E-04	129
42	477.0	2.599	4.74E-03	129

TABLE XVI, CONTINUED

Line No.	Wavelength nm	Energy, ev	f-number	Ref.
43	493.2	2.514	4.74E-03	130
44	437.1	2.836	1.69E-03	129
45	426.9	2.904	1.05E-03	129
46	247.8	5.003	9.40E-02	127
47	193.1	6.421	8.20E-02	127
48	176.7	7.016	1.41E-02	128
49	175.1	7.081	1.20E-01	127
50	165.7	7.482	1.70E-01	127
51	160.6	7.720	5.34E-03	128
52	160.5	7.725	3.67E-02	128
53	156.1	7.942	9.10E-02	127
54	154.4	8.030	1.97E-03	128
55	154.3	8.035	2.60E-03	128
56	151.3	8.194	1.16E-02	128
57	151.1	8.205	1.47E-03	128
58	149.3	8.301	7.40E-03	128
59	149.3	8.304	9.07E-04	128
60	148.1	8.371	1.10E-02	127
61	148.0	8.377	5.01E-03	128
62	147.0	8.434	1.42E-02	128
63	146.3	8.474	9.30E-02	127
64	145.9	8.498	7.00E-03	127
65	143.1	8.664	1.30E-01	127
66	135.7	9.136	5.26E-03	128
67	135.6	9.143	3.62E-02	128
68	132.8	9.336	3.80E-02	127
69	131.2	9.450	1.93E-02	128
70	131.2	9.450	2.55E-03	128
71	129.0	9.611	1.14E-02	128
72	128.8	9.626	1.43E-03	128
73	127.8	9.701	1.95E-02	128
74	127.8	9.701	3.80E-03	127
75	127.7	9.709	6.30E-02	127
76	127.5	9.724	7.22E-03	128
77	127.5	9.724	8.85E-04	128
78	126.5	9.801	4.88E-03	128
79	126.0	9.840	2.90E-02	127
80	119.2	10.401	7.19E-03	128
81	119.1	10.410	4.15E-02	128
82	115.7	10.716	2.61E-02	128
83	115.7	10.716	3.43E-03	128

TABLE XVI, CONCLUDED

Line No.	Wavelength nm	Energy, ev	f-number	Ref.
84	114.0	10.875	7.05E-01	128
85	114.0	10.875	1.55E-02	128
86	113.9	10.885	1.95E-03	128
87	112.8	10.991	9.80E-03	128
88	112.8	10.991	1.20E-03	128
89	101.8	12.179	1.05E+00	128
90	94.5	13.122	2.70E-01	127
91	91.1	13.605	2.95E-01	128

TABLE XVII LINES OF NEUTRAL OXYGEN, 01

Line No.	Wavelength nm	Energy, ev	f-number	Ref.
1	5484.5	0.226	1.90E-01	128
2	5274.5	0.235	1.97E-01	128
3	1820.1	0.681	9.72E-01	128
4	1799.0	0.689	9.84E-01	128
5	1609.7	0.770	2.15E-03	128
6	1591.1	0.779	2.17E-03	128
7	1402.1	0.884	1.63E-01	127
8	1255.8	0.987	1.61E-01	128
9	1245.7	0.995	1.62E-01	128
10	1128.9	1.098	7.50E-01	127
11	1095.0	1.132	1.73E-01	127
12	926.3	1.338	9.00E-01	127
13	844.9	1.467	8.98E-01	127
14	777.6	1.594	9.22E-01	127
15	736.5	1.683	1.62E-02	127
16	701.5	1.767	3.98E-02	127
17	641.9	1.931	1.48E-02	127
18	615.1	2.016	6.64E-02	127
19	596.2	2.080	3.97E-03	128
20	532.7	2.327	1.40E-02	127
21	443.9	2.793	5.60E-03	127
22	391.4	3.168	2.29E-03	127
23	371.6	3.336	1.28E-02	128
24	334.0	3.712	1.43E-02	128
25	130.5	9.500	3.10E-02	127
26	121.7	10.187	1.30E-01	127
27	115.2	10.762	9.00E-02	127
28	112.6	11.011	1.85E-02	128
29	105.0	11.808	4.89E-03	128
30	104.6	11.853	1.99E-02	128
31	102.7	12.072	1.00E-02	127
32	101.9	12.167	1.88E-03	128
33	99.8	12.427	3.50E-02	127
34	99.0	12.524	4.70E-02	127
35	98.0	12.654	5.24E-03	128
36	97.6	12.702	2.13E-02	128
37	97.3	12.738	1.54E-02	128
38	96.0	12.915	7.01E-02	128
39	95.3	13.008	2.01E-03	128
40	95.0	13.051	1.05E-02	128
41	93.8	13.223	1.88E-02	128
42	93.7	13.232	2.22E-02	128

TABLE XVII, CONCLUDED

Line No.	Wavelength nm	Energy, ev	f-number	Ref.
43	93.7	13.236	6.57E-03	128
44	93.0	13.334	4.27E-03	128
45	92.5	13.397	2.93E-03	128
46	92.2	13.450	1.50E-02	127
47	91.8	13.501	5.60E-03	128
48	91.4	13.559	4.97E-03	128
49	91.3	13.585	4.94E-02	128
50	89.5	13.856	2.14E-03	128
51	89.2	13.898	3.35E-02	128
52	88.3	14.033	5.82E-03	128
53	87.9	14.108	3.70E-02	127
54	87.8	14.116	3.85E-02	128
55	86.2	14.386	2.23E-03	128
56	85.9	14.428	2.61E-02	128
57	83.1	14.925	2.50E-02	128
58	81.7	15.181	2.54E-02	128
59	81.2	15.276	6.91E-03	128
60	81.2	15.276	7.70E-03	127
61	80.5	15.405	1.22E-02	128
62	78.8	15.726	6.52E-03	128
63	78.4	15.810	1.44E-02	128
64	77.6	15.979	6.62E-03	128
65	77.2	16.064	2.43E-02	128
66	77.1	16.078	2.49E-03	128
67	76.9	16.120	9.71E-03	128
68	75.9	16.335	2.53E-03	128
69	75.7	16.376	1.64E-02	128
70	73.5	16.873	2.83E-02	128
71	72.6	17.084	2.32E-02	128
72	70.2	17.671	7.32E-03	128
73	69.8	17.757	1.61E-02	128
74	68.8	18.026	2.79E-03	128
75	68.6	18.068	1.09E-02	128

TABLE XVIII LINES OF IONIZED CARBON, CII

Line No.	Wavelength nm	Energy, ev	f-number	Ref.
1	392.0	3.163	1.43E-01	131
2	283.7	4.370	1.33E-01	131
3	251.1	4.937	1.36E-01	131
4	133.5	9.287	2.70E-01	127
5	103.6	11.967	5.90E-02	127
6	90.4	13.713	5.20E-01	127
7	85.8	14.443	4.60E-02	127
8	80.8	15.340	1.23E-01	128
9	68.7	18.039	2.60E-01	127
10	65.1	19.039	4.88E-01	128
11	64.2	19.321	1.65E-01	128
12	63.6	19.494	1.05E-02	128

TABLE XIX LINES OF IONIZED OXYGEN, OII

Line No.	Wavelength nm	Energy, ev	f-number	Ref.
1	83.3	14.880	4.30E-01	127
2	79.7	15.566	7.00E-02	127
3	71.8	17.258	2.50E-01	127
4	67.3	18.427	6.30E-02	127
5	64.4	19.252	1.50E-01	127

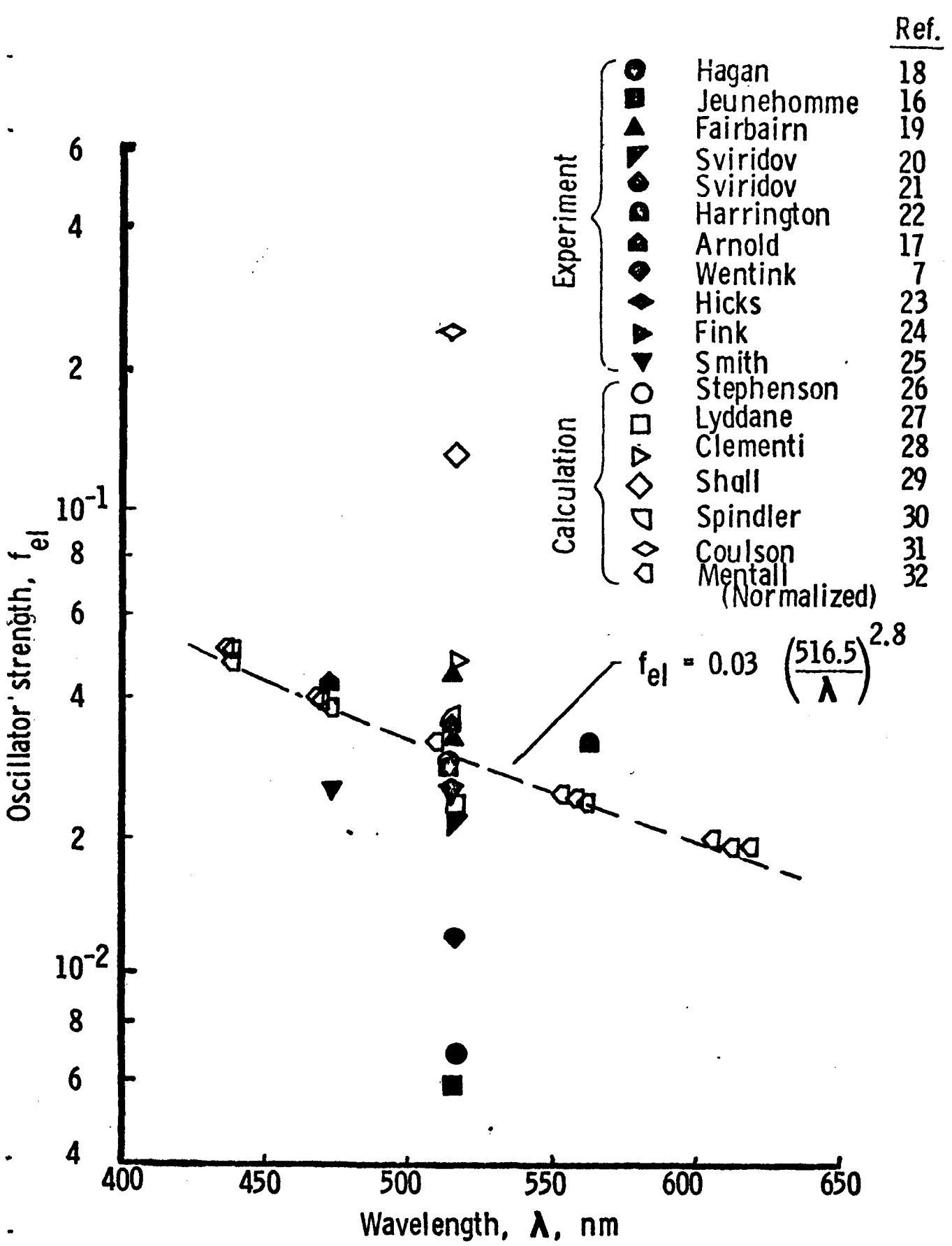

Figure 1. - Electronic oscillator strengths for C_2 Swan band system.

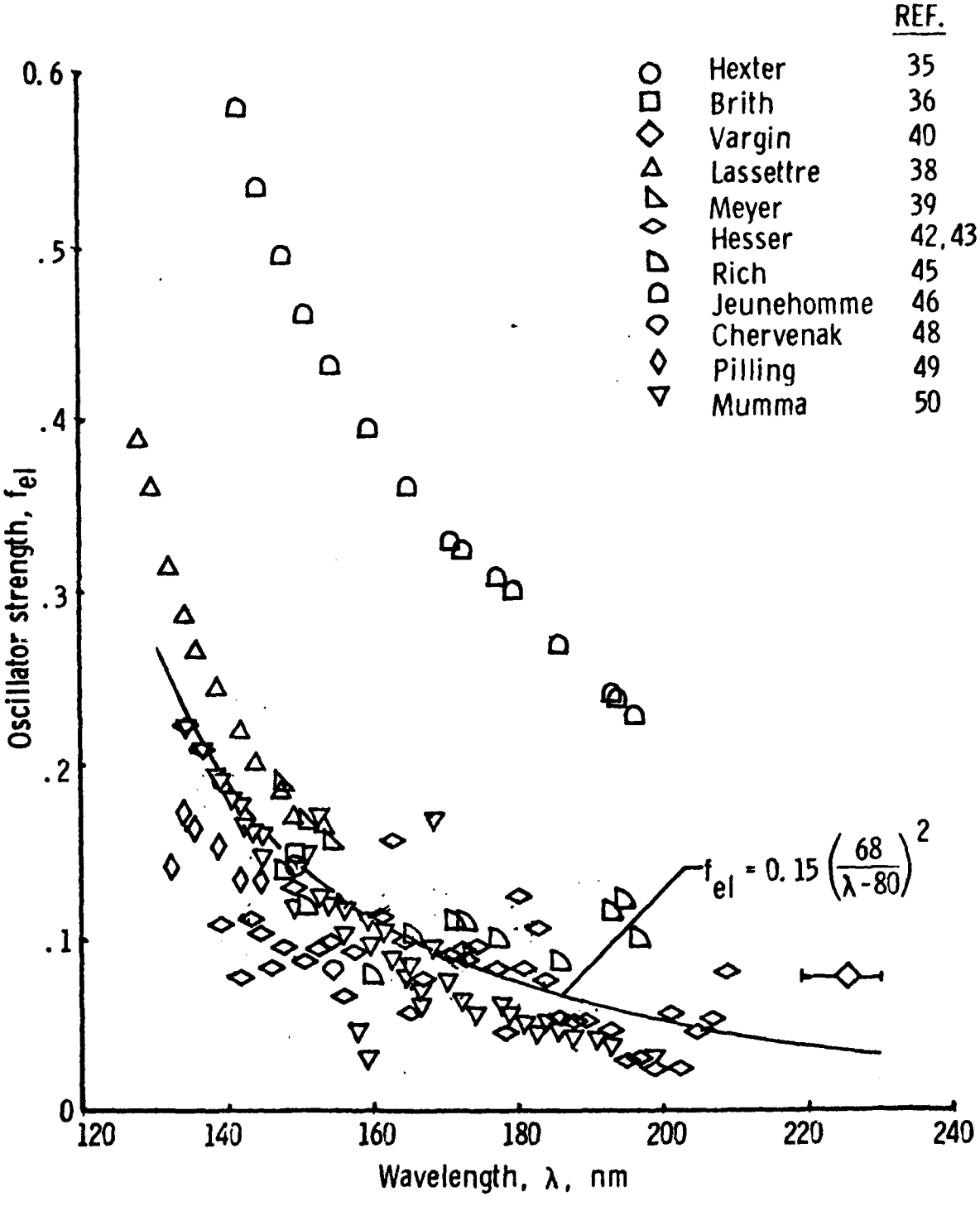

Figure 2. - Electronic oscillator strengths for CO Fourth Positive band system.

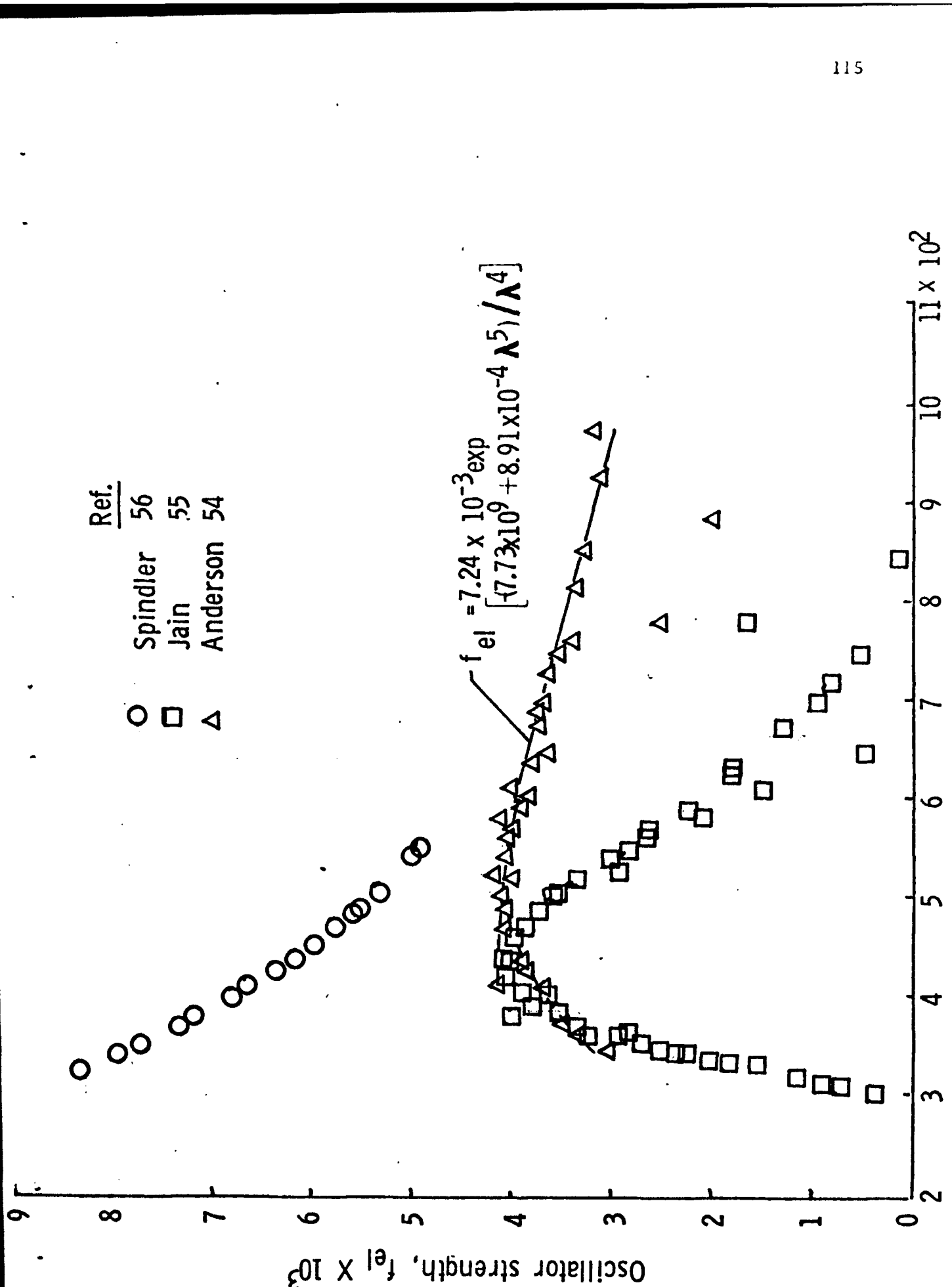

Figure 3. - Electronic oscillator strengths for CO^+ Comet-Tail band system.

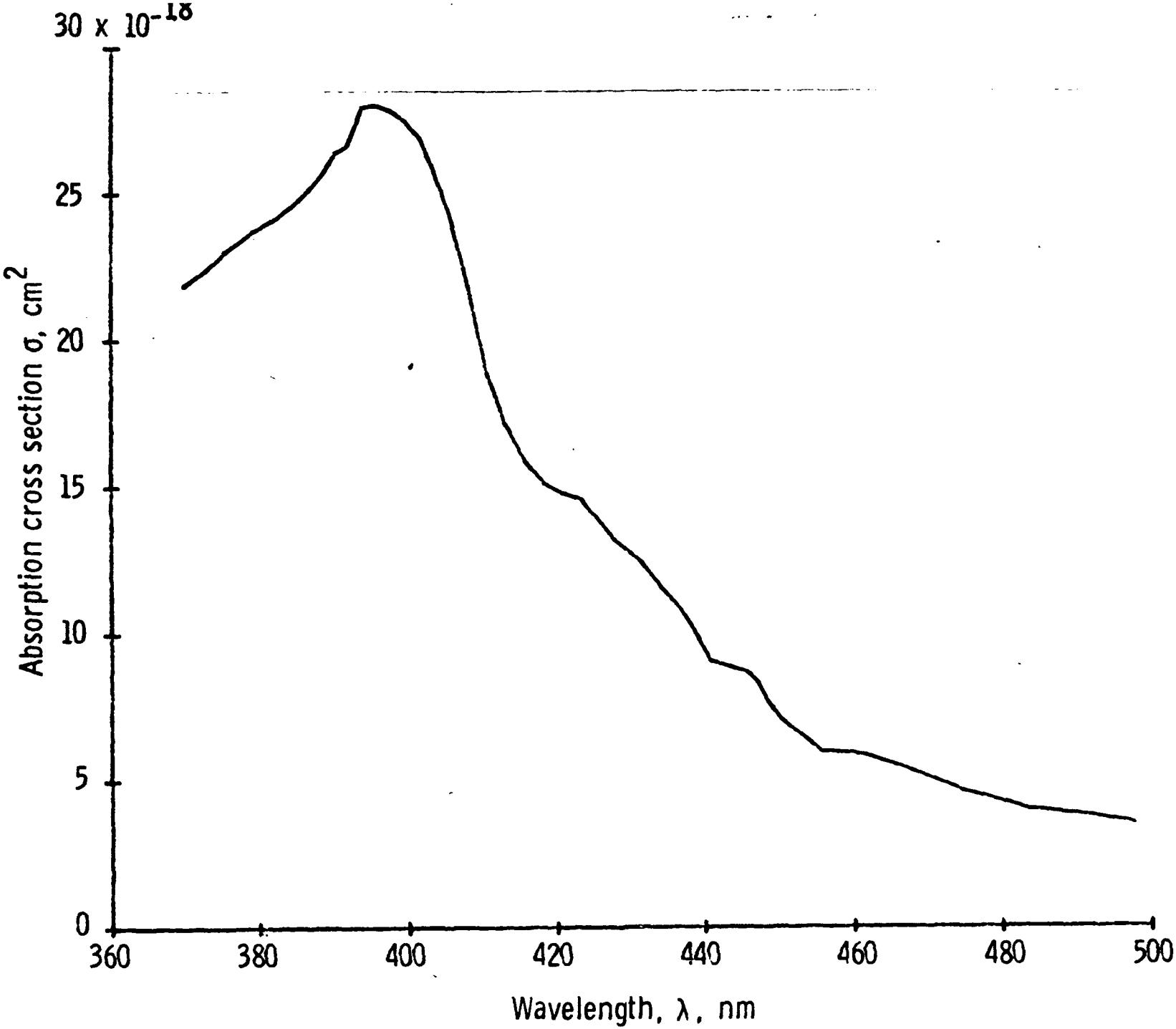

Figure 4.- Absorption cross section for C_3 (from Brewer and Engelke, reference 96). N = 3.268E+16 cc^{-1}.

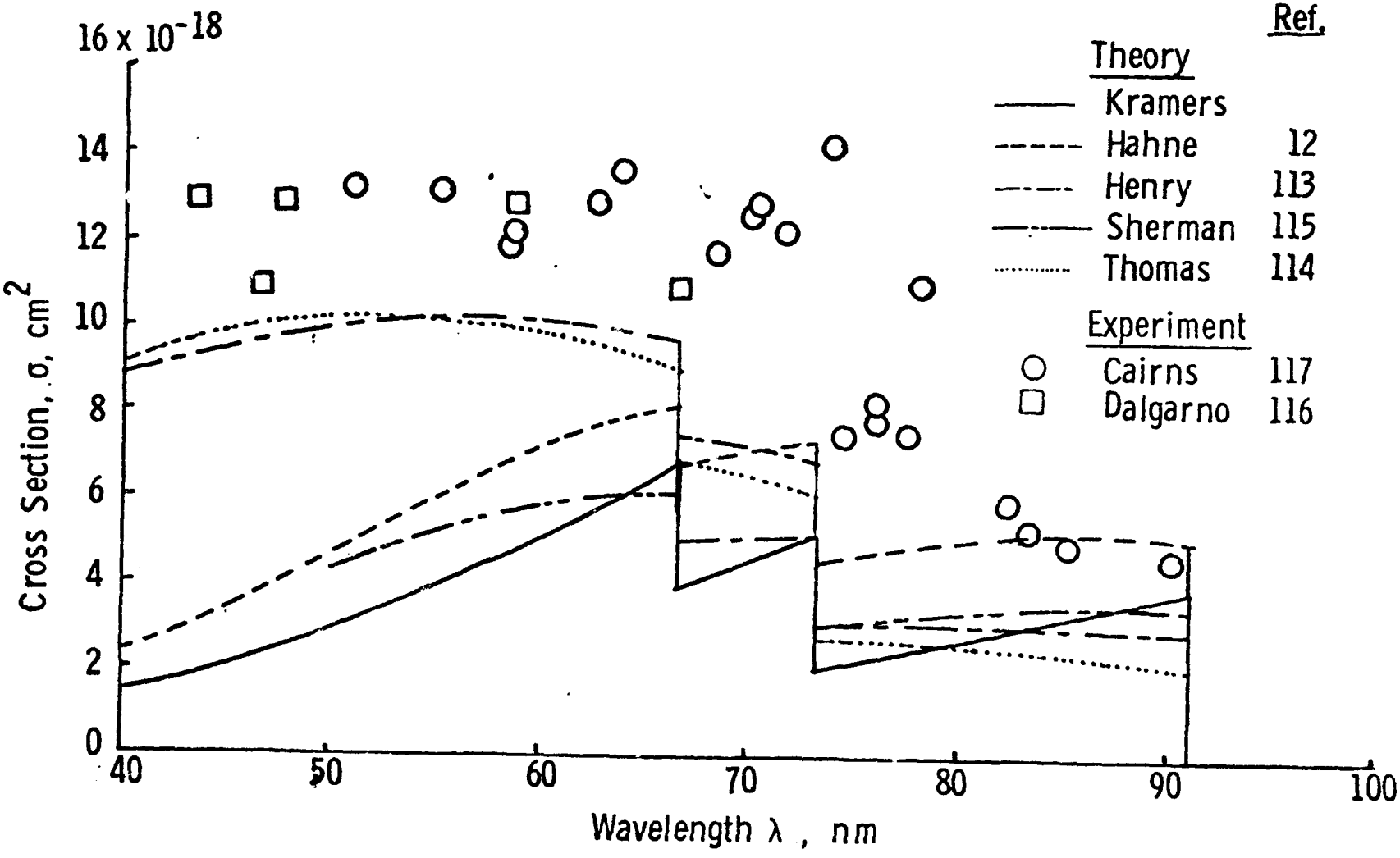

(a) $O(^3P) + h\nu \rightarrow O^+ (^4S^o, {}^2D^o, {}^2P^o) + e^-$.

Figure 5. - Photoionization cross section of atomic oxygen.

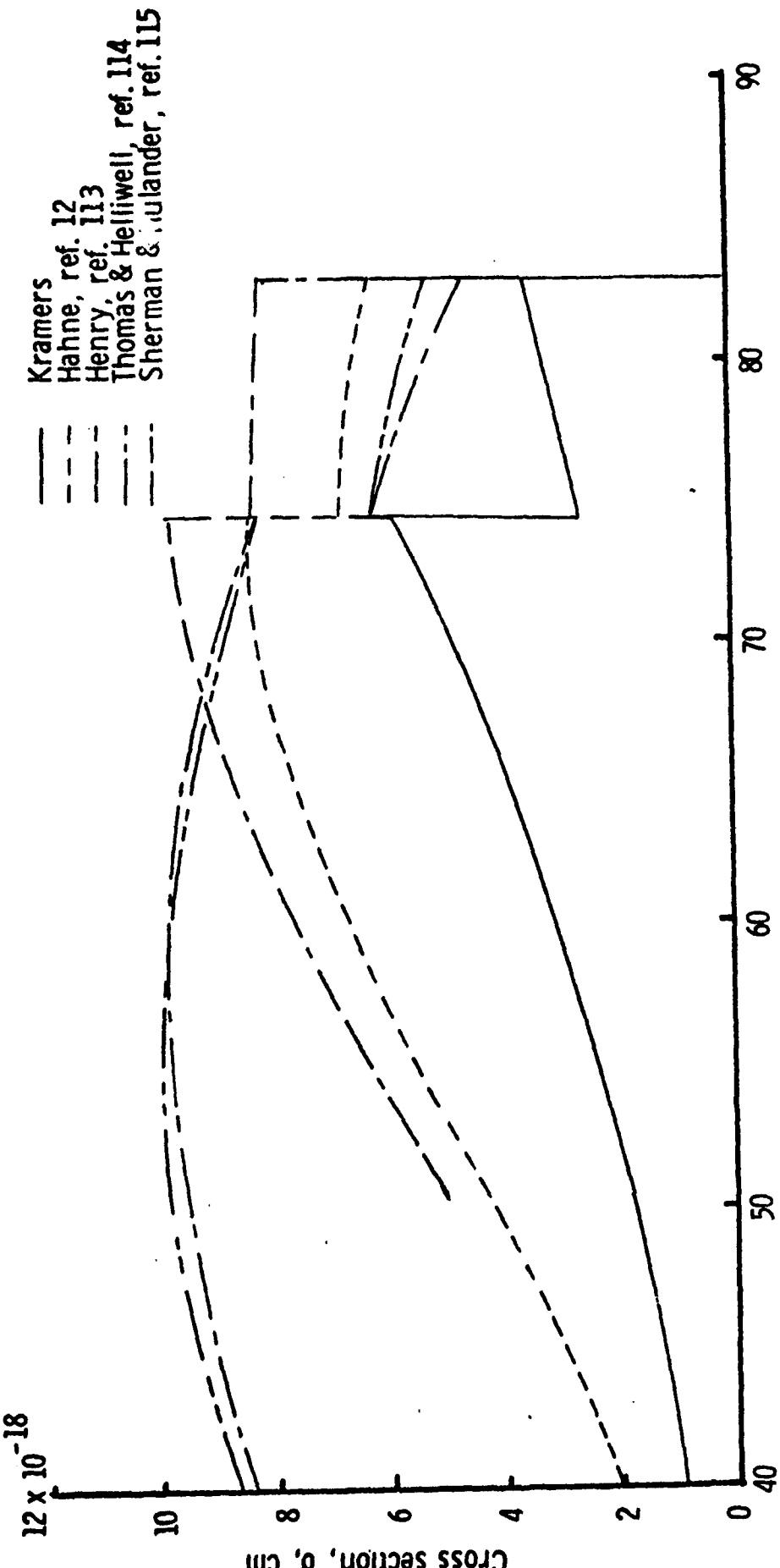

(b) $O(^1D) + h\upsilon \rightarrow O^+ (^2D^o, ^2P^o) + e^-$.

Figure 5.- Continued.

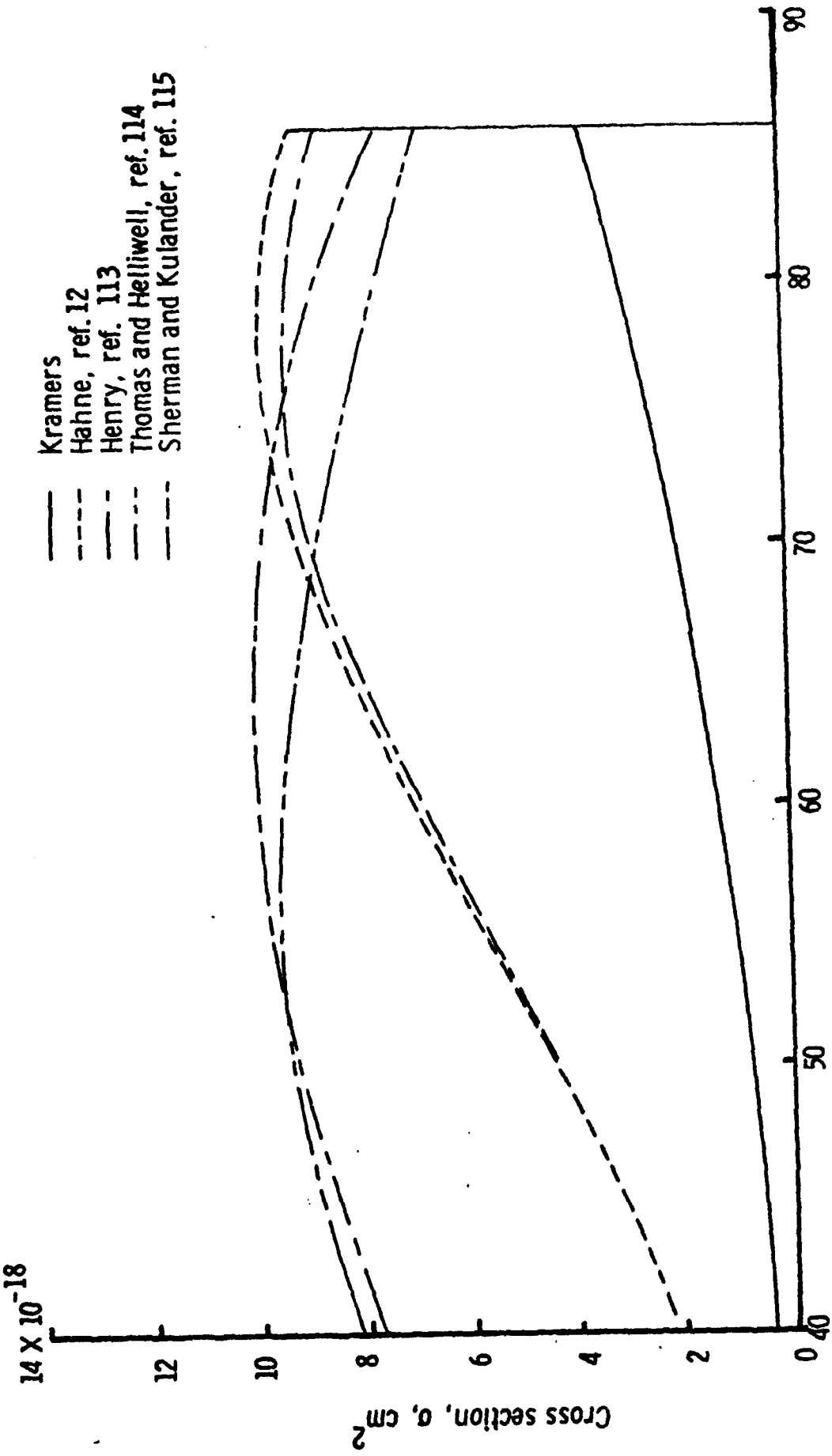

(c) $O(^1S) + h\upsilon \rightarrow O^+ (^2P^o) + e^-$.

Figure 5. - Concluded.

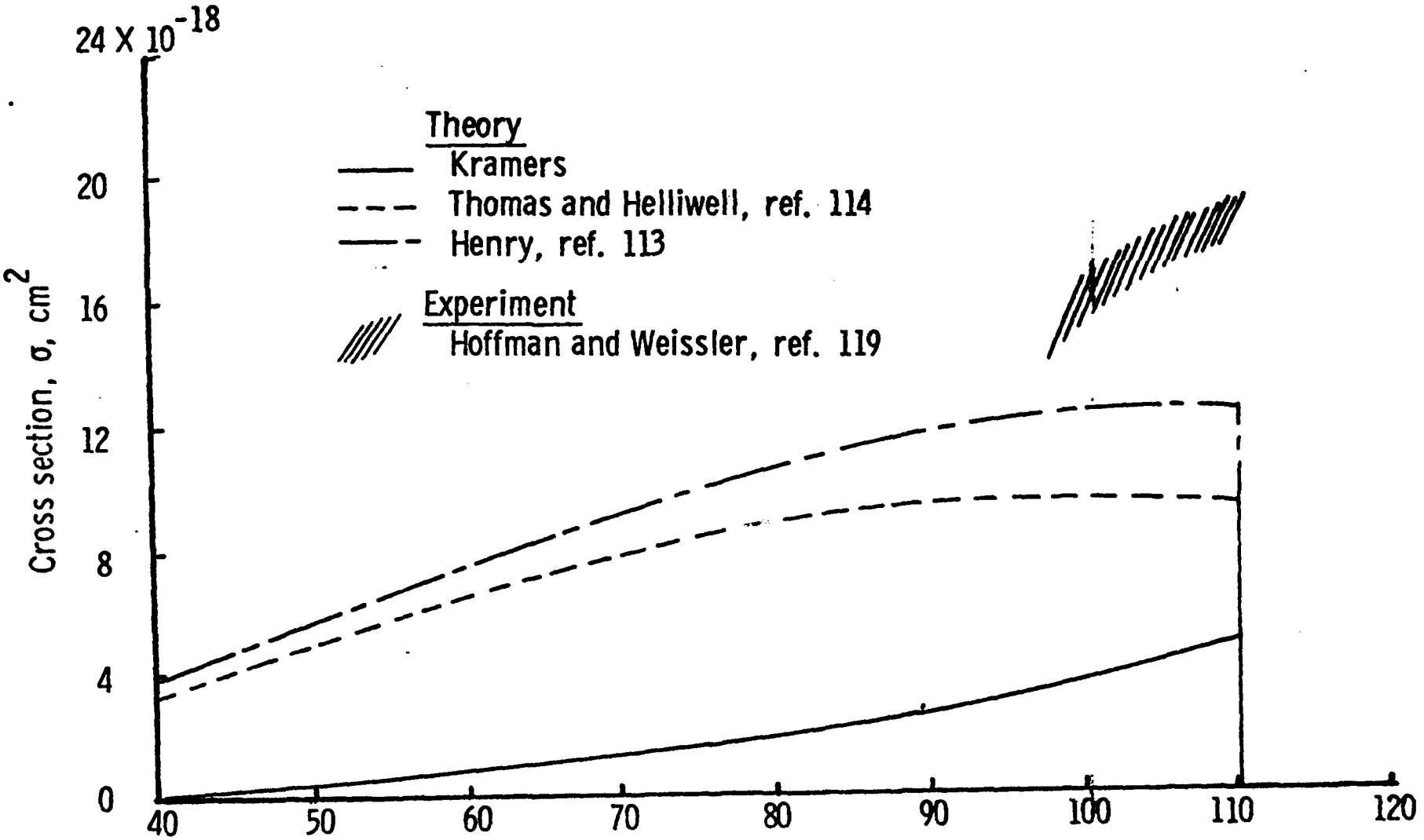

(a) $C(^2P) + h\nu \rightarrow C^+(^2P^o) + e^-$.

Figure 6. - Photoionization cross section for atomic carbon.

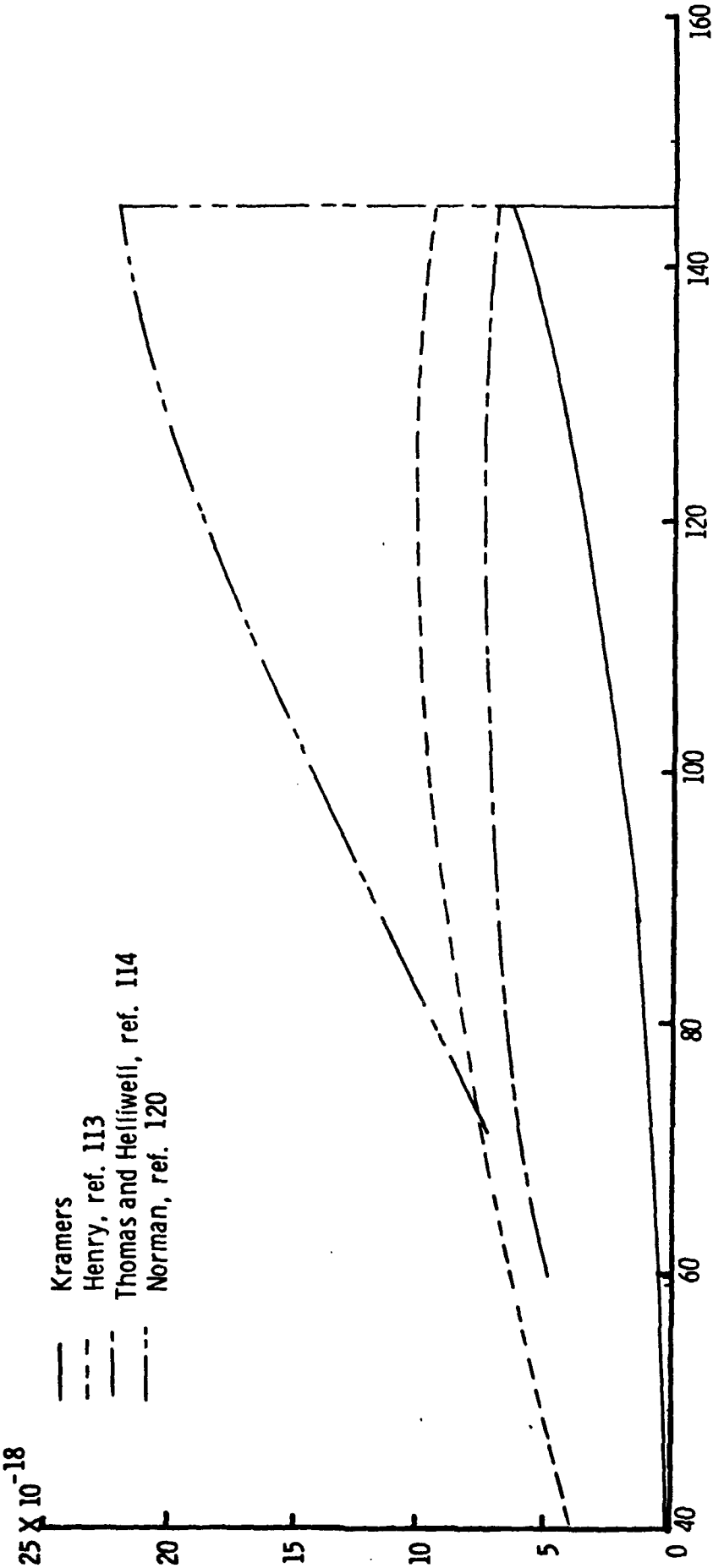

(b) $C(^1S) + h\upsilon \rightarrow C^+ (^2P^o) + e^-$.

Figure 6. - Continued.

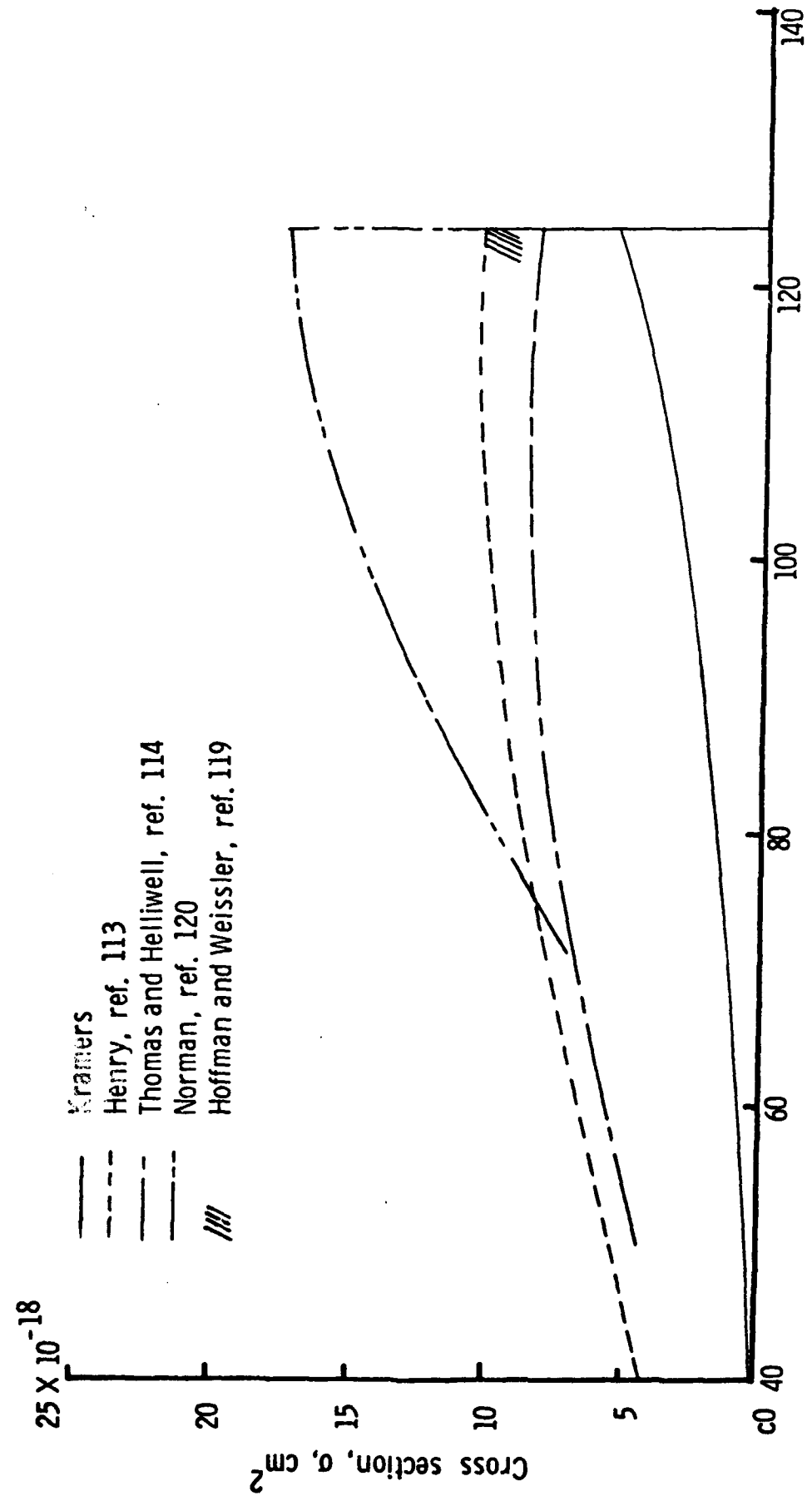

(c) $C(^1D) + h\nu \rightarrow C^+(^2P^o) + e^-$.

Figure 6. - Concluded.

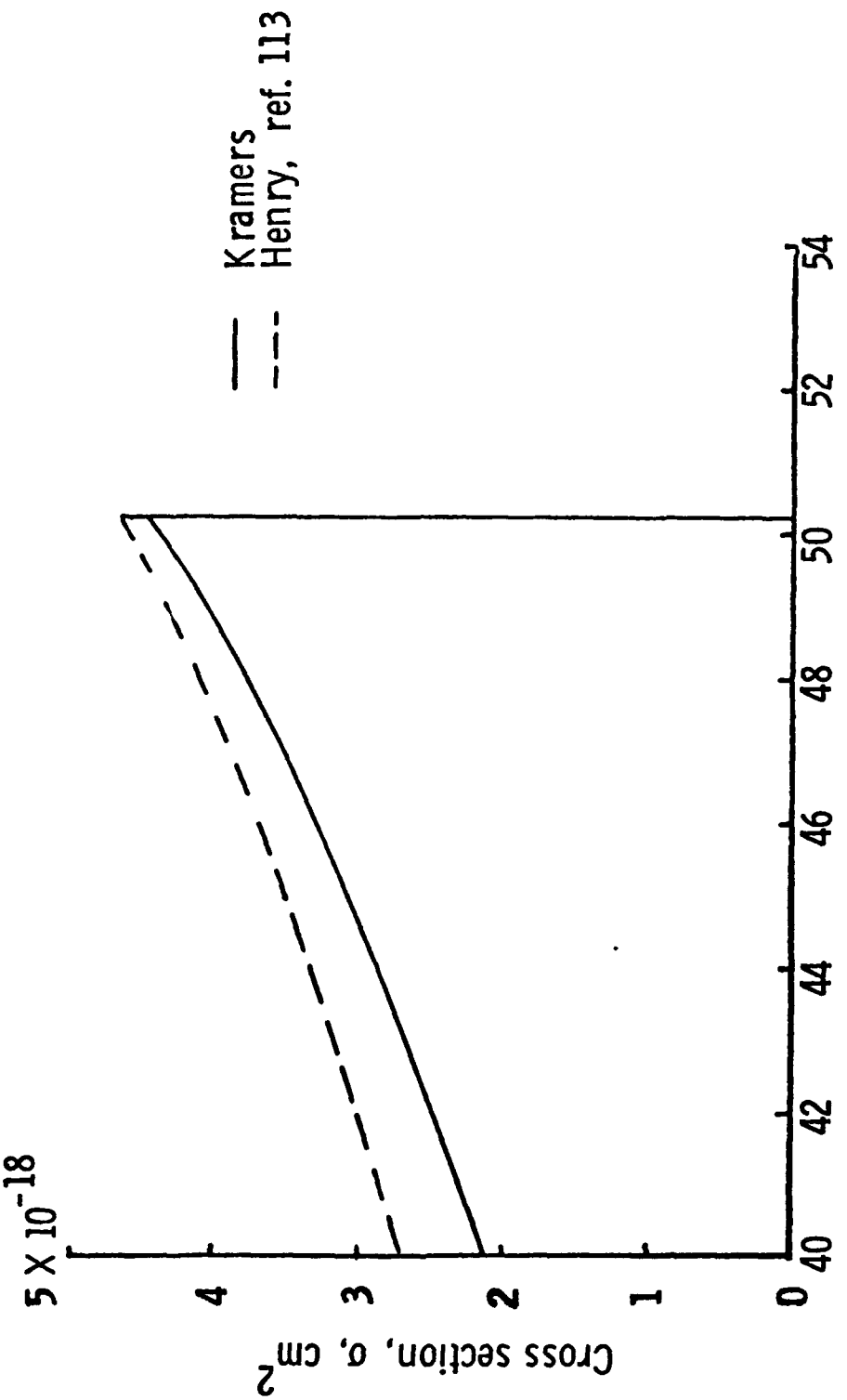

Figure 7.- Photoionization cross section for carbon ion, $C^+ (^2P) + h\nu \rightarrow C^{++} (^1S) + e^-$.

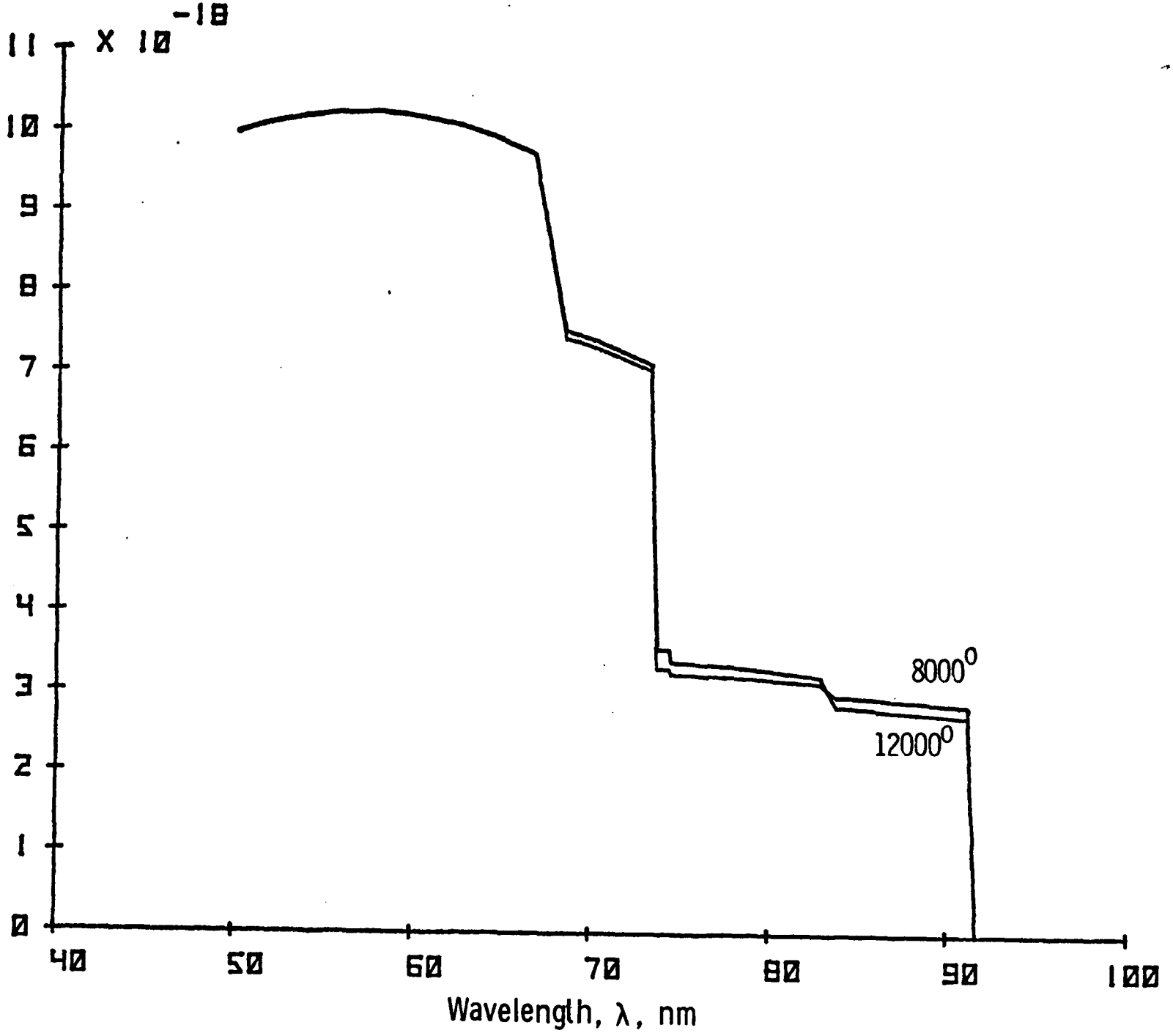

Figure 8. - Absorption coefficient per particle for free-bound transitions of oxygen.

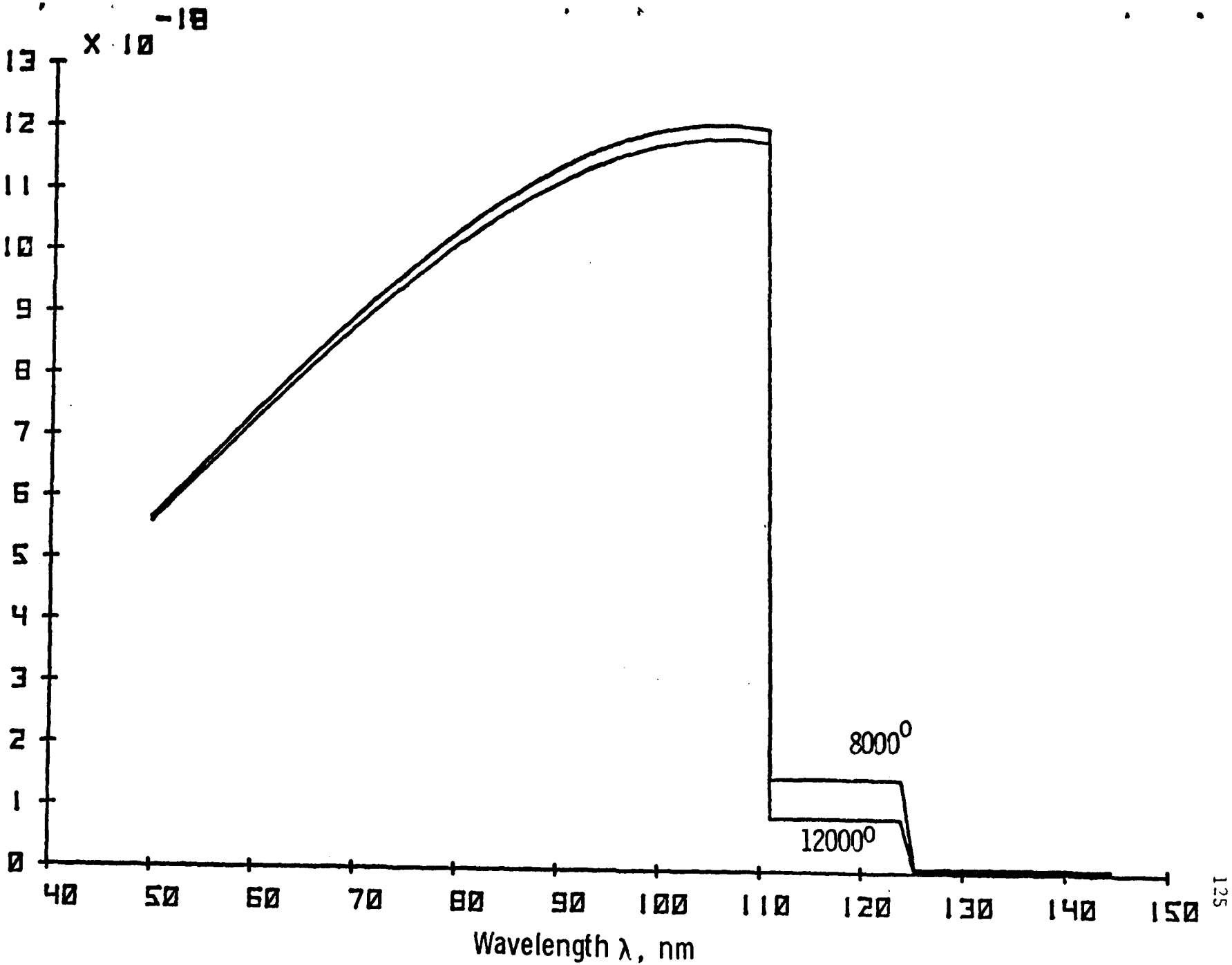

Figure 9. - Absorption coefficient per particle for free-bound transitions of carbon.

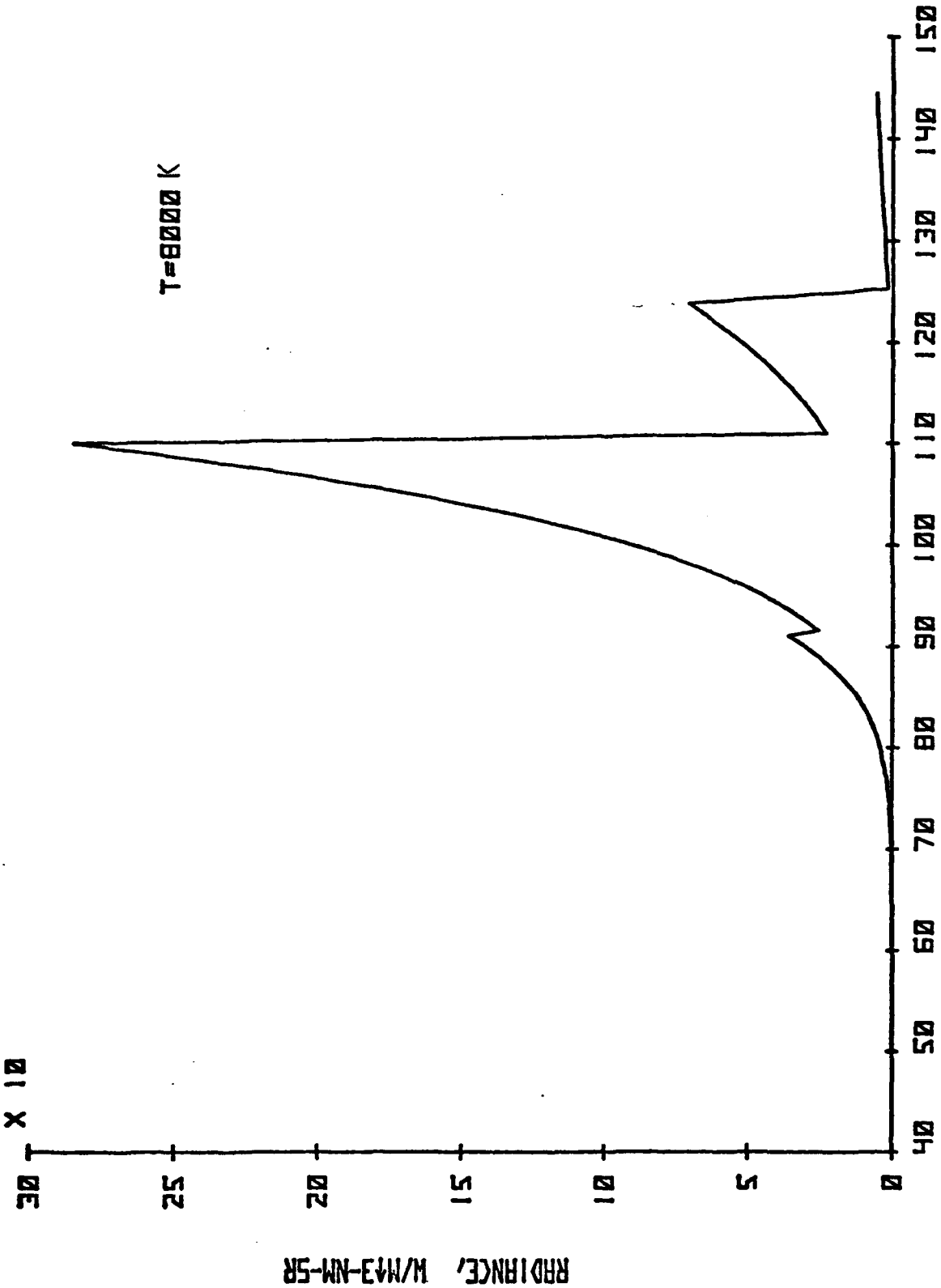

(a) T = 8000 K, 1 atm. pressure.

Figure 10 - Radiance of heated CO_2 due to free-bound transitions of atomic carbon and oxygen.

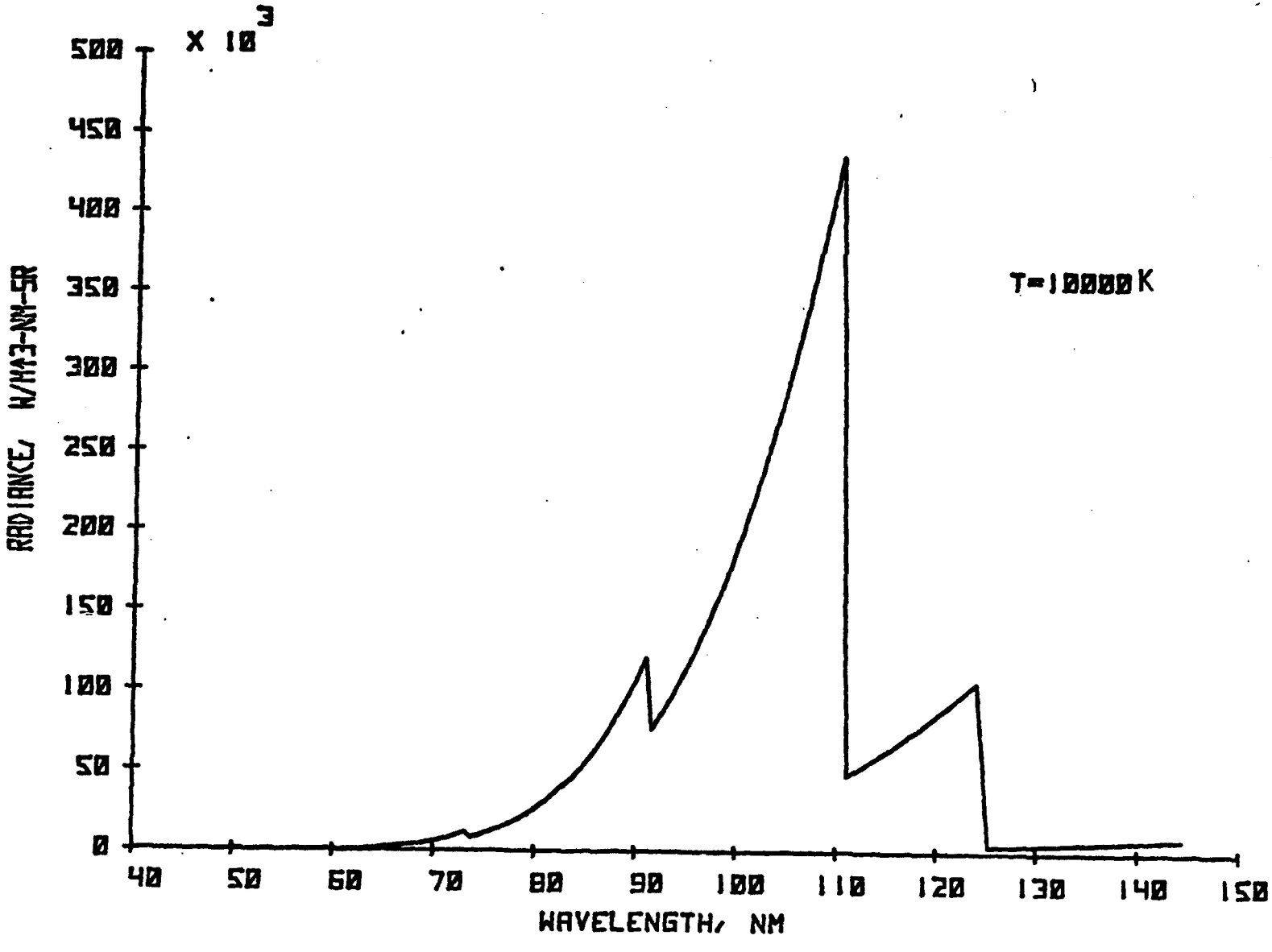

(b) T = 10000 K, 1 atm. pressure.

Figure 10. - Continued.

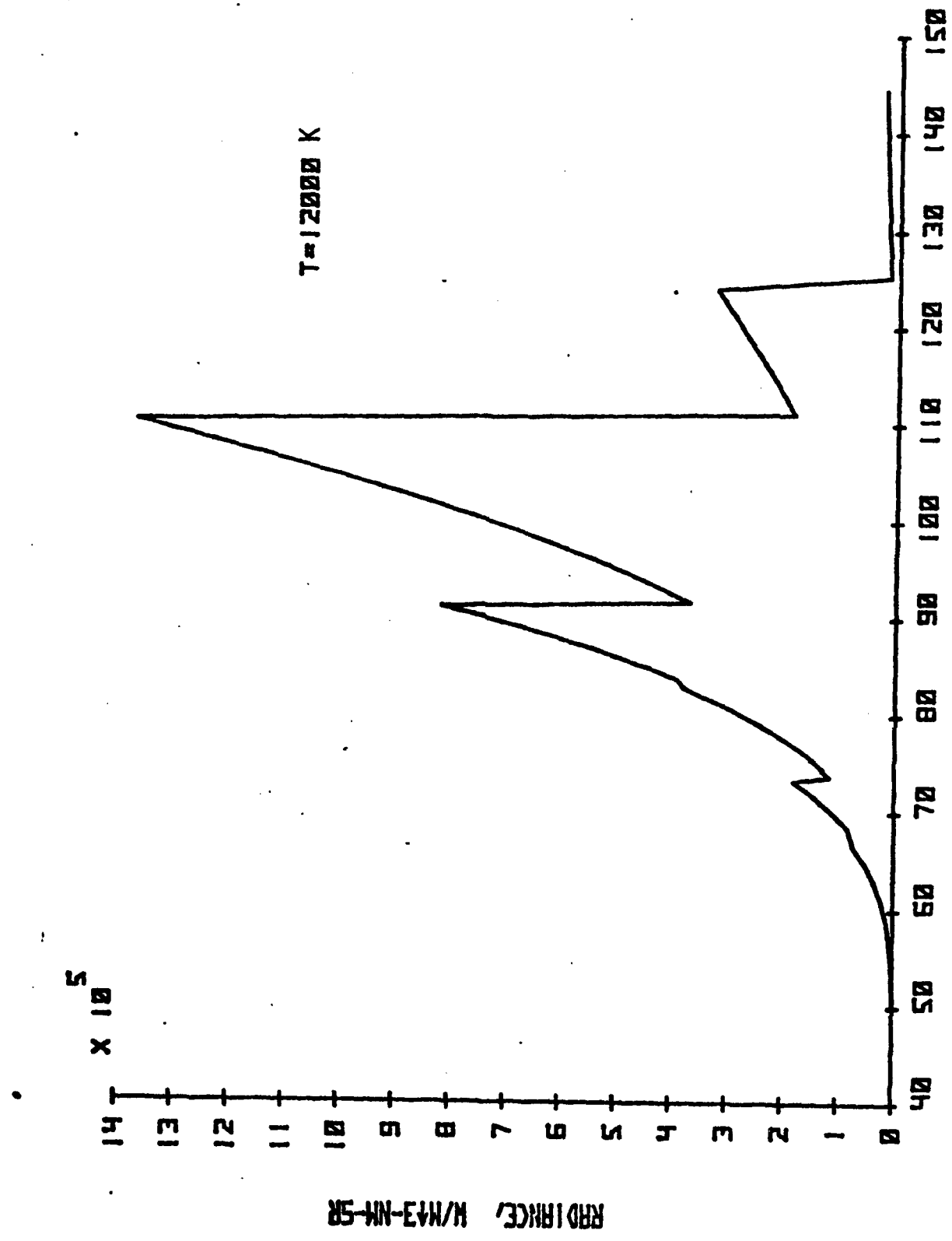

(c) T = 12000 K, 1 atm. pressure.

Figure 10.- Concluded.

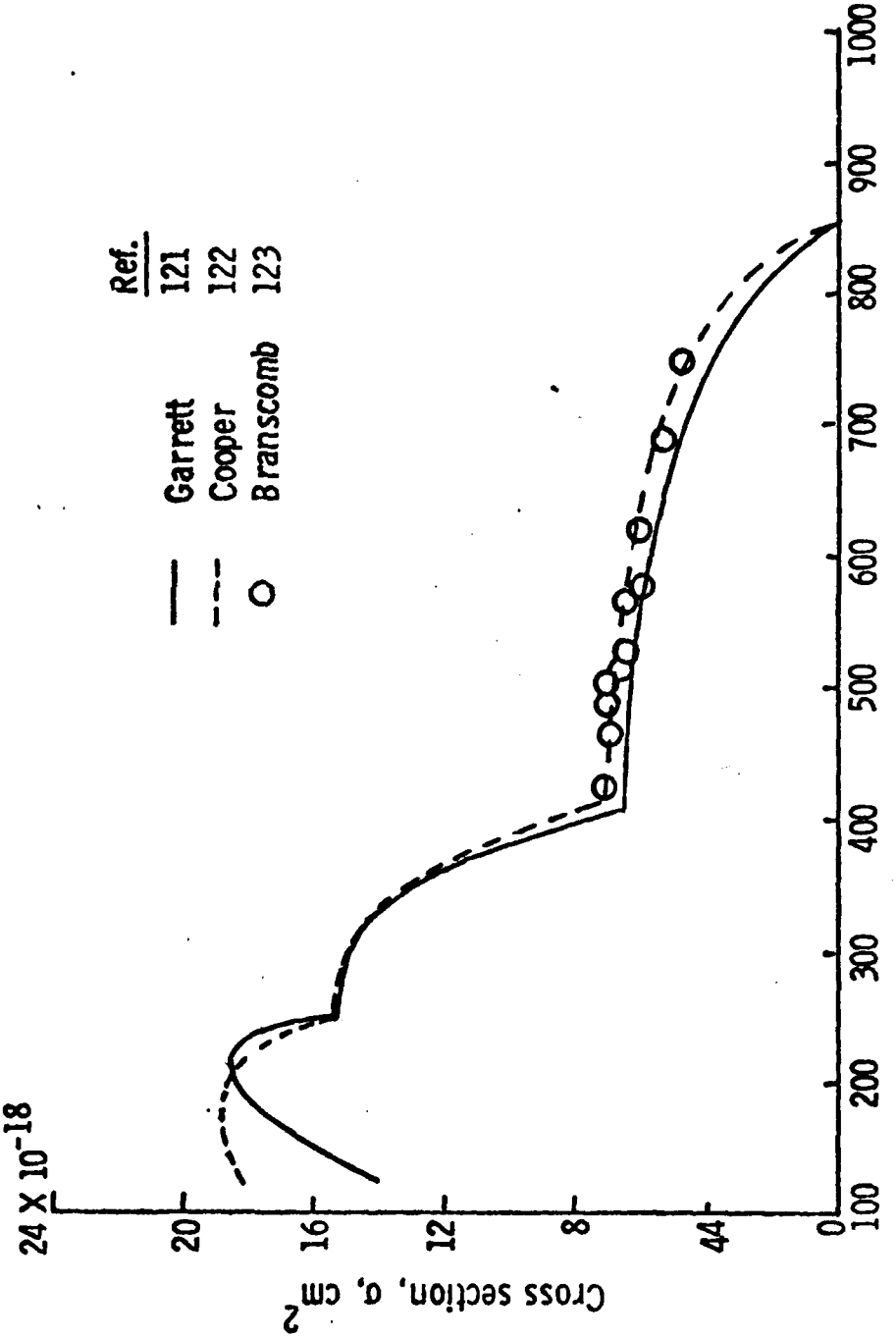

Figure 1E - Cross section for detachment of the negative oxygen ion.

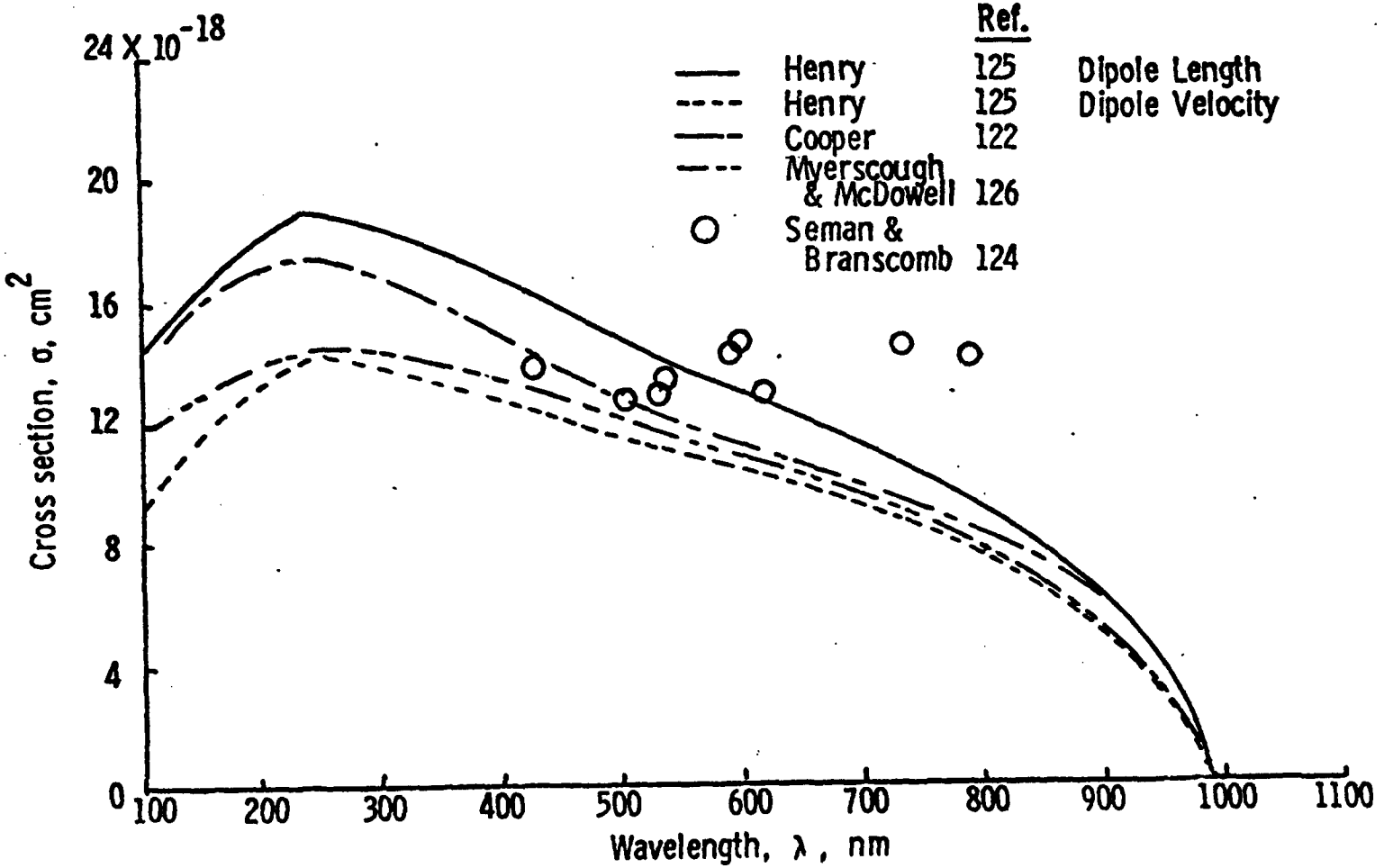

Figure 12.- Cross section for detachment of the negative carbon ion.